



**Monitoring of Air Pollutants using Active and Passive Sampling Techniques**

**Jas Raj Subba**

**A Thesis Submitted in Partial Fulfillment of the Requirements for the Degree of  
Doctor of Philosophy in Chemistry**

**Prince of Songkla University**

**2016**

**Copyright of Prince of Songkla University**

**Thesis Title**            Monitoring of Air Pollutants using Active and Passive Sampling  
Techniques

**Author**                    Mr. Jas Raj Subba

**Major Program**        Chemistry

---

**Major Advisor :**

.....

(Assoc. Prof. Dr. Proespichaya Kanatharana)

**Examining Committee :**

.....Chairperson

(Assoc. Prof. Dr. Pakawadee Sutthivaiyakit)

.....

**Co-advisor :**

(Assoc. Prof. Dr. Proespichaya Kanatharana)

.....

(Asst. Prof. Dr. Chongdee Thammakhet)

.....

(Asst. Prof. Dr. Chongdee Thammakhet)

.....

(Assoc. Prof. Dr. Lupong Kaewsichan)

The Graduate School, Prince of Songkla University, has approved this thesis as partial fulfillment of the requirements for the Doctor of Philosophy Degree in Chemistry.

.....

(Assoc. Prof. Dr. Teerapol Srichana)

Dean of Graduate School

This is to certify that the submitted work is the result of the candidate's own investigations.  
Due acknowledgement has been made of any assistance received.

.....Signature  
(Assoc. Prof. Dr. Proespichaya Kanatharana)  
Major Advisor

.....Signature  
(Mr. Jas Raj Subba)  
Candidate

I hereby certify that this work has not been accepted in substance for any degree, and is not being currently submitted in candidature for any degree.

.....Signature

(Mr. Jas Raj Subba)

Candidate

**Thesis Title** Monitoring of Air Pollutants using Active and Passive Sampling Techniques  
**Author** Mr. Jas Raj Subba  
**Major** Chemistry  
**Academic** 2015

### Abstract

Monitoring of air pollutants is being focused in this thesis. Both active and passive sampling techniques were used with emphasis on simple, cost effective and portable devices. The first project used a cost effective printed circuit board (PCB) passive sampler to monitor BTX in Hat Yai city, one of the largest commercial hub of southern Thailand. Sampling was done by exposing the PCB passive samplers in different locations of Hat Yai city covering high to low exposure areas. After sampling BTX were desorbed from the PCB passive samplers using a laboratory-built thermal desorption system passed through an on-line micro-preconcentrator before being detected by gas chromatography with flame ionization detector (GC-FID). At optimum GC-FID conditions the analysis technique provided linear dynamic range of 0.06–5.6  $\mu\text{g}$  for benzene, 0.07–2.2  $\mu\text{g}$  for toluene and 0.23–2.5  $\mu\text{g}$  for xylene with  $R^2 > 0.99$  and limit of detections of 6.6, 6.8 and 19 ng, respectively. The ambient concentration of BTX was found in the range of N.D.–11.3 $\pm$ 1.6 for benzene, 4.5 $\pm$ 0.76–49.6 $\pm$ 3.7 for toluene and 1.0 $\pm$ 0.21–39.6 $\pm$ 3.1  $\mu\text{g m}^{-3}$  for xylene. The results suggested that benzene concentration is slowly increasing in Hat Yai while toluene and xylene are below the WHO recommended levels.

The second project was the monitoring of  $\text{SO}_2$  and  $\text{NO}_2$  in an industrial area of Bhutan using standard colorimetric methods. Active air sampling of  $\text{SO}_2$  and  $\text{NO}_2$  was done in the spring of 2015 (March – May) to see the distribution of these two pollutants from the point source of emission (factories and industries) and to obtain a baseline data for future references. A small compact portable active sampler was developed in the laboratory and was validated before using it for real field monitoring. The developed system provided good linearity with  $R^2 > 0.99$  and limit of detection of 0.03  $\mu\text{g mL}^{-1}$  for  $\text{SO}_2$  and 0.03  $\mu\text{g mL}^{-1}$  for  $\text{NO}_2$ . Twenty five sampling sites were selected and sampling was carried out three

times a day (morning, afternoon and evening) in each sampling site. The average concentration of SO<sub>2</sub> and NO<sub>2</sub> was found in the range of 0.45–4.46 µg m<sup>-3</sup> and 0.56–5.68 µg m<sup>-3</sup>, respectively. These were still below the maximum permissible limits set by World Health Organization of 350 µg m<sup>-3</sup> for 1 h mean exposure of SO<sub>2</sub> and 200 µg m<sup>-3</sup> for 1 h mean exposure of NO<sub>2</sub>. And they were also below the maximum permissible limits set by National Environment Commission of Bhutan of 80 µg m<sup>-3</sup> for 24 h average.

## Acknowledgements

This thesis would not have been complete, without the help, guidance and support of many people. I remain thankful to all the people involved in completing this thesis successfully.

I am very much thankful and grateful to Associate Professor Dr. Proespichaya Kanatharana, my course advisor for guiding me throughout the course of my project. I would also like to thank to Assistant Professor Dr. Chongdee Thammakhet my co-advisor for her tireless continuous support throughout my studies. And I would also extend my hearty thanks to Associate Professor Dr. Panote Thavarungkul for her critical and valuable timely feedbacks during the course of my project.

I would also like to thank:

The examination committee members of this thesis for their valuable time and feedback;

Prince of Songkla University, PhD scholarship for supporting financially to carry out this project.

Staffs of Department of Chemistry for their timely help during the course of my project;

Trace Analysis and Biosensor Research Center (TAB-RC), Chemistry Department, Faculty of Science and Graduate School, Prince of Songkla University;

My wife, son, daughter, parents, brothers and all the good supporting friends for their unmeasurable love, support, encouragement and big understanding.

Last but not the least to all my laboratory friends in TAB-RC who were there to help me any time I want in need of any help during the entire course of my project.

Jas Raj Subba

### **Relevant of the Research Work to Thailand**

The main purpose of this Doctoral thesis in Analytical Chemistry is to make use of active and passive sampling technique for monitoring of air pollutants from an ambient air. This thesis is based on monitoring of volatile organic compounds (VOCs) like benzene, toluene and xylene (BTX) in Hat Yai city using the laboratory-built printed circuit board (PCB) passive sampler and analysed by using thermal desorption system coupled with gas chromatograph with flame ionization detector (GC-FID). The second part of this thesis describes about the use of standard colorimetric method for the determination of sulfur dioxide (SO<sub>2</sub>) and nitrogen dioxide (NO<sub>2</sub>) from the ambient air. For which the portable active sampler was modified, validated and used for sampling of sulfur dioxide and nitrogen dioxide from an industrial area of Bhutan. These methods can be applied for monitoring of VOCs, SO<sub>2</sub> and NO<sub>2</sub> in all parts of Thailand. Therefore it is particularly useful for the Ministry of Public Health, the Ministry of Environment and Natural Resources and the Ministry of Industry and Ministry of Education.

**Contents**

	<b>Page</b>
List of Tables	xvi
List of figures	xix
CHAPTER 1 : Introduction	1
1.1 Background and Rationale	1
1.2 Objectives of the research	2
1.2.1 Sampling of BTX in Hat Yai City using a cost effective laboratory- built PCB passive sampler	3
1.2.2 Distribution of SO <sub>2</sub> and NO <sub>2</sub> in the lower atmosphere in an industrial area of Bhutan	3
1.3 Benefits	3
CHAPTER 2: Air Sampling Techniques	4
2.1 Introduction	4
2.2 Whole-air collection techniques	5
2.2.1 Canisters	5
2.2.2 Tedlar bag	8
2.2.3 Impinger sampling	10
2.3 Sorbent Sampling	11
2.3.1 Active Sampling	12
2.3.2 Passive Sampling	15
2.3.2.1 Tube-type passive sampler	17

**Contents (Continued)**

	<b>Page</b>
2.3.2.2 Badge-type passive sampler	18
2.3.2.3 Radial diffusive samplers	19
2.3.3 Solid Phase Microextraction (SPME)	21
2.3.4 Desorption techniques	26
2.3.4.1 Solvent extraction	27
2.3.4.2 Thermal desorption	28
2.3.5 Chemisorption	28
2.3.6 Quality assurance for air sampling	29
CHAPTER 3: Analytical technique for air pollutants determination	30
3.1 Introduction	30
3.2 Analytical method for air pollutants BTX	30
3.2.1 Gas Chromatography (GC)	31
3.2.2 Chemical sensor	33
3.3 Analytical method for SO <sub>2</sub> and NO <sub>2</sub>	35
3.3.1 Spectrophotometry	35
3.3.2 Chemiluminescence	39
3.3.3 Ion-Exchange Chromatography	41
CHAPTER 4: Sampling of BTX in Hat Yai city using cost effective laboratory- built PCB passive sampler	43

**Contents (Continued)**

	<b>Page</b>
4.1 Introduction	43
4.2 Experimental	45
4.2.1 Apparatus and reagents	45
4.2.2 Gas chromatographic system	46
4.2.3 Methodology	46
4.2.4 Optimization of GC-FID conditions	47
4.2.4.1 Carrier gas (N <sub>2</sub> ) flow rate	47
4.2.4.2 Make up gas (N <sub>2</sub> ) flow rate	48
4.2.4.3 Fuel gas (H <sub>2</sub> ) and oxidant gas (air) flow rate	48
4.2.4.4 Injector temperature	48
4.2.4.5 Detector temperature	49
4.2.4.6 Column temperature programming	49
4.2.5 Analytical performance of the GC-FID	50
4.2.5.1 Linear dynamic range of the GC-FID	50
4.2.5.2 Limit of detection (LOD) and limit of quantification (LOQ) of GC-FID	52
4.2.6 Re-development of the printed circuit board (PCB) passive sampler	53
4.2.7 Validation of the PCB passive sampler	53
4.2.8 Analytical performance of the system	56
4.2.8.1 Sampling time	57

**Content (continued)**

	<b>Page</b>
4.2.9 Sampling sites	58
4.3 Results and Discussion	59
4.3.1 Optimization of GC-FID conditions	59
4.3.1.1 Carrier gas (N <sub>2</sub> ) flow rate	60
4.3.1.2 Make up gas (N <sub>2</sub> ) flow rate	64
4.3.1.3 Fuel gas (H <sub>2</sub> ) and oxidant gas (air) flow rates	65
4.3.1.4 Detector temperature	68
4.3.1.5 Injector temperature	70
4.3.1.6 Column temperature programming	71
4.3.1.6.1 Initial column temperature	72
4.3.1.6.2 Initial column holding time	73
4.3.1.6.3 Temperature ramp rate	75
4.3.1.6.4 Final column temperature	76
4.3.1.6.5 Final column holding time	78
4.3.1.7 Summary of GC-FID optimum conditions	80
4.3.2 Analytical performance of the GC-FID	81
4.3.2.1 Linear dynamic range of the GC-FID	81
4.3.2.2 Limit of detection (LOD) and limit of quantification (LOQ)	84
4.3.3 Re-development of the printed circuit board (PCB) passive sampler	86

**Content (continued)**

	<b>Page</b>
4.3.4 Optimization of the thermal desorption and on-line micro-preconcentrator system	87
4.3.4.1 The desorption temperature of the laboratory-built thermal desorption system	87
4.3.4.2 The desorption time of the laboratory-built thermal desorption system	89
4.3.4.3 Adsorption time of the on-line micro-preconcentrator	90
4.3.4.4 Heating potential of on-line micro-preconcentrator	92
4.3.4.5 Heating time of the on-line micro-preconcentrator	93
4.3.4.6 Analytical performance of the system	95
4.3.4.7 Sampling time	98
4.3.4.8 Application of the PCB passive samplers	99
4.3.4.9 Concentration of BTX in Hat Yai city	100
4.3.4.10 Conclusion	103
CHAPTER 5: Distribution of SO <sub>2</sub> and NO <sub>2</sub> in the lower atmosphere in an industrial area of Bhutan	105
5.1 Introduction	105
5.2 Experimental	107
5.2.1 Apparatus and reagents	107
5.2.2 Methodology	108

**Content (continued)**

	<b>Page</b>
5.2.2.1 Standard colorimetric method for SO <sub>2</sub> (West-Gaeke method)	108
5.2.2.1.1 Principle of the West and Gaeke method	109
5.2.2.2 Colorimetric method for determination of NO <sub>2</sub> (Saltzman method)	110
5.2.2.2.1 Principle of Saltzman method	110
5.2.3 Preparation of various absorbing solutions and standard solutions	111
5.2.3.1 Trapping solutions for SO <sub>2</sub>	111
5.2.3.2 Trapping solution for NO <sub>2</sub>	112
5.2.3.3 Preparation of standard sulfite solution	112
5.2.3.4 Preparation of standard nitrite solution	112
5.2.4 Sampling train for active sampling	113
5.2.4.1 Analytical performance and method validation	116
5.2.4.1.1 Linearity, limit of detection (LOD) and limit of quantitation (LOQ)	116
5.2.4.1.2 Precision	117
5.2.4.1.3 Calibration of liquid standard and gas standard	117
5.2.4.1.4 Flow rate and sampling time	118
5.2.5 Sampling sites	118
5.2.6 Calculation of ambient concentration of SO <sub>2</sub> and NO <sub>2</sub>	120
5.2.7 Results and discussion	122
5.2.7.1 Analytical performance of the system	122

**Content (continued)**

	<b>Page</b>
5.2.7.1.1 Linear dynamic range (LDR), limit of detection (LOD) and limit of quantification (LOQ)	122
5.2.7.2 Precision	123
5.2.7.3 Calibration of liquid and gas standards	124
5.2.7.4 Flow rate and sampling time	125
5.2.7.5 Sampling result	125
5.2.8 Conclusion	129
CHAPTER 6 : Conclusion	130
References	132
Vitae	150

### List of Tables

<b>Tables</b>		<b>Page</b>
2.1	Advantages and disadvantages of the whole-air sampling by using canister	8
2.2	Advantages and disadvantages of active sampling	14
2.3	Active sampling for organic compounds in air samples	15
2.4	Advantages and disadvantages of passive sampling	20
2.5	Examples and applications of commercially available SPME fibers	25
2.6	Advantages and disadvantages of SPME	26
3.1	Application of metal oxides gas sensor for detection of BTX	34
4.1	Optimization parameters for column program temperature of GC-FID	49
4.2	The HETP calculated from the chromatograms obtained from the analysis of 5.0 ppm of BTX standard gases at various carrier gas flow rate (n = 5)	63
4.3	Peak area of 5.0 ppm of BTX at various make up gas flow rate (n = 5)	64
4.4	Peak area of 5.0 ppm of BTX at various flow rates of fuel (H <sub>2</sub> ) and oxidant(air) gas (n= 5)	66
4.5	Peak area of 5.0 ppm of BTX at various detector temperature (n = 5)	69
4.6	Peak area of 5.0 ppm of BTX at various injector temperature (n = 5)	70
4.7	Peak area of 5.0 ppm of BTX at various initial column temperature (n = 5)	72
4.8	Peak area of 5.0 ppm of BTX at various initial column holding time (n = 5)	74
4.9	Peak area of 5.0 ppm of BTX at various temperature ramp rate (n = 5)	75

**List of Tables (continued)**

<b>Tables</b>	<b>Page</b>
4.10 Peak area of 5.0 ppm of BTX at various final column temperature (n = 5)	77
4.11 Peak area of 5.0 ppm of BTX at various final column holding time (n = 5)	78
4.12 Summary of optimum GC-FID conditions for the determination of 5.0 ppm BTX standard gas	80
4.13 The peak area of 20 blank injections at optimum GC-FID conditions	85
4.14 LOD and LOQ of the GC-FID for BTX detection	86
4.15 Peak area of 1.0 ppm BTX at various desorption temperature of the laboratory- built thermal desorption system (n = 5)	88
4.16 Peak area of 1.0 ppm BTX at various desorption time of the laboratory- built thermal desorption system (n = 5)	89
4.17 Peak area of 1.0 ppm BTX at various adsorption time of the on-line micro- preconcentrator (n = 5)	91
4.18 Peak area of 1.0 ppm BTX at various heating potential of the on-line micro- preconcentrator (n = 5)	92
4.19 Peak area of 1.0 ppm BTX at various heating time of the on-line micro- preconcentrator (n = 5)	94
4.20 Optimum conditions of the laboratory-built thermal desorption and on-line micro-preconcentrator system	95
4.21 LOD and LOQ of BTX under optimum conditions of thermal desorption system and on-line micro-preconcentrator coupled with GC-FID	98

**List of Tables (continued)**

<b>Tables</b>	<b>Page</b>
5.1 LOD an LOQ of SO <sub>2</sub> and NO <sub>2</sub>	123
5.2 Intraday and interday precision for SO <sub>2</sub> (n = 5)	123
5.3 Intraday and interday precision for NO <sub>2</sub> (n = 5)	124
5.4 Table showing the accuracy of absorbance of SO <sub>2</sub> and NO <sub>2</sub> liquid standard and gas standard (n = 5)	125

## List of Figures

Figures	Page
2.1 Examples of different configurations used in a systems for trapping VOCs in ambient air collected in canisters. (a) the established U.S.EPA TO14 method (U.S. EPA, 1999b), (b) method used by Chang <i>et al.</i> , (2003) (Chang et al., 2003) (c) method used by Tolnai <i>et al.</i> , (2000) (Tolnai et al., 2000) and (d) method used by Mangani <i>et al.</i> , (2003) (Mangani et al., 2003).	7
2.2 Tedlar bag ( <a href="http://www.keikaventures.com/s_tedlar.php">http://www.keikaventures.com/s_tedlar.php</a> )	9
2.3 Schematic diagram showing sampling of air using midjet impingers	11
2.4 Single-bed tube for active sampling (Sigma-Aldrich)	13
2.5 Multi-adsorbent tubes for active sampling (Sigma-Aldrich)	14
2.6 Examples of tube-type passive sampler (A) tube-type (Gibson et al., 1997) (B) Orsa 5 ( <a href="http://www.laborbedarf-kohl.de">http://www.laborbedarf-kohl.de</a> )	17
2.7 Badge-type passive sampler (A) Passive sampler (Zhou and Smith, 1997) (B) Badge-type ( <a href="http://www.skcinc.com/catalog/index.php">http://www.skcinc.com/catalog/index.php</a> )	18
2.8 Schematic diagram of a radial diffusive sampler (A) radial diffusive sampler (Woolfenden, 2010) (B) Radiello diffusive sampler (Carrieri et al., 2014).	20
2.9 Commercial SPME device made by Supelco (Kataoka et al., 2000)	21
2.10 Modes of SPME operation: (A) direct extraction (B) Headspace SPME (C) membrane-protected SPME (Pawliszyn, 2012)	23
3.1 Schematic diagram of a typical gas chromatograph	33

**List of figures (continued)**

<b>Figures</b>	<b>Page</b>
3.2 Reaction mechanism of SO <sub>2</sub> with methyl red in excess of Br <sub>2</sub> (Geetha and Balasubramanian, 2000)	36
3.3 Reaction mechanism of iodine monochloride with SO <sub>2</sub> (Kumar et al., 2006)	37
3.4 Reaction mechanism of SO <sub>2</sub> in presence of formaldehyde and pararosaniline	38
3.5 Reaction mechanism of NO <sub>2</sub> with N-1-naphthylethylenediamine dihydrochloride (Tanaka et al., 1998)	39
3.6 Chemiluminescence detector for NO <sub>x</sub>	40
3.7 Schematic diagram of Ion-exchange chromatography system	42
4.1 The y-residuals of a regression line (Miller and Miller, 2005)	51
4.2 Schematic diagram of the laboratory-built thermal desorption system coupled with on-line micro-preconcentrator	54
4.3 Hanging of PCB passive sampler	57
4.4 Map showing the locations of sampling sites (S1 to S16)	59
4.5 The van Deemter plot	60
4.6 The van Deemter plots of BTX at 5.0 ppm (n = 5)	63
4.7 Effect of the make-up gas flow rate on the peak area of 5.0 ppm BTX (n = 5)	65
4.8 Effect of the fuel and oxidant gas flow rate on the peak area of 5.0 ppm benzene (n = 5)	67

**List of Figures (continued)**

<b>Figures</b>	<b>Page</b>
4.9 Effect of the fuel and oxidant gas flow rate on the peak area of 5.0 ppm toluene (n = 5)	67
4.10 Effect of the fuel and oxidant gas flow rate on the peak area of 5.0 ppm xylene (n = 5)	68
4.11 Effect of the detector temperatures on the peak areas of 5.0 ppm BTX standard gas (n = 5)	69
4.12 Effect of the injector temperatures on the peak areas of 5.0 ppm BTX standard gas (n = 5)	71
4.13 Effect of the initial column temperatures on the peak areas of 5.0 ppm of BTX standard gas (n = 5)	73
4.14 Effect of the initial column holding time on the peak areas of 5.0 ppm of BTX standard gas (n = 5)	74
4.15 Effect of the temperature ramp rate on the peak areas of 5.0 ppm of BTX standard gas (n = 5)	76
4.16 Effect of the final column temperature on the peak areas of 5.0 ppm of BTX standard gas (n = 5)	77
4.17 Effect of the final column holding time on the peak areas of 5.0 ppm of BTX standard gas (n = 5)	79
4.18 Optimum column temperature programming for the analysis of BTX	79
4.19 Chromatogram of BTX 5.0 ppm at optimum GC-FID conditions	81

**List of Figures (continued)**

<b>Figures</b>	<b>Page</b>
4.20 Linear dynamic range of GC-FID for the determination of benzene	82
4.21 Linear dynamic range of GC-FID for the determination of toluene	83
4.22 Linear dynamic range of GC-FID for the determination of xylene	83
4.23 Schematic diagram showing the development of PCB passive sampler	86
4.24 Effect of the desorption temperature of the laboratory-built thermal desorption system on the peak area of 1.0 ppm BTX gas (n = 5)	88
4.25 Effect of the desorption time of the laboratory-built thermal desorption system on the peak area of 1.0 ppm BTX gas (n = 5)	90
4.26 Effect of the adsorption time of the on-line micro-preconcentrator on the peak area of 1.0 ppm BTX gas (n = 5)	91
4.27 Effect of heating potential of the on-line micro-preconcentrator on the peak area of 1.0 ppm BTX gas (n = 5)	93
4.28 Effect of heating time of the on-line micro-preconcentrator on the peak area of 1.0 ppm BTX gas (n = 5)	94
4.29 Linear dynamic range of benzene at various mass uptake on the PCB passive sampler after desorption using the thermal desorption system coupled with the on-line micro-preconcentrator and GC-FID system	96
4.30 Linear dynamic range of toluene at various mass uptake on the PCB passive sampler after desorption using the thermal desorption system coupled with the on-line micro-preconcentrator and GC-FID system	97

**List of Figures (continued)**

<b>Figures</b>	<b>Page</b>
4.31 Linear dynamic range of xylene at various mass uptake on the PCB passive sampler after desorption using the thermal desorption system coupled with the on-line micro-preconcentrator and GC-FID system	97
4.32 The amount of BTX ( $\mu\text{g}$ ) adsorbed on to the PCB passive sampler for various exposure time	99
4.33 Concentrations of BTX at different sampling sites in	101
5.1 Reaction mechanism of West and Gaeke method for determination of $\text{SO}_2$	109
5.2 Reaction mechanism for Saltzman method of determination of $\text{NO}_2$	110
5.3 Schematic diagram of active sampler assembled in the laboratory	113
5.4 Map showing the industrial area of Bhutan and sampling stations	120
5.5 Linear plot of $\text{SO}_2$ in the concentration range of 0.05-1.0 ppm ( $n = 5$ )	122
5.6 Linear plot of $\text{NO}_2$ in the concentration range of 0.05-1.0 ppm ( $n = 5$ )	122
5.7 Histogram showing the ambient concentration of $\text{SO}_2$ and $\text{NO}_2$ in morning afternoon, evening and average at different sampling stations with distance in km.	126

## CHAPTER 1

### Introduction

#### 1.1 Background and Rationale

Air quality has become a very important concern for everyone and every country. Research has shown that polluted air highly impacts the environment and overall health of living beings. Therefore, clean air is so vital in promoting a healthy life span of flora and fauna. In spite of this fact, very little attention is given to the effect of anthropogenic activities on the quality of ambient air in many mega cities (Kirchner et al., 2005). With the rapid increase in human population, there is a huge demand for increased housing, expanded industrial infrastructure, and additional transportation. If these activities are poorly managed, it will lead to a range of environmental problems, such as; degradation of indoor and outdoor air quality (Ng et al., 2005), as well as, increased respiratory health problems of children (Franklin, 2007). The deterioration of outdoor air quality is brought about by air pollution that mainly results from increased vehicle emissions (Beckerman et al., 2008; Škarek et al., 2007) and higher levels of industrial pollutants in the atmosphere (Singer et al., 2004) that comes with industrialization and urbanization (Bell et al., 2006; Sivacoumar et al., 2001).

Air pollutions are classified into primary and secondary pollutants. Those that are directly released into the ambient air from sources like factories, exhaust gases from vehicles, smokes from firewood or cigarette are classified as primary air pollutants (Cavalcante et al., 2006; Lü et al., 2010), while secondary air pollutants are formed from the interaction of primary air pollutants. Examples of primary air pollutants are volatile organic compounds (VOCs), persistent organic compounds (POPs), and SO<sub>2</sub>. There are also some pollutants which are both primary and secondary. Nitrogen dioxide (NO<sub>2</sub>) fall into this latter category. Acid rain has been already recognized as a major regional scale problem in many countries and NO<sub>x</sub> and SO<sub>2</sub> is the major contributor of acid rain in China

(Meng et al., 2008). As a result, it has great impact on forest and natural water ecosystems, in addition to building erosion. Due to the adverse health effects on humans of these pollutants they should be monitored on regular basis (Billionnet et al., 2011; Ciarrocca et al., 2011; Lupo et al., 2011; Llop et al., 2010; Liu et al., 2012; Lei and Wuebbles 2013).

The global scale analysis of data on air pollution shows that the quality and availability of information is highly diverse. In Europe, air quality is regulated by the directive of the European Union 2008/50/EC, which commits the member states to monitor and report periodically about the status of air pollutions to the European Commission (Barrero et al., 2015). Whereas in many other parts of the world measurements of air pollutions are irregularly conducted or not at all. The reason may be because modern air pollution monitoring equipment is very sophisticated, expensive and requires highly skilled operators. Therefore, suitable analytical methods are still continuing being developed and applied for the monitoring of air pollutants with the aim of protecting human health and environment in general. Two groups of air pollutants *i.e.* benzene, toluene, and xylene (BTX) which are VOCs and SO<sub>2</sub> and nitrogen dioxide (NO<sub>2</sub>) are being focused in this thesis.

## **1.2 Objectives of the research**

The aims of this research are to re-develop and re-validate the printed circuit board (PCB) passive sampler and apply for the monitoring of ambient VOCs air pollutants benzene, toluene and xylene (BTX) in outdoor ambient air and to monitor SO<sub>2</sub> and NO<sub>2</sub> in an industrial area of Bhutan using simple colorimetric methods to set-up a baseline data. In order to achieve these objectives two projects were carried out as follows;

### **1.2.1 Sampling of BTX in Hat Yai city using a cost effective laboratory-built PCB passive sampler**

In this project, a PCB passive sampler which was developed and validated for the monitoring of styrene and xylene in copy print shops (Saelim et al., 2013) has been re-developed and re-validated for the monitoring of BTX in outdoor ambient air in Hat Yai city of Thailand.

### **1.2.2 Distributions of SO<sub>2</sub> and NO<sub>2</sub> in the lower atmosphere in an industrial area of Bhutan**

In this work, standard colorimetric methods (West and Gaeke, 1956, Saltzman 1949) were used for monitoring of SO<sub>2</sub> and NO<sub>2</sub> in an industrial area of Bhutan. The sampling is based on the collection of ambient air directly into the absorbing solutions and measuring the absorbance of the colour developed directly using a portable spectrophotometer.

### **1.3 Benefits**

It is expected that the easy to prepare, low cost, and portable PCB passive sampler can be effectively used for the monitoring of VOCs in an ambient outdoor air. Through the monitoring of BTX in Hat Yai city their concentrations can be compared with other big cities in the world. For the monitoring of SO<sub>2</sub> and NO<sub>2</sub> using colorimetric methods which are cost effective, simple and portable, this will be the first baseline data of these two pollutants in an industrial area of Bhutan.

## CHAPTER 2

### Air Sampling Techniques

#### 2.1 Introduction

Air sampling is done mainly to identify the target analyte, characterize the chemical exposure, as well as estimate and evaluate the exposure. Information obtain is vital in making key decisions about risk and hazard assessment, public health, and biological monitoring. One of the important reason to monitor air borne chemical exposure is to help in preventing potential damage that the exposure might impart to humans (Kennedy, 2010).

Since, sampling of air is very crucial in any monitoring process, care should be taken especially with sampling volume and the analytical technique used. While sampling air, it must be noted that the sampling volume and the sensitivity of analytical method should be compatible, and the sampling process must be carefully considered (Zielinska and Fujita, 1994). Besides this, one should consider the trace levels of pollutants in the atmosphere. If pollutants are present in trace levels, an enrichment method is often required in order to obtain acceptable limits of detection (LOD) (Ras et al., 2009). In any analytical procedure, sampling is usually the most important step. Any errors made in this step cannot be corrected later in the process of analysis.

The sampling of air from the atmosphere have various procedures, which are either pre-concentration on sorbent tube or whole air sample taken in canister (Kumar and Viden, 2007). Furthermore, air can be sampled directly into absorbing solutions called impinger sampling.

## **2.2 Whole-air collection techniques**

Whole-air collection techniques involve collection of air into a container and is one of the simplest way to collect air. Collection of whole-air can be either be active (requires pump) or passive (no pump required). The samples collected are usually carried to a laboratory for further analysis by gas chromatography (GC) by injecting them directly or by injecting them into the GC only after pre-concentration step (Ras et al., 2009). For whole-air collection several types of containers can be used like gas-tight syringes, glass bulbs, bags, or metal containers. However, plastics bags and stainless-steel containers are usually the most widely used (Wang and Austin, 2006).

### **2.2.1 Canisters**

Whole-air collection using canisters was first used in the USA in the 1980s, when the Environmental Protection Agency (EPA) adopted and evaluated the canister method (TO-14 and TO-14A) targeting 40 nonpolar VOCs (Król et al., 2010). This air sampling method provides an alternative to techniques based on sorbent-bed adsorption. Both polar and nonpolar compounds in trace levels in ambient air can be collected using canister (Wang and Austin, 2006). The internal surface of the canister is usually treated with a pure chrome-nickel oxide layer or by chemically bonding a thin fused-silica layer to the stainless steel surface. And prior to use, the canister must be carefully cleaned and evacuated in order to avoid any contamination (Kumar and Viden, 2007).

Sampling of air using canister is performed in two modes, that is grab sampling or time integrated sampling. Samples can be collected with sub-atmospheric pressure conditions (passive) or pressurized condition with pump (active) (Ras et al., 2009). Collection of air in a canister using pump allows the sample to be pressurized and the collection of larger sample volumes. If the gas volumes collected exceeds the canister

volume, than forced flow at high pressure has to be applied. This does not directly affect the degree of enrichment of the air components (Skov et al., 2001). If large volume of air need to be collected, it may take 30-40 hour to several days to fill a canister (Król et al., 2010). While collecting sample into the canister as whole-air sampling care must be taken with regard to air matrix like the water from the humidity in ambient air. Research have shown that moisture content plays a crucial role in recoveries of polar and non-polar VOCs from canisters. It was found that several VOCs stored in dry canisters showed decreased in concentration due to lack of moisture, which is essential to cover the active sites on the interior surface of the canister, preventing from physical adsorption or chemical interaction. And in presence of high moisture content, there was dissolution of target analytes in condensed water (Kumar and Viden, 2007). The moisture content from the gas streams can be removed by using desiccants (Zou et al., 2003), adsorbents (Rao et al., 2007), cryocondensation (Chang et al., 2005; Heo et al., 2001) and permeation (Mangani et al., 2003).

After the whole-air sampling using a canister, depending on the target analyte and on the detector sensitivity preliminary enrichment may have to be done before the chromatographic analysis. Usually such enrichment can be carried out using a sorbent or a cryogenic trap filled with glass beads (Chiu et al., 2005). Figure 2.1 shows different configurations for trapping VOCs in ambient air collected in canister before analysis by gas chromatography. Table 2.1 shows the summary of advantages and disadvantages of whole-air sampling by using a canister.

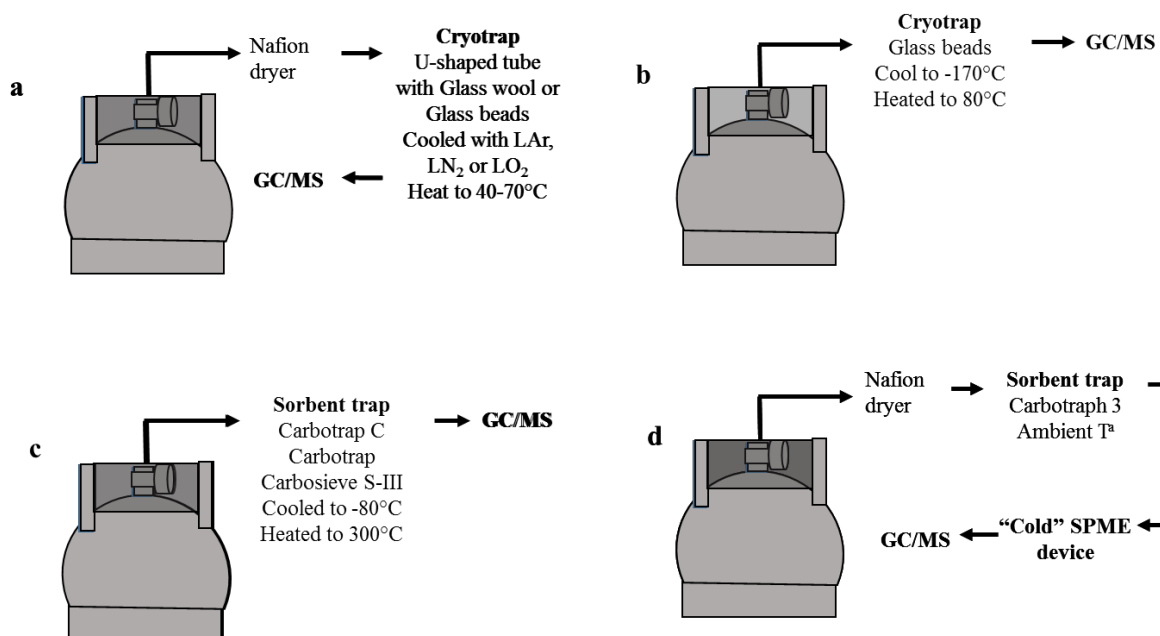


**Figure 2.1** Examples of different configurations used in a systems for trapping VOCs in ambient air collected in canisters. (a) the established U.S.EPA TO14 method (U. S. EPA, 1999), (b) method used by Chang *et al.*, (2003) (Chang et al., 2003) (c) method used by Tolnai *et al.*, (2000) (Tolnai et al., 2000) and (d) method used by Mangani *et al.*, (2003) (Mangani et al., 2003).

**Table 2.1** Advantages and disadvantages of the whole-air sampling by using canister

<b>Advantages</b>	<b>Disadvantages</b>
<ul style="list-style-type: none"> <li>• Air sample is collected without any breakthrough</li> <li>• No degradation problem of trapping material</li> <li>• Moisture has no effect upon sampling</li> <li>• Analysis can be done many times</li> </ul>	<ul style="list-style-type: none"> <li>• Complex sampling apparatus</li> <li>• Hard to clean up the apparatus</li> <li>• Flow rate tends to fluctuate especially at the end of sampling</li> <li>• Because of the presence of reactive species, loss of target analyte may occur</li> </ul>

### 2.2.2 Tedlar bag

Collection of whole-air sampling can be done using plastics bags such as Tedlar, Teflon or aluminized Tedlar. The name Tedlar is a trade name for a polyvinyl fluoride film developed by DuPont Corporation in the 1960's (Eurofins Air Toxics, 2014) and is widely used in a variety of applications, both in industrial hygiene and environmental. Tedlar bags are simple to use, inexpensive and available in various sizes, normally from 500 mL to 100L. And they can be reused after cleaning by repeatedly filling them with pure nitrogen or ultrahigh-purity air (Król et al., 2010; Ras et al., 2009). The use of Tedlar bags for air sampling are recommended by the European Environment Agency (EPA) and United State Environmental Protection Agency (U.S. EPA). Tedlar bags may be used to collect samples containing common solvents, hydrocarbons, chlorinated solvents, sulfur compounds, atmospheric and biogenic gases and many other classes of compounds. Compounds with low vapor pressures such as Naphthalene are not appropriate for Tedlar bags as recovery is very low even under short sample storage

times. Low molecular compounds such as Helium and Hydrogen can diffuse through the Tedlar bag material resulting in poor storage stability (Eurofins air toxics, 2014). Figure 2.2 shows the typical Tedlar bag air sampling device.



**Figure 2.2** Tedlar bag

([http://www.keikaventures.com/s\\_tedlar.php](http://www.keikaventures.com/s_tedlar.php))

Some of the advantages of using Tedlar bag for air sampling are, they are cheap and can be used for different volumes of collection. Tedlar bag can be reused again after cleaning them with high purity nitrogen gas (Król et al., 2010). However, there are some disadvantages of using Tedlar bag like contamination levels is these bags are substantial due to outgassing of the container material. Some of the Tedlar bags are permeable to certain chemicals and have been observed to lose significant amount of sample when stored for prolonged periods (Beauchamp et al., 2008). Tedlar bags also shows memory effect from previous sample collections. Beside this, collecting samples in a bag requires an air sample to be pumped in, which may add up a potential source of contamination. Humidity condition during storage can affect the degradation constant of

sampled compounds, high relative humidity provide higher stability than low relative humidity (Hsieh et al., 2003). To limit the impact of humidity a double-layer Tedlar bag with a drying agent between the two films could be employed (Cariou and Guillot, 2006).

### **2.2.3 Impinger sampling**

The first impinger was created by Greenburg Smith impinger in 1922 (Marple, 2004). Since then, impingers have been successfully used for aerosol sampling (Dart and Thornburg, 2008). Although impingers was traditionally used for sampling of micron-sized particles, these days researchers have begun to investigate the use of impingers to collect fine and ultrafine particles, including viruses (Hogan Jr et al., 2005). Miljevic et al. (2009), worked on determination and collection efficiency of an SKC special midget impinger with fritted nozzle (170  $\mu\text{m}$ ) and in-house designed impingers with frit porosity grade 1 (100-160  $\mu\text{m}$ ) and 2 (40-100  $\mu\text{m}$ ) (Miljevic et al., 2009). Impingers were successfully used for the sampling and analysis of various air pollutants like  $\text{SO}_2$  (West and Gaeke, 1956) and  $\text{NO}_2$  (Saltzman, 1949). Figure 2.3 shows the schematic diagram of sampling with midget impingers.

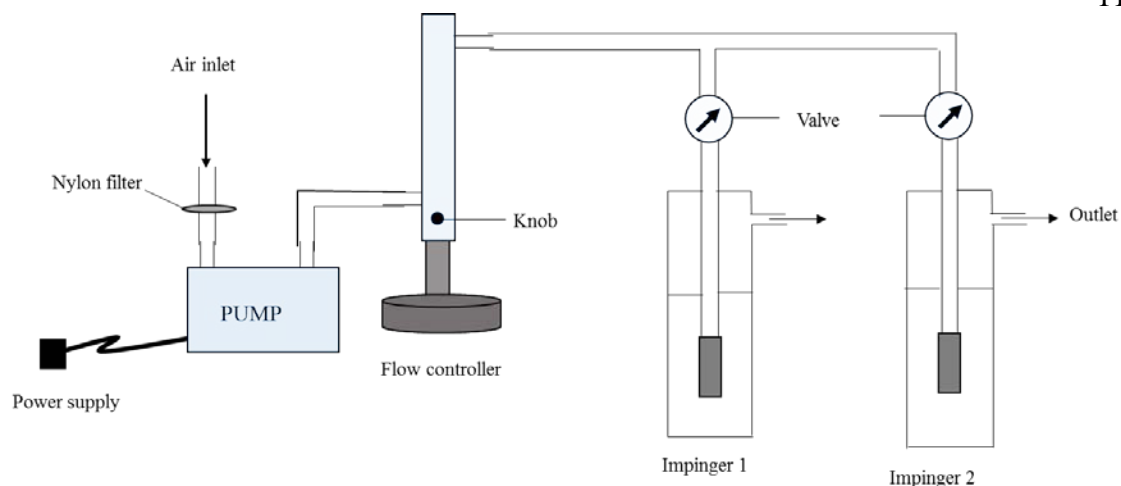


**Figure 2.3** Schematic diagram showing sampling of air using midget impingers

### 2.3 Sorbent Sampling

Sampling on sorbents is comparatively easier than canister sampling. In fact adsorptive enrichment on solid sorbents is a technique often used to combine preconcentration with sampling, either by an active or passive sampling (Demeestere et al., 2007). For sorbent sampling, one of the important criteria is the selection of suitable adsorbent as it depends on the sample matrix and on the compound to be collected. Beside this, the quantity of the substance which can be captured on the adsorbent depends on the ambient conditions like temperature, pressure, concentration, humidity, amount of sorbent and sampling speed (Kumar and Viden, 2007). While selecting a suitable sorbent one need to consider following criteria to be considered like, the break-through of the analytes has to be avoided, usually combination of more than one adsorbent can overcome this problem (Harper, 2000). Another criteria to be considered is about the degradation problem of some adsorbents, Carbotrap B, Carbotrap C and Carbosieve SIII are the most resistant adsorbents to degradation while Tenax TA and Tenax GC are reported to form artifacts (Helmig and Greenberg, 1994). One should avoid contamination of sorbents before and after sampling.

Build-up of contaminants on the sorbents during storage was also reported (Helmig, 1996). Retention of moisture content on sorbents must be avoided as it may pose undesirable effects on chromatographic analysis. Moisture content may cause degradation of chromatographic column (Kumar and Viden, 2007).

### 2.3.1 Active Sampling

Active sampling generally make use of a pump which will pump the air sample into the solid sorbents or an adsorbing solution. If air sample is pumped into the solid adsorbent, the compounds of interest gets adsorbed by the sorbent in the tube and is returned to the laboratory for analysis, giving a result as a “mass per tube”. The “mass per tube” is then divided by the volume of air to give final ambient concentration of air in microgram per cubic meter. In active sampling, flow rates can vary in the range of 10-1000 mL/min, collecting sample volumes of 0.1-150 L (Kumar and Viden, 2007).

There are sampling tubes filled with only one type of adsorbent or with multi-sorbent based on target analytes (Figure 2.4). For example, tubes filled with only one sorbent have been used effectively to monitor some VOCs in ambient air (Marlet and Lognay, 2010). Tubes filled with Chromosorb 106 was used for trapping VOCs in indoor air (Srivastava and Devotta, 2007) and tubes filled with Anasorb CSC were used for trapping VOCs in ambient air (Gariazzo et al., 2005). But if analytes of broad volatility range need to be determined, then it is often useful to select more than one adsorbent and to arrange them in order of increasing adsorbents strength weakest to strongest adsorbent (Figure 2.5) (Kuntasal et al., 2005; Ras-Mallorquí et al., 2007). The different adsorbents can either be placed in a single sample tube separated using steel gauze or glass wool plugs or in separate tubes linked together with inert couplings. In either case, the adsorbents should be arranged in succession of increasing adsorbent strength (TO-17, 1999). Adsorbents may also be used by cooling down cryogenically to enable the collection of volatile analytes. This helps to maintain sufficient adsorption capacity and reduces the amount of adsorbent (Ras et al., 2009).

The presence of ozone and humidity can interfere in sorbent trapping resulting into significant loss of analyte, especially for reactive, unsaturated compounds. This effect is also influenced by the adsorbent used for sampling, as in the case of Tenax. But if carbon-based adsorbents are used interferences from ozone is minimum (Dettmer and Engewald, 2002). Interference caused by water must be also avoided, it is because water vapour can compete with the analytes for the active points of the adsorbent (Marion et al., 2011). Under wet conditions the pores can be filled with water. Water vapour can condense in the small pores of adsorbent and then this water droplet can either displace adsorbed organic molecules, or react with them or form an immiscible phase (Domeño et al., 2004). Therefore, in order to avoid this, moisture traps are commonly used. For example, while using active coconut charcoal to trap benzene, silica-gel trap is attached to the sampling tube (Rao et al., 2007). Similarly, ambient VOCs can be collected using a moisture trap of calcium chloride attached to sampling tubes filled with activated carbon (Elbir et al., 2007). The advantages and disadvantages of active sampling is summarized in Table 2.2 and the applications of active sampling for organic compounds in air sample are summarized in Table 2.3.

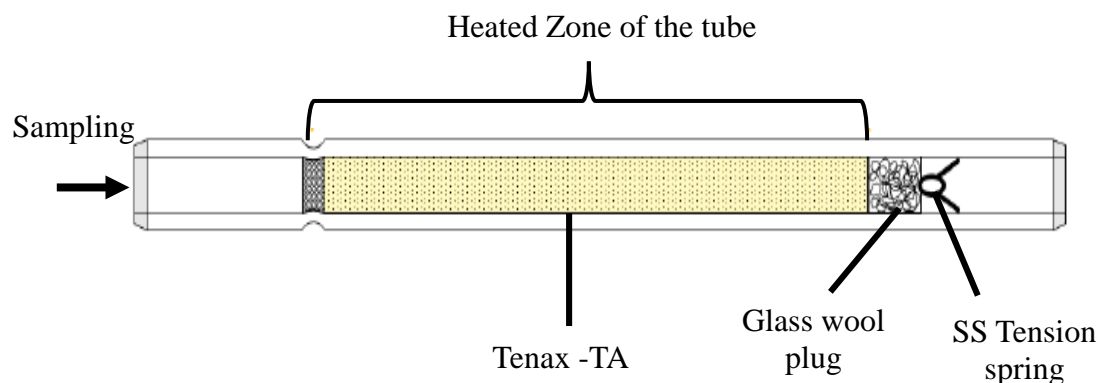


**Figure 2.4** Single-bed tube for active sampling (Sigma-Aldrich)

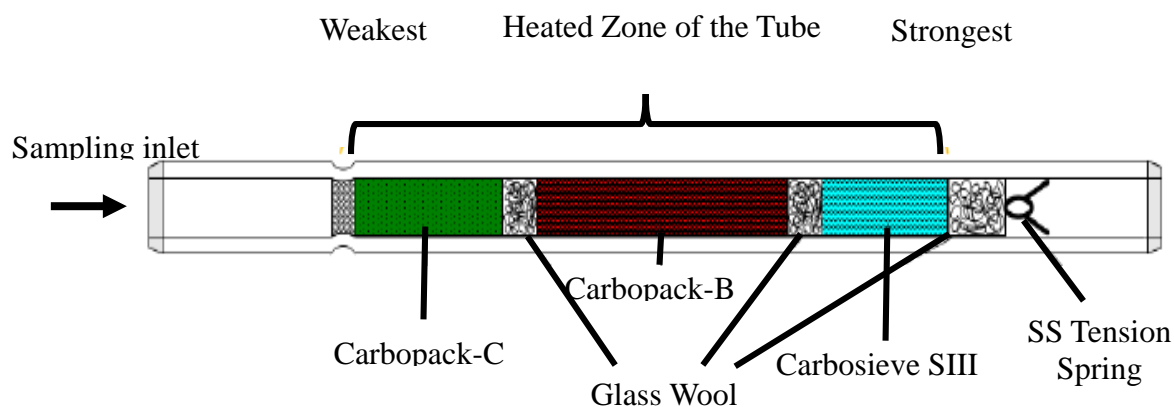


**Figure 2.5** Multi-adsorbent tubes for active sampling (Sigma-Aldrich)

**Table 2.2** Advantages and disadvantages of active sampling

Advantages	Disadvantages
Preconcentration efficiency is very high	Need of pump or electricity and flow-meters
Because of the multi-adsorbant beds, wide range of analytes can be preconcentrated	There is risk of component breakthrough if excessive flow rates are used
Calibration is much easier as compared to passive sampler	Diffusion of analytes introduces significant errors in active sampling
Use of moisture trap can avoid the interference from the moistures	Transport of power equipment (pumps, ventilators) to the sampling site is troublesome
Large-volume of samples can be collected	High cost of a single measurement

**Table 2.3** Active sampling for organic compounds in air samples

Analyte	Adsorbent	Desorption mode	Analysis technique	References
VOCs	Multi-adsorbent tube (Carbotrap, Carbopack X and Carboxen 569)	Thermal desorption	GC-MS	(Gallego et al., 2008)
VOCs	Tenax-TA <sup>TM</sup>	Thermal desorption	GC-MS	(Ongwandee et al., 2011)
Carbonyl compounds	Sep-Pak silica gel cartridge	Solvent desorption	HPLC-UV	(Feng et al., 2004)
Non-methane VOCs	Carbopack-B	Thermal desorption	GC-ECD	(Karbiwnyk et al., 2002)
BTEX	Activated coconut shell charcoal	Solvent desorption	GC-MS	(Martins et al., 2007)

### 2.3.2 Passive Sampling

Passive sampling may be defined as any sampling technique based on free flow of analyte molecules from the sampling medium to a collecting medium, as a result of a difference in concentration of the analyte between the two media (Kumar and Viden, 2007). Net flow of analyte molecules from one medium to the other continues until equilibrium is established in the system or until the sampling session is terminated by the user (Górecki and Namieśnik, 2002). Passive sampling technique has been widely applied for environmental monitoring due to its simplicity, cost effectiveness and portable nature (Bogdal et al., 2013; Kot-Wasik et al., 2007; Sanjuán-Herráez et al., 2014; Vrana et al., 2014). Moreover, passive sampling can be used where there is no electricity, many samples can be collected at the same time (Hazrati and Harrad, 2007; Tao et al., 2008) and for sampling it does not require any trained technical staff (Campos et al., 2010). Passive sampling is particularly suited for the determination of time-weighted average concentrations (Górecki and Namieśnik, 2002).

In passive sampling, the net transport of analyte across the barrier occurs mainly due to analyte molecular diffusion following Fick's law equation 2.1 (Seethapathy et al., 2008)

$$Q = \frac{AD(C_1 - C_0)t}{L} \quad (2.1)$$

Where Q is the uptake amount of the analyte ( $\mu\text{g}$ ), A is the cross section of the diffusion path ( $\text{cm}^2$ ), D is the molecular diffusion coefficient of the analyte ( $\text{cm}^2\text{s}^{-1}$ ),  $C_1$  is the concentration of the analyte adsorbed by the sampler ( $\text{mgm}^{-3}$ ).  $C_0$  is the concentration of the analyte at the surface of the sampler ( $\text{mgm}^{-3}$ ), t is the exposure time (s), and L is the total diffusion length from the membrane to passive sampler (cm).

Passive samplers can have many different forms, depending on the sampling principle and the sampled medium. Gas sampling passive samplers are most widely used. Passive air samplers are manufactured by numerous suppliers of analytical equipment (such as Perkin-Elmer, Draeger, 3M, SKC, and DuPont) (Górecki and Namieśnik, 2002). Passive samplers for air sampling are broadly classified as tube, radial, badge and cartridge-type (Krupa and Legge, 2000) which have substantially different uptake rates, thus suitable for different applications. Badge and radial type provide higher uptake rates since they have shorter diffusion path and larger surface area, thus they are suitable of a short-term monitoring such as personal or occupational exposure (Kot-Wasik et al., 2007) comparatively tube-type samplers have longer axial diffusion path and smaller surface area as a result it provides lower uptake rates and are suitable for long-term monitoring (Kot-Wasik et al., 2007).

### 2.3.2.1 Tube- type passive sampler

Tube-type passive sampler are with a small cross-sectional area and long diffusion length (Figure 2.6). The rate of atmospheric sampling can be finely adjusted, the sampling

rate would be very slow (Król et al., 2010). This type of passive sampler are not very responsive to air movement. The sorbent used in these samplers includes Tenax TA, Chromosorb, Chrompack and GCB. In most cases, adsorbed analytes are released by thermal desorption system (Ras et al., 2009).

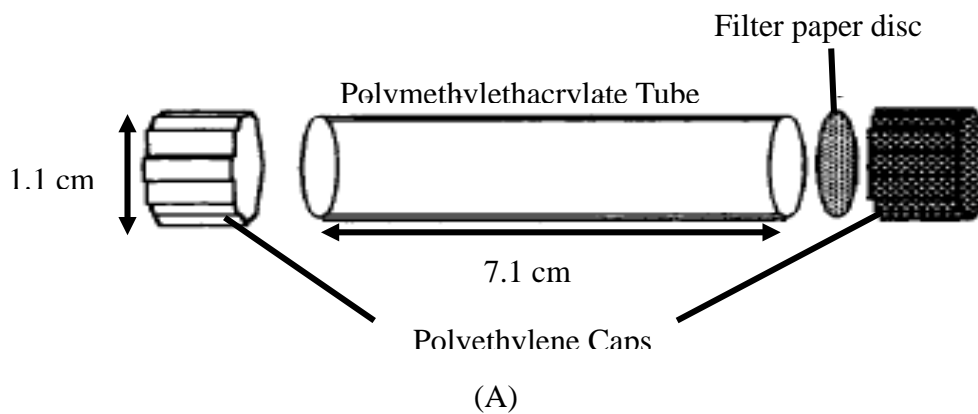
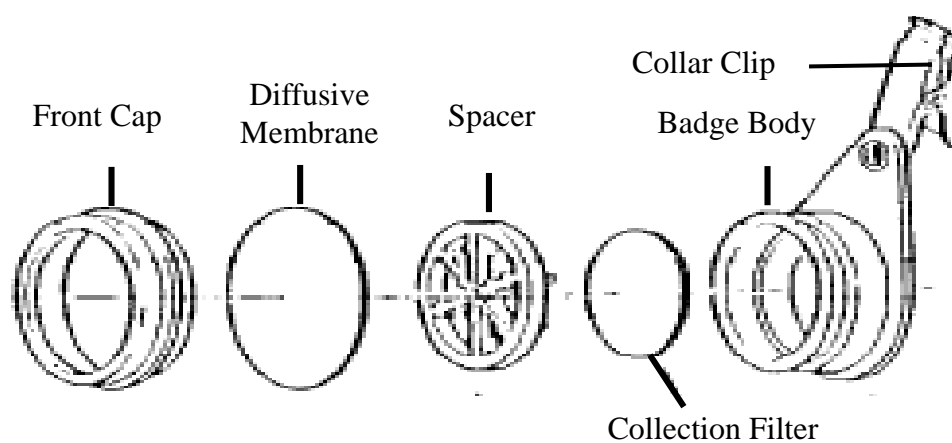


**Figure 2.6** Examples of tube-type passive sampler (A) tube-type (Gibson et al., 1997) (B)

Orsa 5 (<http://www.laborbedarf-kohl.de>)

### 2.3.2.2 Badge-type passive sampler

Badge-type of passive sampler comparatively have higher adsorption rates than tube-type passive samplers, it is because of their shorter diffusion length and more surface areas (Strandberg et al., 2005). Badge-type of sampler is not suitable for thermal desorption but can be easily desorbed by using suitable solvents (Figure 2.7)



(A)



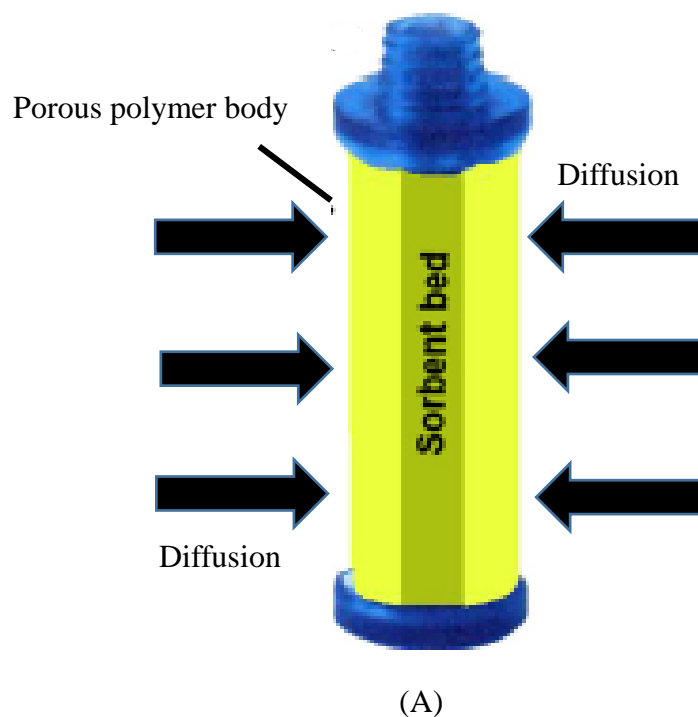
(B)

**Figure 2.7** Badge-type passive sampler (A) Passive sampler (Zhou and Smith, 1997) (B)

Badge-type (<http://www.skinc.com/catalog/index.php>)

### 2.3.2.3 Radial diffusive samplers

Radial diffusive samplers have 100 times more area than the tube-type and the badge-type passive samplers, and short diffusion path. Therefore, overall sampling time using radial passive sampler will be less. Radial passive samplers are commercially available as Radiello (Figure 2.8), which have a diffusion path parallel to the cartridge radius and a greater cross-sectional area, allowing higher uptake rates (Ras et al., 2009). Radiello samplers have been widely evaluated and used for monitoring of various environmental pollutants (Carrieri et al., 2014; Roukos et al., 2011). However, radial diffusive samplers frequently reach sorbent saturation with analytes, with an associated risk of inverse diffusion (Strandberg et al., 2005). After sampling, the cartridge can either be analyzed by using solvent extraction (Plaisance et al., 2007) or alternatively using thermal desorption (Roukos et al., 2011).





(B)

**Figure 2.8** Schematic diagram of a radial diffusive sampler (A) radial diffusive sampler (Woolfeden, 2010) (B) Radiello diffusive sampler (Carrieri et al., 2014)

Advantages and disadvantages of passive sampling is summarized in Table 2.4

**Table 2.4** Advantages and disadvantages of passive sampling

Advantages	Disadvantages
Simple and portable	Not suitable of short-term sampling
More number of samplings can be done at a time simultaneously	Low preconcentration capacity in comparison to active sampling
Low cost	Efficiency influenced by sampler design
Do not require any trained technical staff	Sensitive to temperature and air movement
Useful for long-term sampling	Enrichment factors for each analyte must be determined
No risk factor involved for collector	Problems of contamination more pronounced than those in active sampling

### 2.3.3 Solid Phase Microextraction (SPME)

Solid-phase microextraction (SPME) is a solvent-free sample preparation technique that combines sampling, isolation and enrichment into one single step (Pawliszyn, 1997). SPME was first reported by Pawliszyn and co-workers in 1990 (Arthur and Pawliszyn, 1990). When it was discovered, SPME device consists basically of a silica fibre, coated with a thin layer of a suitable polymeric sorbent or immobilized liquid, fixed within the needle of a syringe-like arrangement (Figure 2.9) (Spietelun et al., 2011). SPME is compatible with analyte separation and detection by gas chromatography (Beránek and Kubátová, 2008) and high-performance liquid chromatography (Malik et al., 2006).

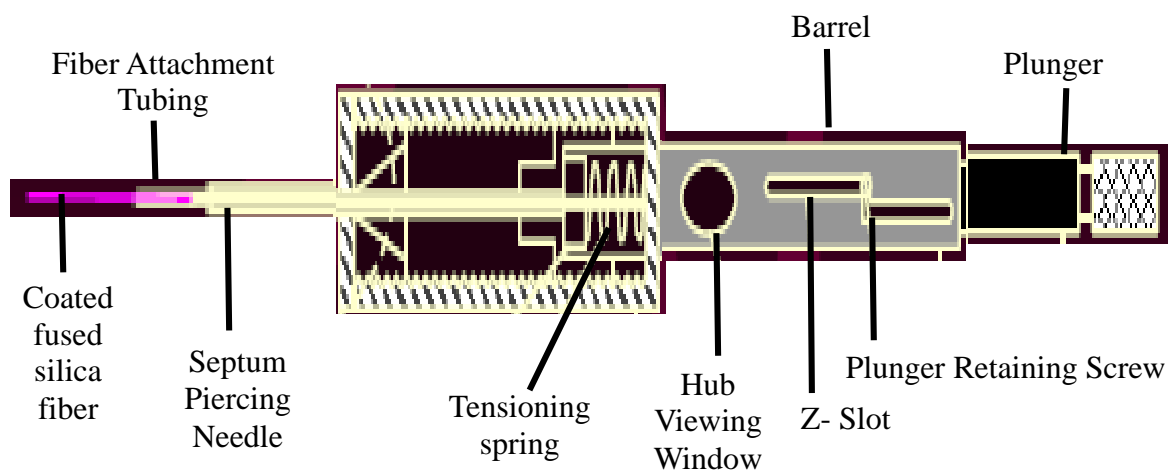


**Figure 2.9** Commercial SPME device made by Supelco (Kataoka et al., 2000)

In SPME, equilibria are established among the concentrations of an analyte in the sample, and in the polymer coating on the fused silica fiber. The amount of analyte (mass of analyte) adsorbed by the coating at equilibrium is directly related to the concentration of the analyte in the sample and can be calculated as (Musteata and Pawliszyn, 2007)

$$n = \frac{K_{fs} V_f C_0 V_f}{K_{fs} V_f + V_s} \quad (2.2)$$

Where  $C_0$  is the initial concentration of a given analyte in the sample

$K_{fs}$  is the fiber coating-sample matrix distribution constant

$V_f$  is the fiber-coating volume,

$V_s$  is the sample volume

$n$  is the amount of analyte extracted by the fiber coating

Equation 2.2 indicates that the amount of analyte extracted onto the coating ( $n$ ) is proportional to the analyte concentration in the sample ( $C_0$ ). But if the sample volume is very large, *i.e.*  $V_s \gg K_{fs} V_f$ , this equation can be simplified as;

$$n = K_{fs} V_f C_0 \quad (2.3)$$

SPME sampling can be done in 3 basic modes: (a) direct extraction (Purcaro et al., 2013; Tankiewicz et al., 2013) (b) headspace extraction (Holopainen et al., 2013; Liu et al., 2014) and (c) extraction with membrane protection (Ge and Lee, 2012; Sarafraz-Yazdi et al., 2012) (Figure 2.10)

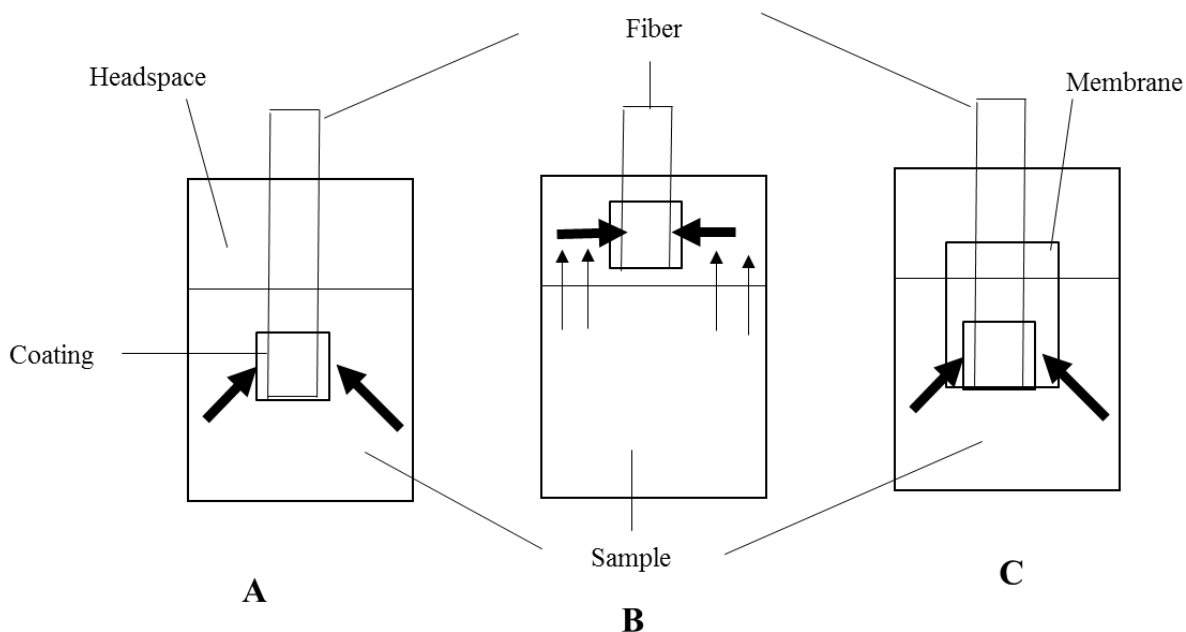


**Figure 2.10** Modes of SPME operation: (A) direct extraction (B) Headspace SPME (C) membrane-protected SPME (Pawliszyn, 2012).

In direct extraction (Figure 2.10 A), the coated fiber is inserted directly into the sample matrix and the analytes get transferred directly from the sample matrix to the extracting phase. To facilitate rapid extraction, some level of agitation is required to transport the analytes from the bulk to the sample to the vicinity of the fiber. In the headspace mode (Figure 2.10 B), the analytes are extracted from the gas phase equilibrated with the sample. The headspace mode allows matrix modifications without affecting the fiber. In a system consisting of a liquid sample and its headspace, the amount of an analyte extracted by the fiber coating does not depend on the location of the fiber; therefore, the sensitivity of headspace sampling is the same as the sensitivity of direct sampling as long as the volumes of the two phases are the same in both sampling modes. In membrane-protected SPME (Figure 2.10 C), the fiber is separated from the sample with a selective membrane, which lets the analytes through while blocking the interferences. The main purpose for the use of the membrane barrier is to protect the fiber against adverse effects caused by high-molecular-weight compounds when very dirty samples are analyzed. Membrane-protected SPME enables the analysis of less-volatile compounds. The

extraction process in this type of SPME is substantially slower than direct extraction because the analytes need to diffuse through the membrane before they can reach the coating. This can be overcome by using thin membranes and an increase in extraction temperature (Pawliszyn, 2000).

Table 2.5 shows the list of the commercially available SPME fibers. The choice of the fiber coating depends mainly on the nature of the target analytes. The general rule for selecting the right fiber is by following the principle “like dissolves like”. Apart from affinity considerations, PDMS fibers are popular for several applications, because of their ruggedness and stability (Augusto and Luiz Pires Valente, 2002). (Ji et al., 2006)

**Table 2.5** Examples and applications of commercially available SPME fibers

<b>Fiber types</b>	<b>Analytes</b>	<b>Determination technique</b>	<b>References</b>
100 $\mu\text{m}$ PDMS	VOCs, BTEX, PAHs Volatiles	GC/HPLC	(Tang and Isacson 2008)
30 $\mu\text{m}$ PDMS	PAHs non-polar and semi volatile	GC	(Tang and Isacson 2008)
7 $\mu\text{m}$ PDMS	PAH non-polar and high molecular weight	GC	(Tang and Isacson 2008)
65 $\mu\text{m}$ PDMS/DVB	VOC, BTEX volatiles, amines,	GC	(Ji et al., 2006)
75/80 $\mu\text{m}$ CAR/PDMS	VOC, BTEX, gases and low molecular weight compounds	GC/ICP	(Popp and Paschke, 1997)
50/30 $\mu\text{m}$ DVB/CAR/PDMS	PAH, semi-volatile volatile compounds	GC	(Tang and Isacson 2008)
85 $\mu\text{m}$ PA	Pesticides, Polar, semi- volatile compounds	GC/HPLC	(Barták and Čáp, 1997; Boyd-Boland and Pawliszyn, 1995)

The quality of the commercial SPME fibers depends on the manufacturer and sometimes the performance is different from batch to batch. This requires an optimization of each fiber before use. Moreover the SPME fibers are fragile and can be easily broken. Care should be taken during the agitation process, since high agitation might damage the fiber resulting into poor result. The formation of gas bubbles on the fiber surface is sometimes difficult to prevent, and it affects the mass transfer rates and leads to problems of poor reproducibility. The main advantages and disadvantages of SPME are summarized in Table 2.6.

**Table 2.6** Advantages and disadvantages of SPME (Spietelun et al., 2011)

<b>Advantages</b>	<b>Disadvantages</b>
Simple to operate	Not very selective
Relatively short extraction time	The fibers are mechanically weak
Lack of artefacts	Provide sample-to-fiber low recoveries
No need of expensive or complex equipment	Whole sample is used
Possibility of full automation	Gas standards are required for calibration
Easy interfacing with GC systems	Storage stability is poor (less than 1 h except under refrigeration).
Applicability to both in situ and in vivo sampling	Equilibrium composition varies widely with temperature

#### **2.3.4 Desorption techniques**

Monitoring of VOCs from the environmental air matrix is a complex process, because of the presence of low concentration of VOCs, from ppb down to ppt. Therefore, for a reliable determination of VOC levels in air requires the most efficient and sensitive sampling, preconcentration and analysis techniques. In this respect, adsorptive enrichment of solid sorbents is a well-established technique which allows sampling and preconcentration in one step. After the preconcentration step, analytes are removed from the sorbent and then determined by gas chromatography. The most common desorption methods used for determining VOC levels are solvent extraction and thermal desorption (Ramírez et al., 2010).

#### 2.3.4.1 Solvent extraction

Solvent extraction is the most common extraction method used for VOCs desorption. This method is very simple, compatible with high molecular mass and thermally unstable compounds and allows the preconcentration of high volumes of air (Ramírez et al., 2010). The main sorbent used for solvent extraction is activated charcoal (NIOSH, 2003). Activated charcoal has a very complex surface structure containing a wide range of functional groups which allow the adsorption of a wide range of compounds (Matisová and Škrabáková, 1995). The desorbing solvent most commonly used with activated charcoal is carbon disulfide due to its high volatility, its high adsorption heat on activated charcoal and its effectiveness at dissolving non-polar compounds. Moreover, it elutes rapidly at the front of the analysis on the most common GC columns and has a very low response on FID (Harper, 2000).

There are many advantages and disadvantages of solvent extraction desorption method, some of the advantages are this method is cheap and simple, no specialist apparatus are needed, it is compatible with high molecular mass and thermally unstable compounds and allows the preconcentration of high volumes of air. The major disadvantages is that the sample is diluted with the desorbing solvent, moreover polar and reactive compounds have often poor desorption efficiencies, solvents used for extraction are toxic and there is regeneration of adsorbent bed before use (Ramírez et al., 2010).

#### **2.3.4.2 Thermal desorption**

Thermal desorption is a good alternative to solvent desorption and is used in several official methods. This method provides enhanced sensitivity and is compatible with thermally stable polar and apolar compounds (Ramírez et al., 2010). Thermal desorption prevents analyte losses by minimizing sample manipulation and risks of contamination due to solvents. This technique is commonly used for volatile chemical analysis, being the method of choice to determine VOCs in several studies of urban industrial air, indoor and other atmosphere (Ras-Mallorquí et al., 2007; Wu et al., 2004).

The main advantages of thermal desorption methods are the adsorbent are reusable, this method has ease of automation, there is no interferences from a solvent, it has short analysis time, low levels of VOCs is detectable, and there is no sample preparation step. But the main drawback of thermal desorption are; the method is very expensive, possible degradation of the adsorbent, it is not suitable for thermally unstable compounds and compounds with high boiling points (Ramírez et al., 2010).

#### **2.3.5 Chemisorption**

Chemisorption also called as chemical adsorption is usually highly selective and occurs only between certain adsorptive and adsorbent species (Webb, 2003). In chemisorption process the analyte to be measured is absorbed irreversibly in a liquid phase and then it is altered by a chemical reaction with other components present. Usually impingers and bubblers containing liquid as adsorbing solution are used for trapping suitable analytes in this process. And it is mainly used for the collection of high-boiling, reactive gases or polar analytes (Bishop and Mitra, 2007). For this process before carrying out analysis the user must decide on the best reagent for a particular analyte. This technique is very much suitable for the collection of larger volumes of air samples and have been used for the determination of reactive gases such as hydrogen sulphide and Sulphur dioxide, acidic or basic organic vapours of low volatility such as amines, carboxylic acids

and phenols (Kumar and Viden, 2007). This process has been commonly applied for the determination of Sulphur dioxide (Geetha and Balasubramanian, 2000) and nitrogen dioxide from the air (Mousazadeh, 2009).

### **2.3.6 Quality assurance for air sampling**

Monitoring of air involves lots of processes resulting into relatively high uncertainty. This can happen during sampling process, or transporting the equipment for sampling or while storing (Huybrechts et al., 2003), analytes might be lost in the desorption step also (Dewulf et al., 2006). So, to obtain the best result, it is very important to validate the methods. If air sampling is done using adsorbent tubes then it should be properly labeled and sealed, this will avoid contamination that would enter through poor end-fittings (Heo et al., 2001). Blank adsorbent tubes, opened and immediately re-sealed in the field, can be used to measure contamination during transport or storage (Plaisance et al., 2007; Xie et al., 2006). Back-up sections or distributed volume sets can be used to detect breakthrough (Kume et al., 2008). For proper sample collection and recovery dual sampling trains can be used where one of the trains is pre-spiked with the analyte. Adsorbent in the tubes and are used for solvent extraction are for single-use only, but thermal desorption tubes can be reused. This can lead to carry over of poorly desorbed compounds which then appear in later analysis.

## CHAPTER 3

### **Analytical technique for air pollutants determination**

#### **3.1 Introduction**

After sampling of air using different sampling method, it has to be analysed using suitable analytical technique. Therefore, for the monitoring of air pollution, analytical technique need to be considered. There are various kinds of analytical technique used for environmental pollution. But for air pollution the common analytical technique used are gas chromatography, ion chromatography and spectrophotometry.

#### **3.2 Analytical method for air pollutants BTX**

The main analytical method used for the identification and determination of BTX in air sample are gas chromatography and chemical sensor. Out of which gas chromatography technique is being extensively applied (Buczynska et al., 2009; Gallego et al., 2008; Lan and Minh, 2013; Yurdakul et al., 2013). Beside this technique various metal oxides ( $\text{SnO}_2$ ,  $\text{WO}_3$ ,  $\text{ZnO}$ ,  $\text{Cr}_2\text{O}_3$ ,  $\text{TiO}_2$  etc) based gas sensors have so far been investigated for efficient BTX detection (Dutta et al., 2015).

### 3.2.1 Gas Chromatography (GC)

GC is one of the most widely used techniques for analyzing hydrocarbon mixtures. The main advantages of chromatography are the range of measurement (in trace levels), the detection of a wide range of components and the repeatability of the measurements. Chromatography is used in the laboratory, in permanently installed online systems and in the field with portable systems. No matter the locations, style or brand all GC are composed of the same functional component. The main analytical components of the GC are the column, and the detectors. And the principle behind separation involves two different phases, the stationary phase and mobile phase. Nitrogen or Helium are used commonly as the mobile phase. And there are two types of stationary phase, they are gas solid chromatography or adsorption chromatography (GSC) and gas liquid chromatography or partition chromatography (GLC). GSC uses a porous polymer solid, while GLC uses mostly viscous gum like liquid coated on the inert support. The quality of separation depends on how long the components to be separated stay in the stationary phase and on how often they interact with this phase. The type of interaction between component and phase is determined by the functional groups. The polarity of the phase is a function of stationary phase substituents. The GC system consists mainly of column, injector port, detector port and gas supplies Figure 3.1

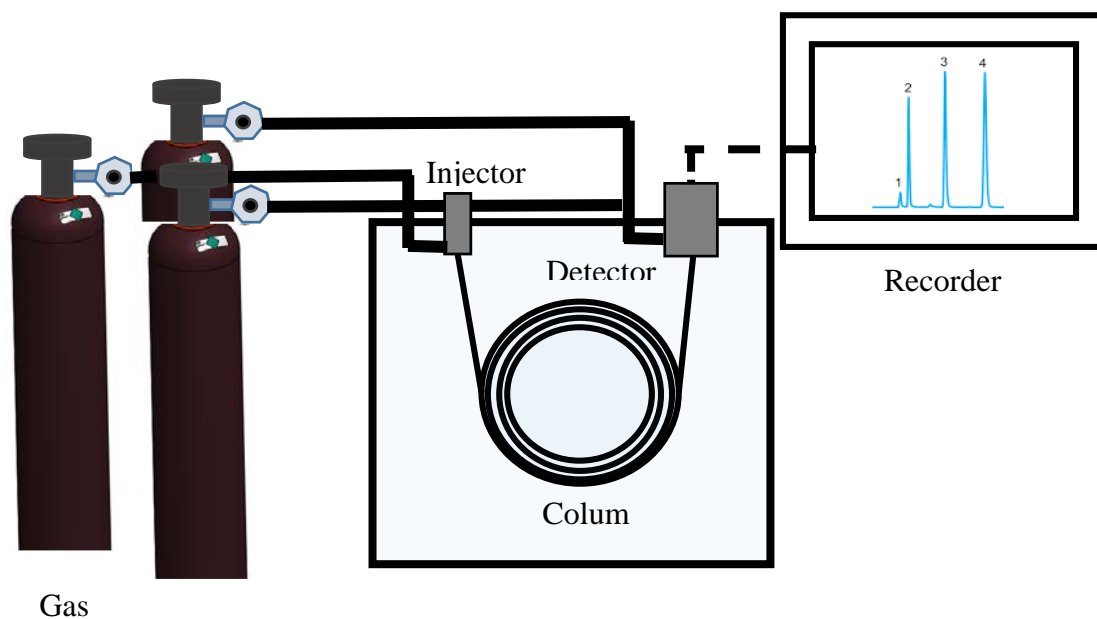
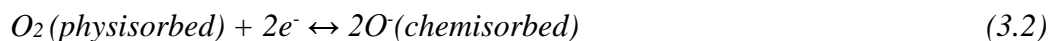


**Figure 3.1** Schematic diagram of a typical gas chromatograph

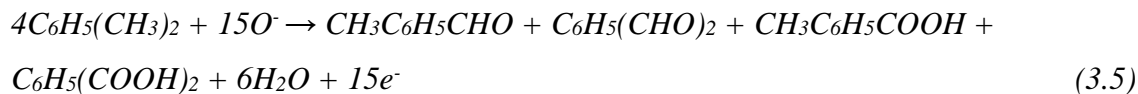
In GC after the components have been separated by the chromatographic columns, they then pass over the detector, which is very important part of the system. Several types of detectors are available for GC, like flame ionization detectors (for ppm-level hydrocarbons) and flame photometric detectors (for ppb-ppm level sulphur detection), but the most common detector used for most hydrocarbon gas analysis is the thermal conductivity detector (low ppm to 100% concentration).

### 3.2.2 Chemical sensor

Gas sensors based on metal-oxides semiconductors may be used in a wide variety of applications including gas monitoring and alarm (Carotta et al., 2001). For BTX detection various metal oxides based gas sensors have been developed and investigated (Table 3.1). Most of these reports indicated that the high optimum operating temperature ranges from 200 to 450°C, which is typical for BTX sensing. Out of many metal oxide sensor Nano-porous p-TiO<sub>2</sub> is one of the latest developed BTX gas sensor (Dutta et al., 2015). Nano-porous surface actively promotes adsorption of oxygen from ambient air and these oxygen often remains in the active state as O<sup>-</sup> (equation 3.1 and equation 3.2). Benzene reacts with this adsorbed oxygen and oxidized to phenol (by hydrogen abstraction due to catalytic effect of oxide surface), at atmospheric pressure, without hampering the aromatic ring. The adsorbed oxygen reacts with benzene to generate electron (equation 3.3).



In-case of toluene and xylene sensing, adsorbed oxygen reacts with methyl groups, instead of C-H bond in aromatic ring (Einaga et al., 2013). Organic acids (benzoic acid, toluic acid and phthalic acid) and aldehydes (benzaldehyde, tolualdehyde and phthalaldehyde) are the resultant product due to oxidation of toluene and xylene (equation 3.4 and equation 3.5). In case of xylene, three isomers (ortho, meta and para-xylene) cannot be separated properly, so, a large number of by products like acids and aldehydes can be formed (Dutta et al., 2015).



Metal oxides gas sensors indicates good sensitivity to ppm or sub-ppm levels of BTX detection and have potential to be employed in real situation. However, one of the major drawbacks of the gas sensors is that they operate at elevated temperatures (Chen et al., 2008; Lin et al., 2011).

**Table 3.1** Application of metal oxides gas sensor for detection of BTX

<b>Metal oxides</b>	<b>Limit of detection (ppm)</b>	<b>Operation temperature (°C)</b>	<b>References</b>
ZnO-TiO <sub>2</sub>	10	370	(Zhu et al., 2004)
SmFeO <sub>3</sub>	1	400	(Mori et al., 2009)
Co <sub>3</sub> O <sub>4</sub>	10	200	(Sun et al., 2011)
WO <sub>3</sub>	0.1	400	(Kanda and Maekawa, 2005)
SnO <sub>2</sub>	0.5	400	(Nicoletti et al., 1999)
NiO-SnO <sub>2</sub>	50	330	(Liu et al., 2011)
ZnO	100	400	(Bai et al., 2011)
Cr <sub>2</sub> O <sub>3</sub>	1	170	(Ma et al., 2012)

### 3.3 Analytical method for SO<sub>2</sub> and NO<sub>2</sub>

There are different kind of analytical techniques used for analysis of SO<sub>2</sub> and NO<sub>2</sub>, common analytical techniques used are ion chromatography, spectrophotometry and chemiluminescence. Spectrophotometric method for determination of SO<sub>2</sub> has been widely used (Kumar et al., 2006, Geetha and Balasubramanian, 2000, Gayathri and Balasubramanian, 2001). Similarly spectrophotometric method has been used for determination of NO<sub>2</sub> (Mousazadeh, 2009, Tanaka et al., 1998).

#### 3.3.1 Spectrophotometry

This techniques if used to measure the amount of light that a sample absorbs. It works on the principle of Lambert-Beer Law. The instrument operates by passing a beam of light through a sample and measuring the intensity of light reaching a detector. In simple words, a beam of photons, strike the analyte molecules, there are chances that some part of photons are absorbed by analyte molecules. This absorption reduces the number of photons in the beam of light, thereby reducing the intensity of the light beam, which can be measured as absorbance at suitable wavelength. And the concentration of an analyte can be determined by measuring the absorbance as suitable wavelength and applying the equation from Lambert-Beer Law (equation 3.6)

$$A = \epsilon_{\lambda} l C \quad (3.6)$$

Where; A represents the absorbance, an optical parameter without dimension accessible with a spectrophotometer, l is the thickness (cm) of the solution through which the incident light is passed, C is the molar concentration and  $\epsilon_{\lambda}$  is the molar absorption coefficient (L mol<sup>-1</sup> cm<sup>-1</sup>) at wavelength  $\lambda$ , at which the measurement is made. This parameter, also called as the molar absorptivity, is the characteristic of the compound being analyzed and depends among other things upon the temperature and the nature of the solvent. Spectrophotometric method applies not only to compounds possessing an

absorption spectrum in that spectral region but equally to all those compounds which, following modification by specific reagents, lead to derivatives which permit absorption measurements (Rouessac and Rouessac, 1994).

Spectrophotometric method for determination of SO<sub>2</sub> and NO<sub>2</sub> has been widely used due to low cost, simple operation and fairly good sensitivity. Methyl red has been used for an indirect method for the determination of SO<sub>2</sub> using spectrophotometric method (Geetha and Balasubramanian, 2000). In this method the determination of SO<sub>2</sub> was done based on the reaction between SO<sub>2</sub> and a known excess of bromine. The unreacted bromine was determined based on its ability to bleach the dye methyl red quantitatively (Figure 3.2)

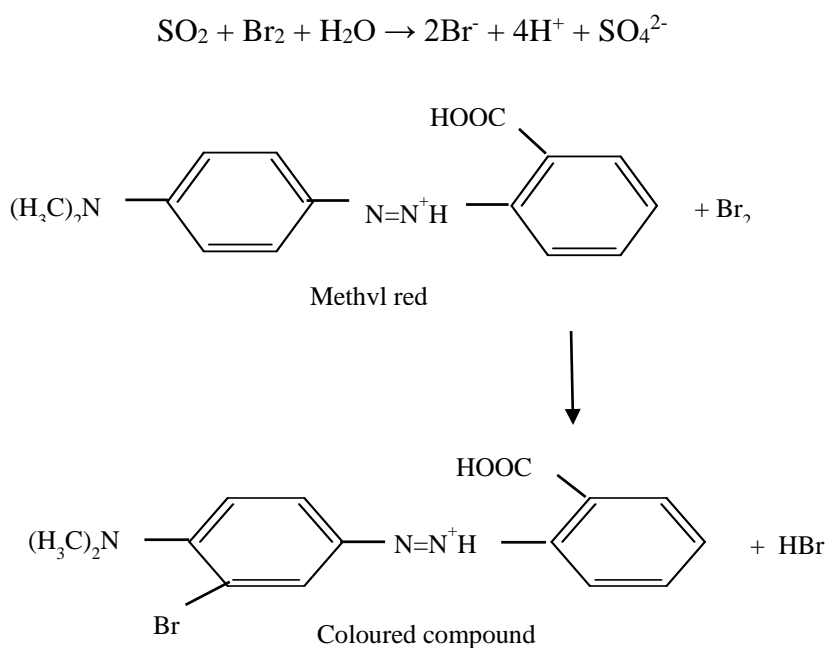


**Figure 3.2** Reaction mechanism of SO<sub>2</sub> with methyl red in excess of Br<sub>2</sub> (Geetha and Balasubramanian, 2000)

The spectrophotometric method based on a redox reaction between SO<sub>2</sub> and iodine monochloride obtained from iodine with chloramine-T in acetic acid has been reported

(Kumar et al., 2006). In this method the reagent iodine monochloride oxidizes  $\text{SO}_2$  to sulfate, thereby reducing itself to iodine. The liberated iodine will also oxidize  $\text{SO}_2$  and reduce itself to iodide. The obtained iodide is expected to combine with iodine to form a brown-coloured homoatomic triiodide anion (460 nm) which forms an ion-pair with the sulfonamide cation, providing exceptional colour stability to the system under an acidic condition, and is quantitatively related to  $\text{SO}_2$  (Figure 3.3).

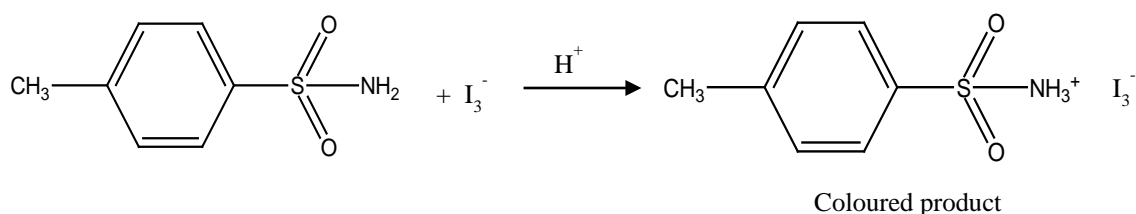
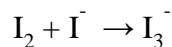
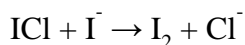
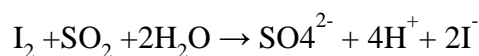
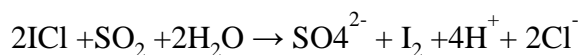


**Figure 3.3** Reaction mechanism of iodine monochloride with  $\text{SO}_2$  (Kumar et al., 2006)

$\text{SO}_2$  has been analysed using spectrophotometric technique by reacting it with formaldehyde and pararosaniline dye. This involves converting the  $\text{SO}_2$  to the sulphite ion using a solution of potassium tetrachloromercurate, and then colorimetrically determining the concentration using a solution of pararosaniline and formaldehyde (Figure 3.4)

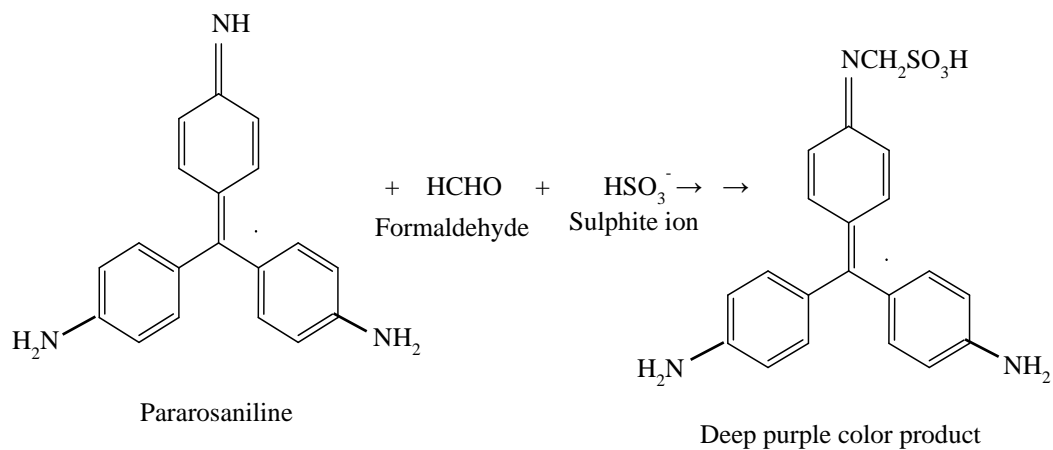


**Figure 3.4** Reaction mechanism of SO<sub>2</sub> in presence of formaldehyde and pararosaniline (Munoz et al., 1989)

Similarly NO<sub>2</sub> has been determined using spectrophotometric method. In this NO<sub>2</sub> was reacted with sulfanilic acid and the product obtained was further reacted with N-1-naphthylethylenediamine dihydrochloride to form a colored compound whose absorbance can be easily measured using spectrophotometry (Tanaka et al., 1998) (Figure 3.5).

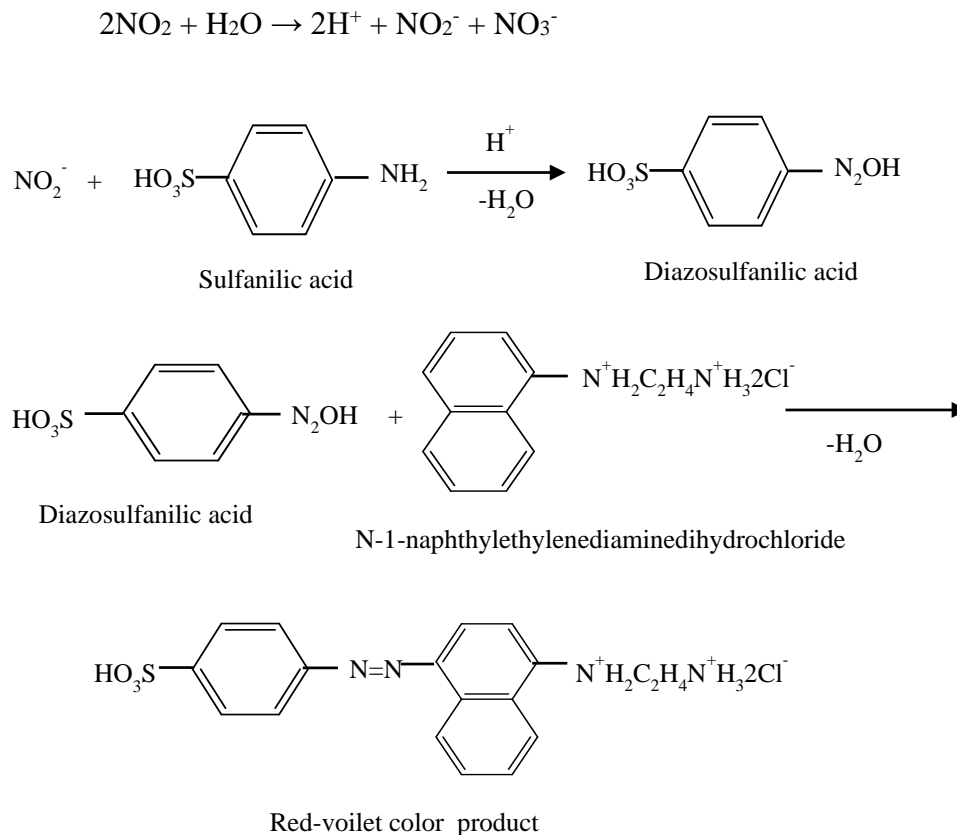


**Figure 3.5** Reaction mechanism of  $\text{NO}_2$  with N-naphthylethylenediamine dihydrochloride (Tanaka et al., 1998)

### 3.3.2 Chemiluminescence

Chemiluminescence is the emission of light energy that results from some chemical reactions (equation 3.7 and 3.8)



This kind of reactions produces some radiation in certain wavelength which is can be measured using chemiluminescence detector. So such phenomena have been used for monitoring of  $\text{NO}_x$ . Figure 3.6 shows a typical layout of a chemiluminescence analyser for  $\text{NO}_x$ . For determination of  $\text{NO}_x$  ozone is generated by the UV radiation of clean air and mixed in a reaction chamber with the sample air. Light from the reaction passes through an optical filter and is detected with a photomultiplier tube. It should be noted that  $\text{NO}_2$  in the sample is not detected in this system. But,  $\text{NO}_2$  can be reduced to  $\text{NO}$  by means of a heated catalyst, such as a stainless steel or molybdenum.

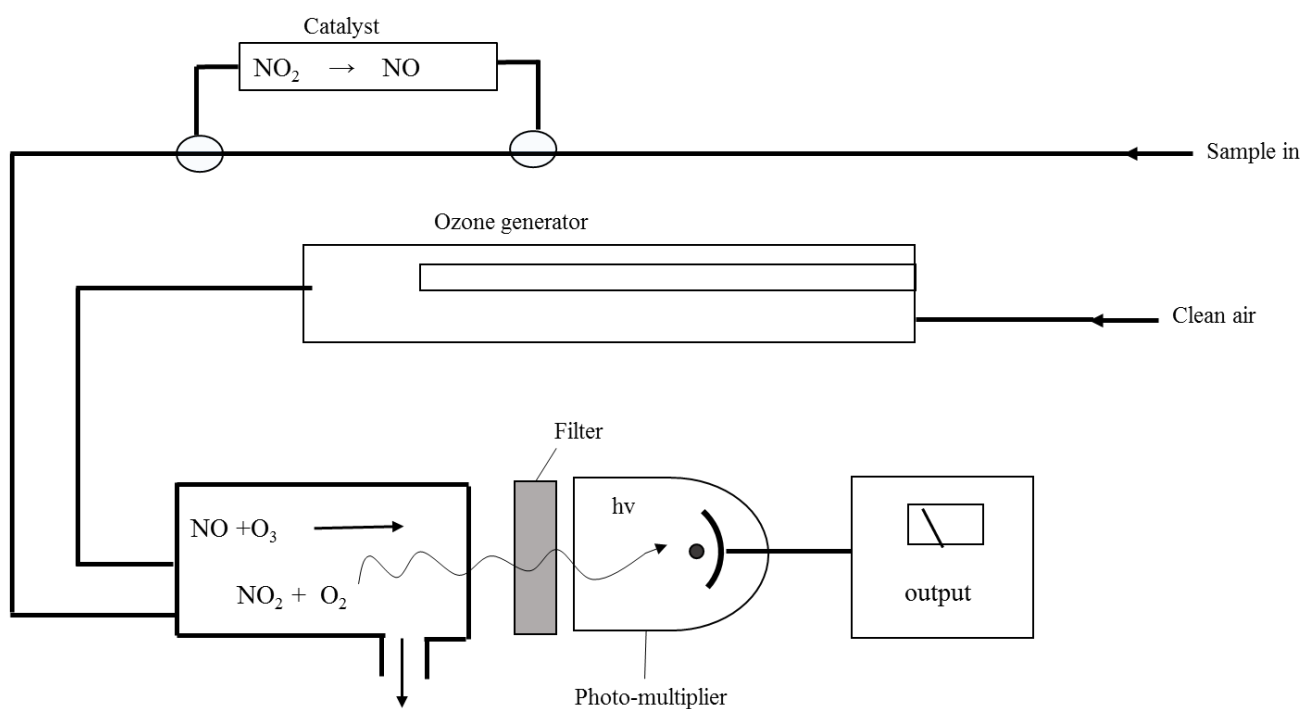


**Figure 3.6** Chemiluminescence detector for  $\text{NO}_x$

### 3.3.3 Ion-Exchange Chromatography

SO<sub>2</sub> and NO<sub>2</sub> are also analysed by using ion-exchange chromatography (IEC) technique (Campos et al., 2010; Moodley et al., 2011; Stranger et al., 2008). In this analysis technique first SO<sub>2</sub> and NO<sub>2</sub> will be converted into their respective ions. IEC is a part of ion chromatography which is an important analytical technique for the separation and determination of ionic compounds, together with ion-partition/interaction and ion-exclusion chromatography (Hadded et al., 1990). Ion chromatography separation is based on ionic interactions between ionic and polar analytes, ions present in the eluent and ionic functional groups fixed to the chromatographic support. In this analysis technique two distinct mechanism occurs; ion exchange due to competitive ionic binding and ion exclusion due to repulsion between similarly charged analyte ions and the ions fixed on the chromatographic support, play a role in the separation in ion chromatography. The separation is based on the formation of ionic bonds between the charged groups of biomolecules and an ion-exchange gel/support carrying the opposite charge (Stanton, 2004) (equation 3.9)



The anion B<sup>-</sup> of the eluent replaced with the analyte anion A<sup>-</sup> bound to the positively charged ion X<sup>+</sup> on the surface of the stationary phase. The adsorption of the analyte to the stationary phase and desorption by the eluent ions is repeated during their elution in the column, resulting in the separation due to ion-exchange (Bhattacharyya, 2012).

IEC mainly consist of a high pressure pump with pressure and flow indicator, to deliver the eluent. An injector for introducing the sample into the eluent stream and onto the column. A column, to separate the sample mixture into the individual components. A detector, to measure the analyte peaks as eluent from the column. A data system for collecting and organizing the chromatograms and data and an oven, optional (Figure 3.7).

The adsorption and desorption processes in IEC are determined by the properties of the three interacting entities; they are the stationary phase, the constituents of the mobile phase and the solute (Kastner, 2005)

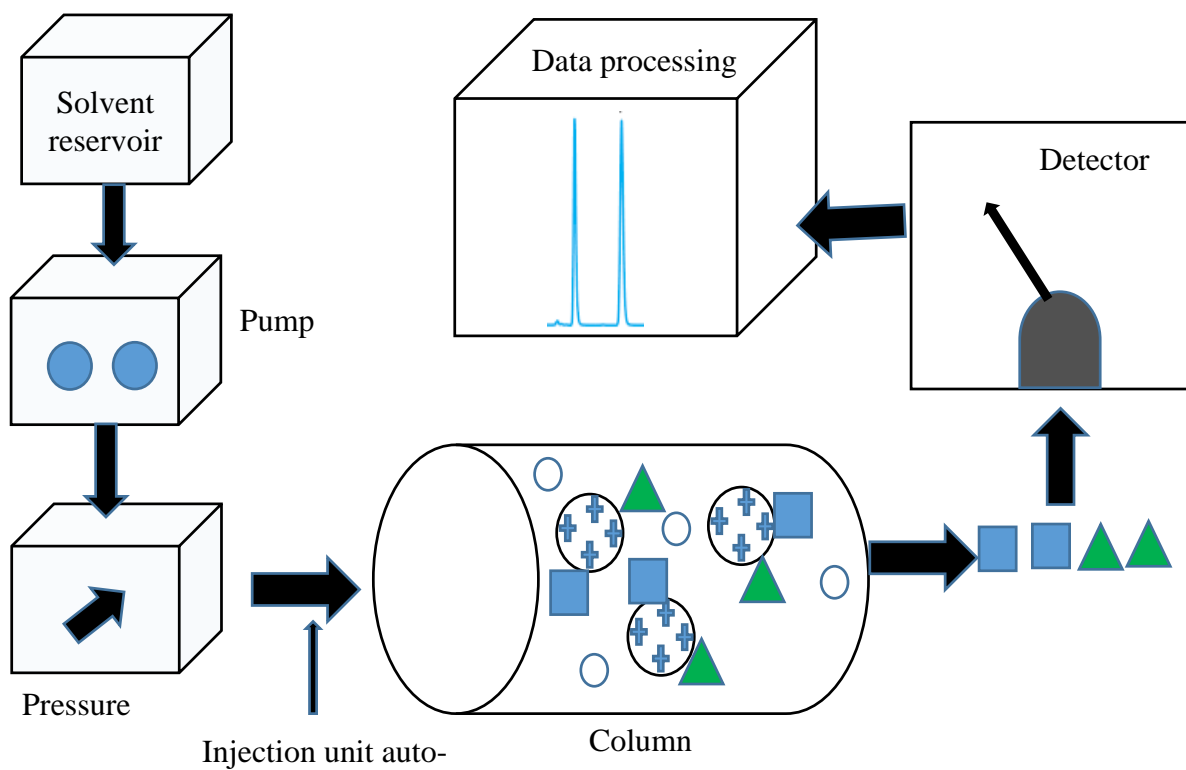


**Figure 3.7** Schematic diagram of Ion-exchange chromatography system

## CHAPTER 4

### **Sampling of BTX in Hat Yai city using cost effective laboratory-built PCB passive sampler**

#### **4.1 Introduction**

Quality of air has become a concern to everyone and to every country. Studies have shown that, deteriorated air quality highly impacts the environment and overall health of living beings. Therefore, clean air is so vital in promoting a healthy life span of flora and fauna. In spite of this fact, very little attention is given to the effect of anthropogenic activities on the quality of ambient air in many mega cities (Kirchner et al., 2005). In most developed cities of the world, air pollutants are increasing and sometimes exceeds the levels set up by the national or international ambient air quality standards (Lee et al., 2002). There are numerous sources of outdoor and indoor air pollutants, out of which the road traffic is one of the major contributors to the levels of pollutants in urban areas (Briggs et al., 2008). Air pollutants like volatile organic compounds (VOCs) mainly come from automobiles. Other sources comprise of solvent utilization, natural gas emission, gasoline evaporation (Srivastava et al., 2005) and biomass burning (Lau et al., 2010).

Out of the many VOCs, benzene, toluene and xylene (BTX) are given special attention because of their adverse effects to human health. Studies have shown that exposure to BTX can cause irritation, imbalance in female hormone level, miscarriages, and low birth weight (Billionnet et al., 2011; Ciarrocca et al., 2011; Llop et al., 2010; Lupo et al., 2011; Mendell, 2007; Slama et al., 2009). The United States Environmental Protection Agency (US EPA) has categorized benzene as carcinogenic to humans. The risk of leukaemia due to the lifetime exposure to benzene is estimated to be 1 in 10,000, 1 in 100,000 and 1 in 1000,000 population at 17, 1.7 and 0.17  $\mu\text{g m}^{-3}$ , respectively (WHO, 2000, US EPA 2011). In view of this high risk, there is no permissible limit for benzene exposure (WHO, 2010, US EPA 2009).

VOCs have become a growing concern in Thailand due to their inappropriate use and management of leakages, improper transferring in production processes and some illegal waste disposal by industrial sector (Laowagul et al., 2008). Ambient VOCs monitoring data in many developing countries is still limited (Cetin et al., 2003). In Thailand, VOCs measurement in the capital city, Bangkok, has been reported for summer of 2006 (Laowagul et al., 2008). Some VOCs like BTX have been studied from time to time (Laowagul et al., 2008; Pimpisut et al., 2005) but data of such a study are not available in other parts of the country.

One of the biggest cities in the south of Thailand is Hat Yai in Songkhla province, with an approximate population of 160,000 (2008) (Pongichan et al., 2014). The city has many large shopping malls and departmental stores along with a large number of street-side vendors and stalls. As per the statistics, more than 400,000 tourists visit Hat Yai city each year (Kuncharin and Mohamed, 2013). Furthermore there are a number of industries surrounding the city and large quantities of air pollutants are being emitted in the area. Because of the various developmental activities and urbanization, it is expected that traffic-related air pollution would be one of the major environmental problems in Hat Yai.

The Ministry of Science, Technology and Environment (MOSTE) of Thailand has set up a monitoring station in Hat Yai city since 1996. Monitoring of particulate matters, sulfur dioxide, nitrogen dioxide, ozone and carbon monoxide are done on a daily basis. However, recent data on the monitoring of ambient concentration of BTX are not available. In contrast BTX are being monitored regularly all over the world, like in Belgium (Buczynska et al., 2009), Australia (EPA Vicoria 2006), Japan (Laowagul and Yoshizumi, 2009), New Zealand (Myers et al., 2005), India (Hoque et al., 2008), and China (Wang et al., 2008 and Liu et al., 2009). Literature shows that BTX monitoring in Hat Yai city was done a decade back (Thammakhet et al., 2004), after which no such studies have been carried out. In a span of ten years a lot of developmental activities have taken place with increased number of people and road-traffic, which might have contributed in deteriorating the air quality of the city. It is important to monitor the air regularly so that the real ambient concentration of the pollutants are known. Therefore, Hat Yai city was chosen for the monitoring of BTX so as to compare its ambient concentration with past studies and also with that of other

bigger cities in and around the world. These comparative studies would show the trend of the air quality which will lead to some preventive action.

In order to monitor the air quality regularly, there is a need of simple and cost-effective sampling and analytical methods capable of achieving very low detection limit. Many of these requirements can be fulfilled by passive sampling techniques (Zabiegała *et al.*, 2002). Passive samplers can be effectively used for large scale and long term monitoring of a wide range of air pollutants, for both indoor and outdoor environment. Thus, in this study a laboratory-built printed circuit board (PCB) passive sampler which was earlier developed and validated for xylene and styrene detection from copy print shops (Saelim *et al.*, 2013) was re-validated and used for sampling and monitoring of BTX in outdoor air in Hat Yai city. This is possible since the PCB passive sampler uses polypyrrole as an adsorbent which can easily adsorb simple VOCs like benzene, toluene and xylene due to pi-pi interaction. Using the re-validated passive samplers, air samples were collected from sixteen sites around the city. Sampling sites were selected to allow for the comparative studies with past studies and also to representatively covering the strategic areas of the city.

## **4.2 Experimental**

### **4.2.1 Apparatus and reagents**

All chemicals used in this study were of analytical grade. Silver nitrate was from Fischer Scientific (Loughborough, UK), sodium tartrate was from BDH Chemical Ltd. (California, USA), propylene glycol was from Farmitalia Carlo Erba SPA (Rodano, Italy), hydrochloric acid (37%), xylene were from LAB-SCAN (Bangkok, Thailand). Benzene and toluene were from Merck KGaA (Darmstadt, Germany) and pyrrole with 98% w/v purity was from Sigma Aldrich (Missouri, USA).

### **4.2.2 Gas chromatographic system**

All analyses were performed by a gas chromatograph coupled with a flame ionization detector (GC-FID) (Shimadzu GC-14A, Kyoto, Japan) with an RTX 624 fused

silica capillary column (30 m, 0.25 mm I.D. and coated with 1.4  $\mu\text{m}$  film thickness; Restek, Philadelphia, USA). High purity nitrogen gas was used as both carrier gas and make up gas (99.995%, Thai Industrial Gases, Samut Prakan, Thailand). High purity hydrogen gas (99.995%, Thai Industrial Gases, Samut Prakan, Thailand) was used as fuel gas and air from an air compressor (Swan, Taiwan) was used as oxidant gas. Data processing was carried out with a Communications Bus Module CBM-102 (Shimadzu, Kyoto, Japan). The gas chromatographic conditions were optimized using a standard gas mixture prepared in a headspace vial (Kolb and Ettre, 2006) from the liquid standard of benzene, toluene and xylene (5.0 ppm) to achieve the best performance of the GC-FID. For the optimization of the gas chromatography system, 100  $\mu\text{L}$  of standard gas mixture was injected.

#### **4.2.3 Methodology**

For the study of BTX in Hat Yai city using PCB passive sampler, it involves methodologies like validation of various analytical procedures and optimization of GC-FID conditions. The method also includes the re-development of PCB passive sampler followed by development and optimization of the laboratory-built thermal desorption system. And after the re-development of the PCB passive samplers application of PCB passive sampler for monitoring of BTX in ambient air of Hat Yai city.

#### 4.2.4 Optimization of GC-FID conditions

Various parameters of GC-FID were optimized based on the criteria short analysis time, high response, good resolution and sharp peak. Parameters like, flow rates of carrier (N<sub>2</sub>), make up (N<sub>2</sub>), fuel (H<sub>2</sub>), and oxidant gas (Air), injector temperature, detector temperature and column temperature were optimized. And since, temperature program was for analysis of BTX thus, initial column temperature, final column temperature, initial holding time, final holding and column ramp rate were also optimized. For optimization process, standard BTX gas were prepared in a headspace 30 mL vial. The headspace vials containing the standard solution of BTX was heated at 60 °C for 10 minutes and 100 µL of the gas phase was injected into the gas chromatographic system. Five measurement replications were done and the optimum value was used for further experiments.

##### 4.2.4.1 Carrier gas (N<sub>2</sub>) flow rate

The separation efficiency of the GC-column depends on the flow rate of the carrier gas. Therefore, carrier gas flow rate is one of the most important parameter of GC that need to be optimized. So, carrier gas flow rate was studied at 1.0, 1.5, 2.0, 2.5 and 3.0 mL min<sup>-1</sup>. A theoretical plate number ( $N$ ) and a height equivalent to a theoretical plate (HETP) were calculated from the retention time, the peak height and the peak area of the analytes obtained from the chromatogram at each flow rate. After which a van Deemter graph was plotted between HETP and flow rate and the optimum flow rate was obtained at the lowest value of HETP.

#### **4.2.4.2 Make up gas (N<sub>2</sub>) flow rate**

The main function of make up gas is to increase the sensitivity of FID and the peak symmetry. It is often added at the exit end of the column to increase the total flow entering the detector. The optimum make up gas flow rate was obtained by considering the flow rate that provided the highest peak area and it was investigated at 20, 30, 40 and 50 mL min<sup>-1</sup>.

#### **4.2.4.3 Fuel gas (H<sub>2</sub>) and oxidant gas (air) flow rate**

FID works on the principle of ionization mechanism. Ionization process needs the heat energy which can be produced from the reaction between fuel gas and oxidant gas. The analytes (organic compounds) gets burn in the jet converting them into their respective ion pairs. In order to obtain the highest ionization efficiency of the flame, fuel gas flow rate were studied at 20, 30, 40 and 50 mL min<sup>-1</sup> and oxidant gas flow rate were studied at 200, 250 and 300 mL min<sup>-1</sup>.

#### **4.2.4.4 Injector temperature**

The role of injector temperature in GC is to heat the injected sample and convert them into the gas phase before entering into the separation column. Thus, in order to make sure, that the injected sample are completely changed into the gas phase, the injector temperature need to be optimized. Usually the injector temperature must be high enough to vaporize the analytes into the gas phase. But it is too high it may cause the analytes in the injected sample to decompose. The injector temperature were investigated at 150, 170, 190 and 210°C and the optimum value was selected at the temperature which provided the highest peak area.

#### 4.2.4.5 Detector temperature

The FID shows the highest response for hydrocarbons detection, being proportional to the number of carbon atoms (Poole and Schuette, 1984). The optimization of detector temperature was done by considering the effect of the temperature on the sensitivity, the analysis time and the life time of the stationary phase. The detector temperature were investigated at 150, 170, 190 and 210°C.

#### 4.2.4.6 Column temperature programming

In GC-FID for detection of organic compounds, usually program column temperature is used. The column temperature programming consist of initial temperature, initial holding time, temperature ramp rate, final column temperature and final holding time. In order to obtain the optimum column temperature programming following parameters were studied as summarized in Table 4.1. The optimum value of the column temperature programming was obtained by considering the best resolution, the highest peak area and the shortest analysis time.

**Table 4.1** Optimization parameters for column program temperature of GC-FID

Step	Parameter	Studied value
1	Initial temperature (°C)	35, 40, 45, 50
2	Initial time (min)	1.0, 1.5, 2.0, 2.5
3	Temperature ramp rate (°C min <sup>-1</sup> )	15, 20, 25, 30
4	Final temperature (°C)	145, 150, 155, 160
5	Final time (min)	1.5, 2.0, 2.5, 3.0

#### 4.2.5 Analytical performance of the GC-FID

The performance of the GC-FID were evaluated, *e.g.*, linear dynamic range (LDR), limit of detection (LOD) and limit of quantitation (LOQ).

##### 4.2.5.1 Linear dynamic range of the GC-FID

To investigate the linearity of the response from the GC-FID, standard BTX solution were prepared in the concentration range of 0.1 – 100 ppm in a 30 mL headspace vial. And the head space vial was placed at 60°C on a water bath. The gas phase of these standard solution (0.1 mL) was injected into the GC-FID at the optimum GC conditions. The linearity was determined from the curve plotted between the peak area ( $\mu\text{V.s}$ ) in  $y$ -axis and the concentration of analytes in  $x$ -axis when the coefficient of determination ( $R^2$ ) was equal or greater than 0.99 (Authority, 2004). However, the random error in the value of the slope and the intercept are very important and thus the equations used for calculating them are to be considered. We must first calculate the statistic  $S_{y/x}$ , which estimates the random errors in the  $y$ -directions equation 4.1. (Miller and Miller 2005).

$$S_{y/x} = \sqrt{\frac{\sum_i (y_i - \hat{y}_i)^2}{n-2}} \quad (4.1)$$

Equation 4.1 utilizes the  $y$ -residual,  $y_i - \hat{y}_i$ , where the  $\hat{y}_i$  – values are the points on the calculated regression line corresponding to the individual  $x$ - values, *i.e.* the fitted  $y$ -values (Figure 4.1)

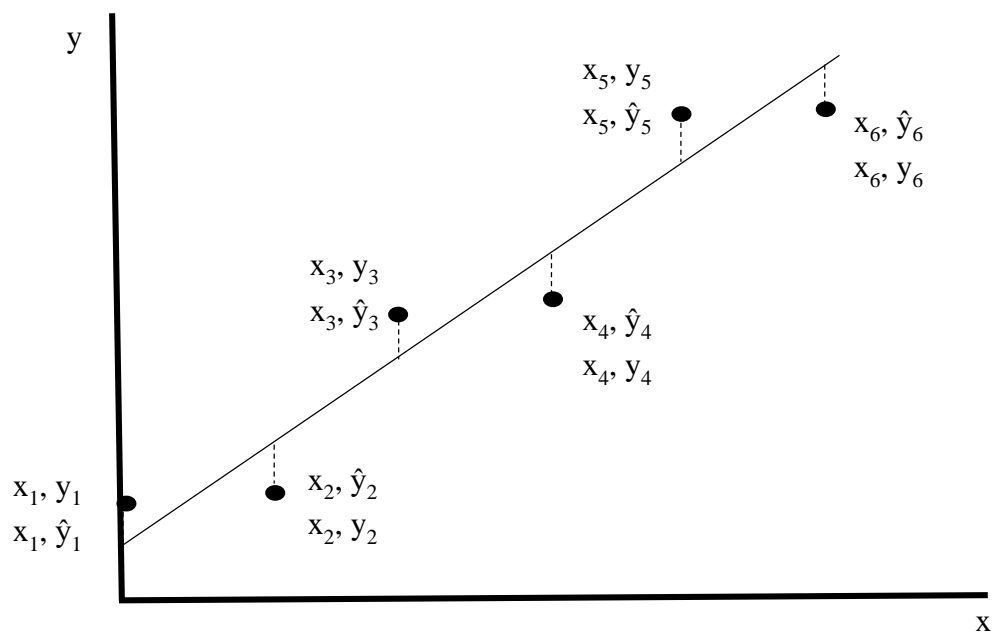


**Figure 4.1** The  $y$ -residuals of a regression line (Miller and Miller, 2005)

A value for  $S_{y/x}$  can be used to calculate  $S_b$  (the standard deviations of slope) and  $S_a$  (the standard deviations of intercept) as shown in equation 4.2 and 4.3 respectively.

$$S_b = \frac{S_{y/x}}{\sqrt{\sum_i (x_i - \bar{x})^2}} \quad (4.2)$$

$$S_a = S_{y/x} \sqrt{\frac{\sum_i x_i^2}{n \sum_i (x_i - \bar{x})^2}} \quad (4.3)$$

#### 4.2.5.2 Limit of detection (LOD) and limit of quantification (LOQ) of GC-FID

LOD was estimated following the International Union of Pure and Applied Chemistry (IUPAC) recommendations by using the concentration corresponding to 3-folds the standard deviation of 20 measurement of the blank divided by the slope of the calibration curve (Long and Winefordner, 1983).

LOQ is defined as the lowest concentration of the analyte in the sample that can be determined with an acceptable precision and an accuracy under the stated operational conditions of the method (Swartz and Krull, 1997). It was investigated by considering the concentration of 10-folds of the standard deviation of 20 measurements of the blank divided by the slope of the calibration curve (Long and Winefordner, 1983).

In this study blank was prepared by mixing 1 mL of methanol in 14 mL of ultrapure water and was added in a 30 mL head space vial. Then the vial was sealed with a rubber septum and aluminum cap and were placed in a the laboratory-built water bath at 60°C for 10 minutes and then 0.1mL of gas phase was injected into the gas chromatographic system that was operated under its optimum conditions.

The LOD and LOQ were calculated using the equation 4.5

$$C_L = \frac{kS_B}{m} \quad (4.5)$$

Where;

$C_L$  = the limit of detection or limit of quantification

$S_B$  = the standard deviation of the response from blank (20 injections)

$m$  = the slope of the calibration curve

$k$  = the number factor chosen according to the confidence level,

$k = 3$  or  $3\sigma$  for the calculation of limit of detection and

$k = 10$  or  $10\sigma$  for the calculation of limit of quantification

#### 4.2.6 Re-development of the printed circuit board (PCB) passive sampler

A printed circuit board (PCB) passive sampler was fabricated using a previously reported procedure (Saelim *et al.*, 2013). In brief, the PCB board was cut into a desired size of  $1 \times 3 \text{ cm}^2$  and polished with alumina slurry. To increase the surface area, the cut pieces were etched with conc. HCl: H<sub>2</sub>O<sub>2</sub>: H<sub>2</sub>O at the volume ratio of 1:2:4 followed by the deposition of silver particles by immersing 2.0 cm of the etched PCB in 3.0 mM of AgNO<sub>3</sub> prepared in propylene glycol. Electropolymerization of polypyrrole by cyclic voltammetry was performed with a potentiostat (model 410, EDAQ, Australia) coupled with an electrochemical cell containing a silver particles modified PCB working electrode, a Ag/AgCl reference electrode and a Pt rod auxiliary electrode. By changing the applied potential from 0.0 to 1.2 V in 15 mL of 0.5 M pyrrole prepared in 0.20 M sodium tartarate solution, with a scan rate of 0.1 Vs<sup>-1</sup> for 100 scans a polypyrrole sorptive layer was electropolymerized onto the Ag particles coated PCB.

#### 4.2.7 Validation of the PCB passive sampler

In the previous work of Saelim and co-workers (Saelim *et al.*, 2013), the passive sampler was validated for the monitoring of xylene and styrene in copy print shops. To use it with BTX in ambient outdoor air it was important to re-validate the PCB passive sampler. This was done using a thermal desorption system coupled with a gas chromatograph with flame ionization detector (GC-FID). Fig. 4.2 shows the schematic diagram of the thermal desorption system. It was built out of a brass block ( $\emptyset$  3.0 cm, and 5.0 cm height) with a 1.8 cm diameter and 4.0 cm deep hole drilled into it to fix the glass chamber. The heat was supplied through a soldering iron rod (70 watt, PX-201, Japan) fitted tightly into a drilled hole at the bottom of the brass block. The temperature of the brass block was monitored by a thermocouple-multimeter (DL 297T digital multimeter, Universal Enterprises, Inc. Korea). The passive sampler was placed inside a glass chamber with an inner diameter of

1.24 cm and a height of 5 cm where the adsorbed analytes were then thermally desorbed (Thammakhet *et al.*, 2004).

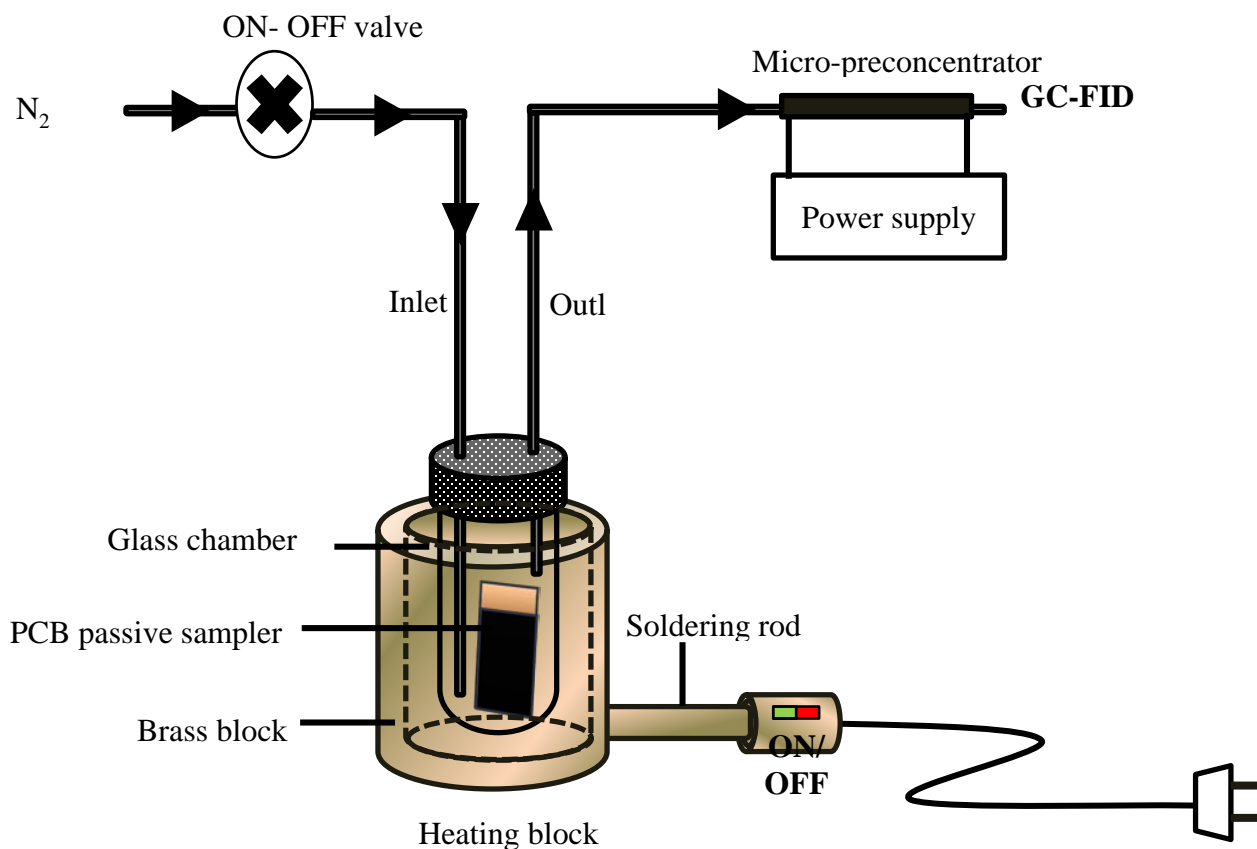


**Figure 4.2** Schematic diagram of the laboratory-built thermal desorption system coupled with on-line micro-preconcentrator,

An on-line micro-preconcentrator was prepared by packing 1.0 mg of multi-walled carbon nanotubes ( $\geq 95\%$  purity) with diameters of 60–100 nm and lengths of 2–5  $\mu\text{m}$  (Shenzhen Nanotech Port Co., Ltd, Shenzhen, China) inside a silico steel tube of 15 cm

long, 0.0525 mm I.D., and 0.725 mm O.D., (Restek Co., Bellefonte, PA, USA). It was placed at the outlet of the glass chamber to preconcentrate the analytes before entering the separation column of the GC-FID.

Operation of the thermal desorption system consists of the following steps. A passive sampler was firstly placed inside an air tight glass chamber which was heated for a certain time so as to desorb the adsorbed analytes. Nitrogen gas was then purged at a rate of  $1.0 \text{ mL min}^{-1}$  into the glass chamber by turning on the valve. The outflow of  $\text{N}_2$  carried the desorbed analytes to the on-line micro-preconcentrator. As the analytes passed through the on-line micro-preconcentrator the multi-walled carbon nanotubes adsorbed the analytes while the  $\text{N}_2$  continued to the injection port of the GC where it mixed with the continuous flow of the  $\text{N}_2$  carrier gas (the total flow rate was controlled at  $1.5 \text{ mL min}^{-1}$  measured by soap a flow meter at detector port before analysis). After an appropriate adsorption time the steel tube of the micro-preconcentrator was heated with a current pulse from the power supply to release the adsorbed analytes into the continuous  $\text{N}_2$  gas flow. Simultaneously the start button of GC-FID is pressed for the analysis of the desorbed analytes. When the analysis is completed, the valve is switch to off position, stopping the flow of  $\text{N}_2$  from the glass chamber until the next cycles.

The GC-FID operation parameters were optimized using standard gases prepared as described in section 2.2. To obtain the highest desorption efficiency, parameters of the thermal desorption system were also optimized. These include desorption time, desorption temperature, heating potential, heating time and adsorption time of the micro-preconcentrator. For the optimization, the PCB passive sampler was first exposed to 1.0 ppm of standard gas of BTX in an air tight 5 mL glass vial for 10 min. The sampler was then transferred to a glass chamber to be thermally desorbed before being analyzed by the GC-FID. The initial conditions of the thermal desorption system coupled with the micro-preconcentrator were:  $190 \text{ }^\circ\text{C}$  and 5 min for the desorption temperature and time, 3.0 V and 0.5 s for the heating potential and time of the micro-preconcentrator with 5 min of adsorption time. Each parameter was optimized while other were kept constant. The optimum value was chosen by using the criteria of the highest peak area and good resolution.

In this study the standard gases of benzene, toluene and xylene were prepared by injecting a known volume of standard solution in a 30 mL air tight head space vial. The principle of headspace analysis was used to generate different gas standard. The concentration of the standard gas was calculated by using the equilibrium equation of headspace analysis (equation 4.6) (Kolb and Ettre, 2006)

$$C_G = \frac{C_o}{K + \beta} \quad (4.6)$$

Where;

$C_G$  = concentration of analyte in gas phase

$C_o$  = original concentration of analyte

$K$  = partition coefficient of each analyte

$\beta$  = phase ratio

#### 4.2.8 Analytical performance of the system

The analytical performances of the chromatographic system coupled with the thermal desorption system were evaluated using BTX standard under optimum conditions. Passive samplers were placed inside the 5 mL air tight glass vials and were exposed to series of BTX standard (0.1 to 100 ppm) for 10 min. Each sampler was then thermally desorbed (section 2.4) and analyzed by the GC-FID. A calibration curve was plotted between the obtained signal and mass of the analytes (calculated from the injected volume of the standard gas concentration) five replications for each concentration. Linearity was determined from the curve plotted between the peak area ( $\mu V.s$ ) and the mass of the analyte ( $\mu g$ ), when the coefficient of determination ( $R^2$ ) was greater than 0.99 (Authority, 2004). The limit of detection (LOD) and limit of quantification (LOQ) were estimated as per the

IUPAC recommendation as the concentration to 3-fold and 10-fold of the standard deviations of 20 blank injections (Long and Winefordner, 1983).

#### 4.2.8.1 Sampling time

For an effective sampling of BTX in ambient outdoor air, the sampling time was investigated. The PCB sampler was first fitted into a holder, covered with a thin stainless steel mesh, placed in an open box and hung upside down (Fig. 4.3). The box protected the passive samplers from the sun and rain. Information related to its purpose was labeled on the box. Five boxes, each with 5 samplers, were hung at a busy cross-road. The first box was collected after a 24 hour (day 1) exposure and analysed in the laboratory. Other boxes were collected after 2, 5, 7 and 14 days of exposure. The mass uptake of the BTX by the passive sampler was calculated by substituting the obtained peak area in the linear equation of the calibration curve. A plot between the uptake versus exposure time was used to determine the suitable sampling time.

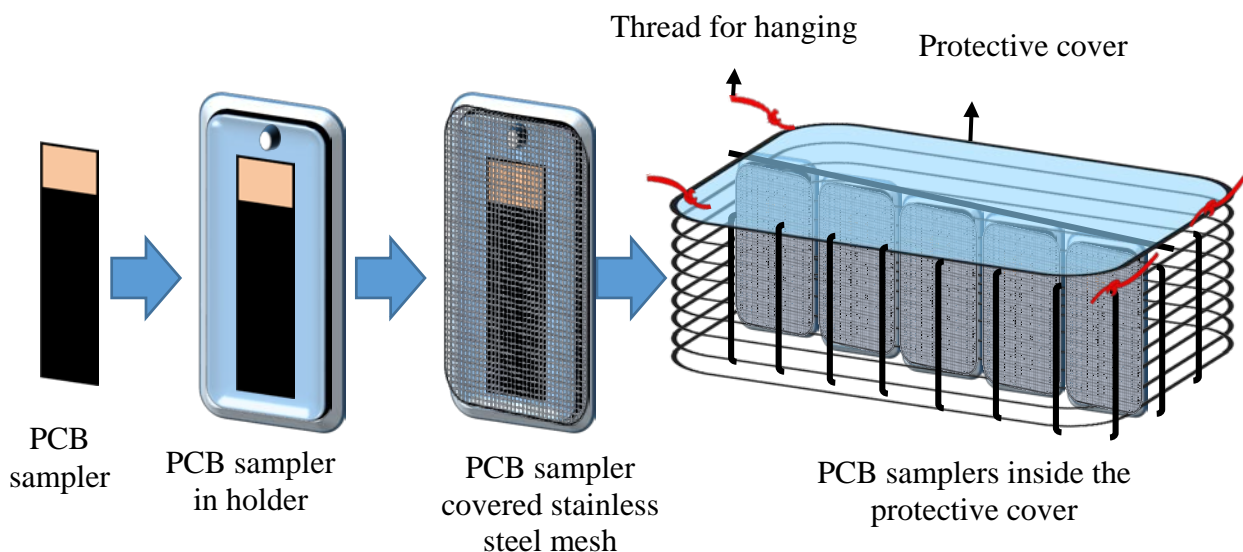


**Fig. 4.3** Hanging of PCB passive sampler

#### 4.2.9 Sampling sites

Hat Yai is a commercial city located in the southern part of Thailand (7.02° N, 100.47° E) near the Malaysia border with approximately 30 kilometers away from the south of the Gulf of Thailand. The city occupies an area of 7,393 square kilometers on the eastern side of the Malaysian peninsula. It is one of the largest commercial hubs of southern Thailand (Pongichan et al., 2014). Record shows that in 2013 the number of registered cars and motorcycles in Hat Yai city was 33,257 and 39,859 (Statistics 2013 Songkhla transport office). Besides, there are numbers of vehicles coming to Hat Yai city from nearby provinces and even from Malaysia. Since Hat Yai is a fast-growing and economically developed city, it is important to detect the air pollutants in ambient air from time to time to monitor air quality.

Samples were collected from sixteen sites (S1-S16) (Fig. 4.4) to cover the representative areas of the city. S1 and S2, at Prince of Songkla University reservoir, were selected as the control because of the very low traffic as compared to other sites. S3, S4 and S5 are along a double lane highway heading to the Malaysian border. It is considered as one of the busiest road of the city with a large volume of traffic flow. S6, S7 and S8 are major roads intersections where a large numbers of automobiles, including big trucks and buses, move through. S9, S10 and S11 are located in the heart of the city, with many shopping malls, big hotels and also a number of street side fried food stalls. S12 and S13 are within a gasoline station, located along one of the busy road. S12 was next to the diesel dispenser and S13 was next to the one for petrol. S14, S15, S16 are on narrow busy roads which connect the city to other provinces. These sites were selected based on the large number of traffic flow to and from the city.



**Figure 4.4** Map showing the locations of sampling sites (S1 to S16)

### 4.3 Results and Discussion

#### 4.3.1 Optimization of GC-FID conditions

Various parameters of GC-FID was optimized to obtain highest response, good separation and short analysis time.

### 4.3.1.1 Carrier gas (N<sub>2</sub>) flow rate

In gas chromatographic system the retention time, peak area and column efficiency is affected by carrier gas flow rate. Therefore, it is important to optimize the carrier gas flow rate so as to get short analysis time, highest peak area and good column efficiency. The optimum carrier gas flow rate was obtained from the lowest HETP value of the van Deemter plot, a plot between the HETP and carrier gas flow rate (Figure 4.5). And theoretical HETP can be calculated from the van Deemter equation (equation 4.7). This equation explains the extent to which a component band spreads as it passes through the column in terms of physical constants and mass transfer effect *e.g.* eddy diffusion, longitudinal diffusion and resistance to mass transfer (Grob and Barry, 2004).

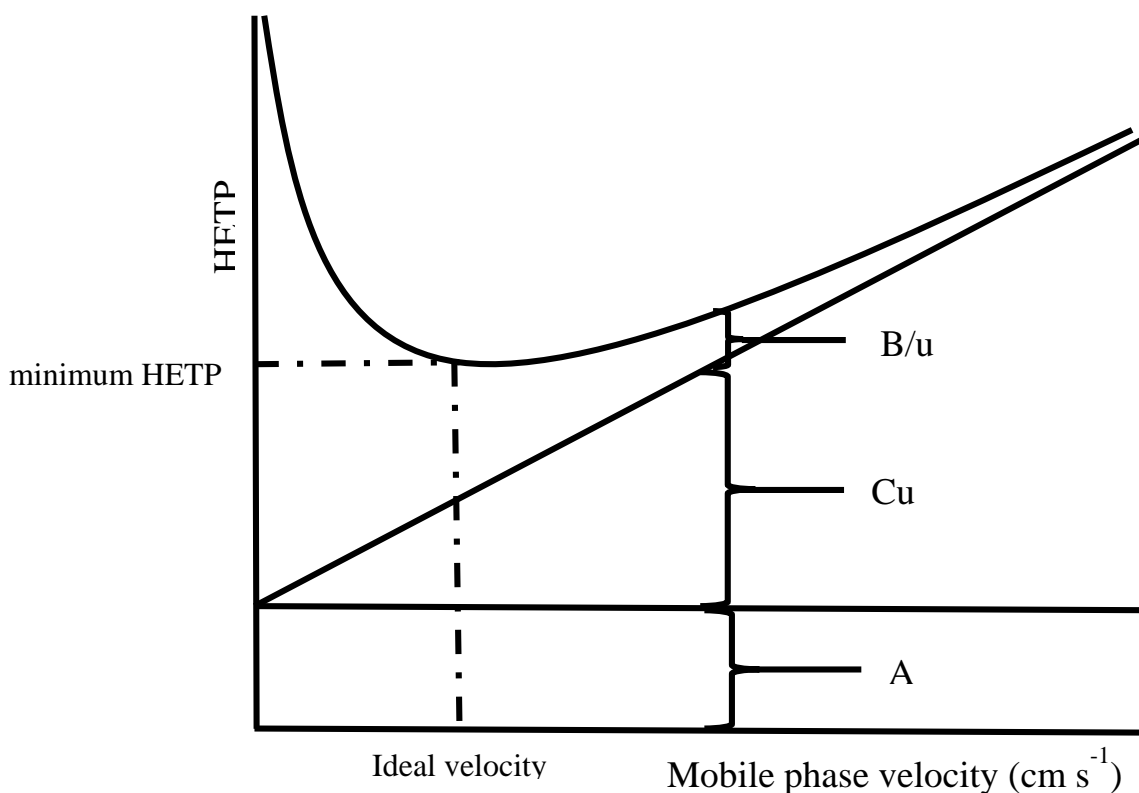


**Figure 4.5** The van Deemter plot

$$\text{HETP}(H) = A + \frac{B}{u} + Cu \quad (4.7)$$

Where;

A is an eddy diffusion or multi-path effect

B is a longitudinal diffusion term

C is a resistance to mass transfer term

u is the linear velocity of carrier gas

The equation 4.7 shows the relationship between the HETP and the flow rate of a carrier gas (u). Optimum column resolution is obtained at the optimum carrier gas flow rate (Grob and Barry, 2004).

In a capillary column unlike pack column the A-term (eddy diffusion) as shown in equation 4.7 do not exist because there is only one flow path but in pack column the flow of the gas passes through the packing materials. Term B/u describes the longitudinal diffusion that represents the diffusion of the analytes in the mobile phase. In capillary column, this term becomes smaller as the velocity increases because less time is available for the solute to diffuse. The C-term (resistance to mass transfer) has the greatest effect on band broadening and its effect in a capillary column is controlled by the mass transfer in the gas phase. Therefore, the equation 4.7 gets modified for a capillary column which is also known as the Golay equation (equation 4.8) (Grob and Barry, 2004).

$$\text{HETP}(H) = \frac{B}{u} + C_g u \quad (4.8)$$

Practically it is very difficult to calculate the terms A, B and C as shown in equation 4.7. However, the plate theory assumes that the column is divided into a number of zones called theoretical plate (*N*). The zone thickness or HETP can be determined by assuming

that there is a perfect equilibrium between gas and liquid phases within each plate. Thus, the column efficiency in terms of HETP can be determined by using equation 4.9

$$\text{HETP} = \frac{L}{N} \quad (4.9)$$

Further, the plate number ( $N$ ) of the column can be calculated from equation 4.10.

$$N = 2\pi(t_R h/A)^2 \quad (4.10)$$

Where;

$L$  is the column length (cm)

$\pi$  is equal to 3.14159

$t_R$  is the retention time (s)

$h$  is the integrated peak height ( $\mu\text{V}$ )

$A$  is the integrated peak area ( $\mu\text{V}\cdot\text{s}$ )

HETP was calculated using equation 4.9 by substituting the  $L$  (column length) which is already known and  $N$  calculated from the peak areas obtained from different flow rates of carrier gas. The experimentally obtained HETPs for BTX gas at each carrier gas flow rate are summarized in Table 4.2. The data in this table were used for plotting a van Deemter plot (Figure 4.6) and  $1.5 \text{ mL min}^{-1}$  was obtained as the optimum flow rate of the carrier gas. The  $1.5 \text{ mL min}^{-1}$  of carrier gas flow rate was chosen as the optimum flow rate it is because at this flow rate, it provided the lowest HETP and provided highest separation efficiency of the column.

**Table 4.2** The HETP calculated from the chromatograms obtained from the analysis of 5.0 ppm of BTX standard gases at various carrier gas flow rate (n = 5)

Carrier gas (N <sub>2</sub> ) flow rate (mL min <sup>-1</sup> )	HETP for benzene (cm)	%RSD	HETP for Toluene (cm)	%RSD	HETP for xylene (cm)	%RSD
1.0	2.160±0.031	1.4	0.340±0.011	3.2	0.640±0.012	1.9
1.5	2.090±0.052	2.5	0.320±0.021	6.5	0.620±0.013	2.1
2.0	2.210±0.061	2.8	0.330±0.012	3.6	0.650±0.012	1.8
2.5	2.22±0.14	6.3	0.350±0.021	6.0	0.730±0.022	3.0
3.0	2.17±0.21	9.6	0.360±0.032	8.9	0.820±0.011	1.3

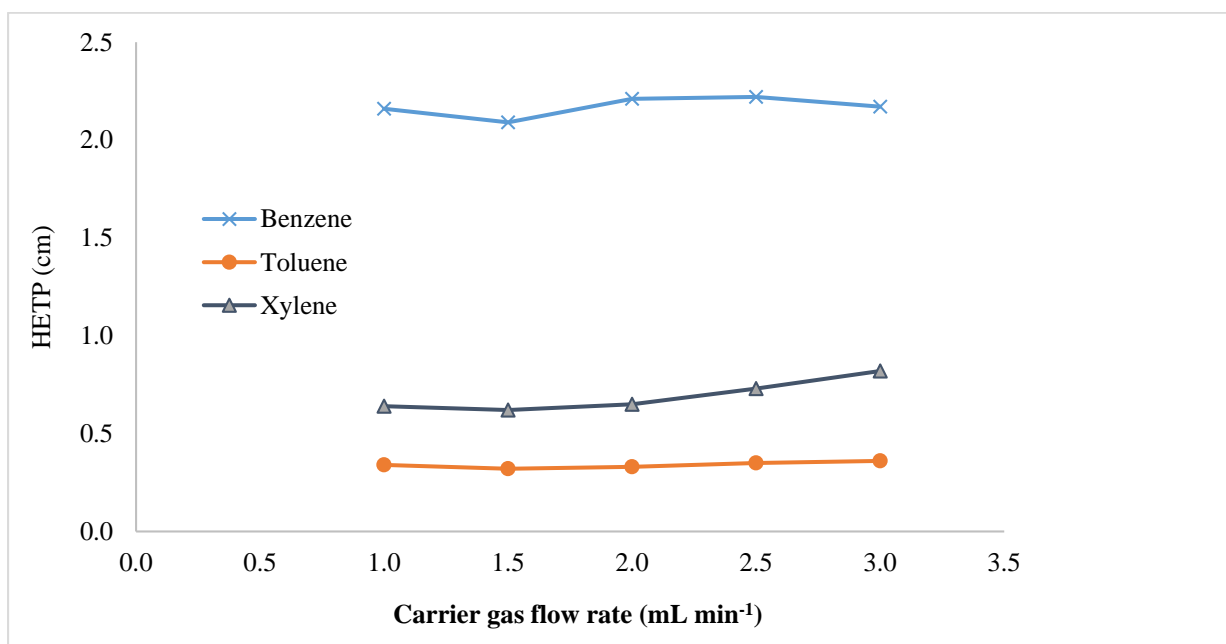


**Figure 4.6** The van Deemter plots of BTX at 5.0 ppm (n = 5)

### 4.3.1.2 Make up gas (N<sub>2</sub>) flow rate

Since the flow of the carrier gas in a capillary column is small, make up gas is used to sweep the analytes into the detector for improving the response of the target analytes (Chasteen 2000; Grob and Barry, 2004). Make up gas flow rate was studied from 20 to 50 mL min<sup>-1</sup>. The peak area of BTX increases with increase of make up gas flow rate 20 to 40 mL min<sup>-1</sup>. After 40 mL min<sup>-1</sup>, the obtained peak area decreases (Table 4.3 and Figure 4.7). Therefore, 40 mL min<sup>-1</sup> was selected as the optimum make up gas flow rate.

**Table 4.3** Peak area of 5.0 ppm of BTX at various make up gas flow rates (n = 5)

Make up gas (N <sub>2</sub> ) flow rate (mL min <sup>-1</sup> )	Peak area (×10 <sup>4</sup> μV.s)					
	Benzene	%RSD	Toluene	%RSD	Xylene	%RSD
20	9.58±0.29	3.0	5.45±0.28	5.1	1.140±0.061	5.3
30	10.52±0.32	3.0	6.02±0.19	3.1	1.35±0.15	11.1
40	12.25±0.56	4.6	7.07±0.13	1.8	1.670±0.072	4.3
50	11.38±0.31	2.7	6.63±0.16	2.4	1.610±0.041	2.5

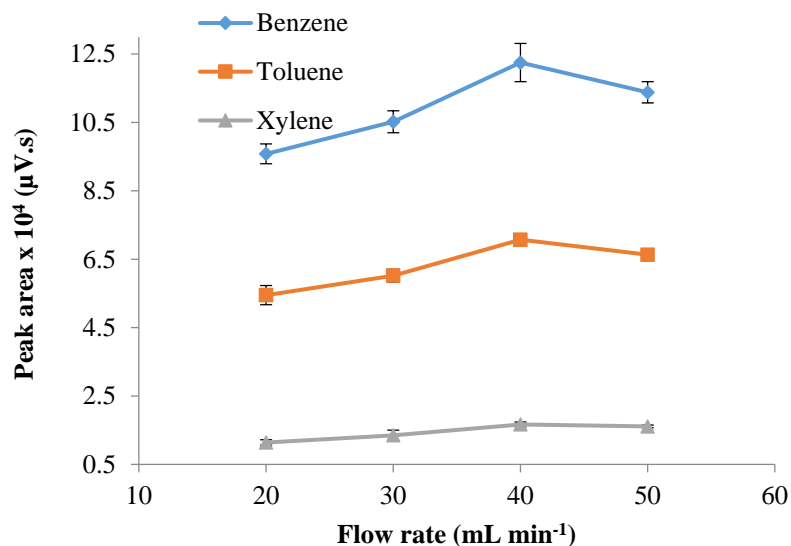


**Figure 4.7** Effect of the make-up gas flow rate on the peak area of 5.0 ppm BTX (n = 5)

#### 4.3.1.3 Fuel gas (H<sub>2</sub>) and oxidant gas (air) flow rates

The process of flame ionization detector involves the ionization mechanism which requires fuel and oxidant gas to make the flame and flow rates of fuel and air can significantly affect the detector sensitivity and the noise levels. The fuel gas and oxidant gas flow rates were simultaneously optimized. The data of the peak area of BTX at different flow rate of fuel gas and oxidant gas are summarized in Table 4.4 and Figure 4.8, Figure 4.9 and Figure 4.10 respectively. The result shows that highest peak area was obtained when the fuel and oxidant gas flow rate were 40 and 250 mL min<sup>-1</sup>.

**Table 4.4** Peak area of 5.0 ppm BTX at various flow rates of fuel (H<sub>2</sub>) and oxidant (Air) gas (n = 5)

Oxidant (air) flow rate (mL min <sup>-1</sup> )	Fuel (H <sub>2</sub> ) gas flow rate (mL min <sup>-1</sup> )	Peak area (×10 <sup>4</sup> μV.s)		
		Benzene	Toluene	Xylene
200	20	4.800±0.041	4.000±0.062	1.110±0.031
	30	10.00±0.11	9.810±0.031	1.310±0.032
	40	12.04±0.41	11.43±0.31	1.650±0.041
	50	11.33±0.54	11.04±0.33	1.560±0.042
250	20	4.300±0.051	4.330±0.031	1.140±0.041
	30	9.900±0.041	9.55±0.11	1.320±0.022
	40	13.05±0.54	12.42±0.49	1.8±0.051
	50	12.25±0.32	11.25±0.25	1.630±0.041
300	20	4.830±0.031	4.390±0.051	1.202±0.021
	30	10.11±0.26	9.840±0.062	1.230±0.031
	40	12.39±0.45	12.05±0.51	1.640±0.052
	50	11.82±0.22	11.64±0.27	1.530±0.031

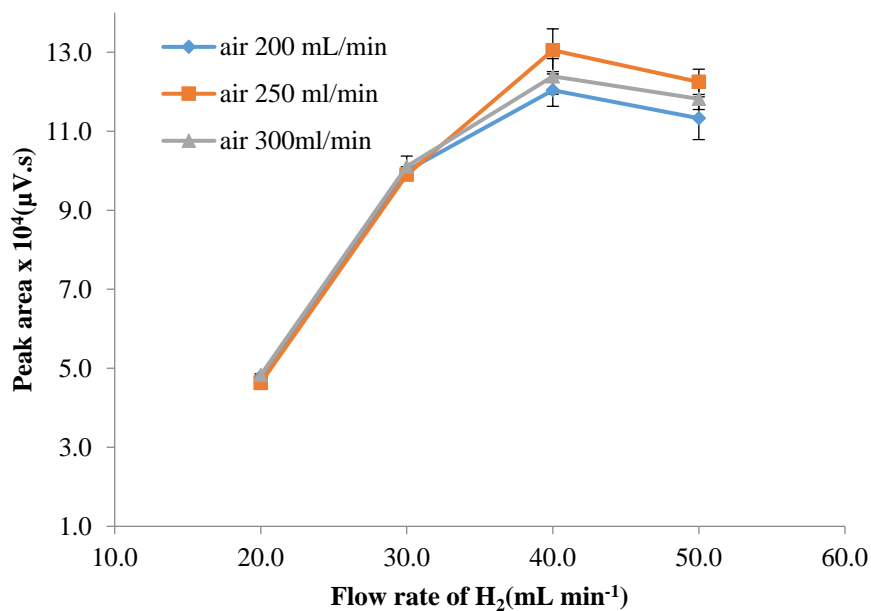


**Figure 4.8** Effect of the fuel and oxidant gas flow rate on the peak area of 5.0 ppm benzene (n = 5)

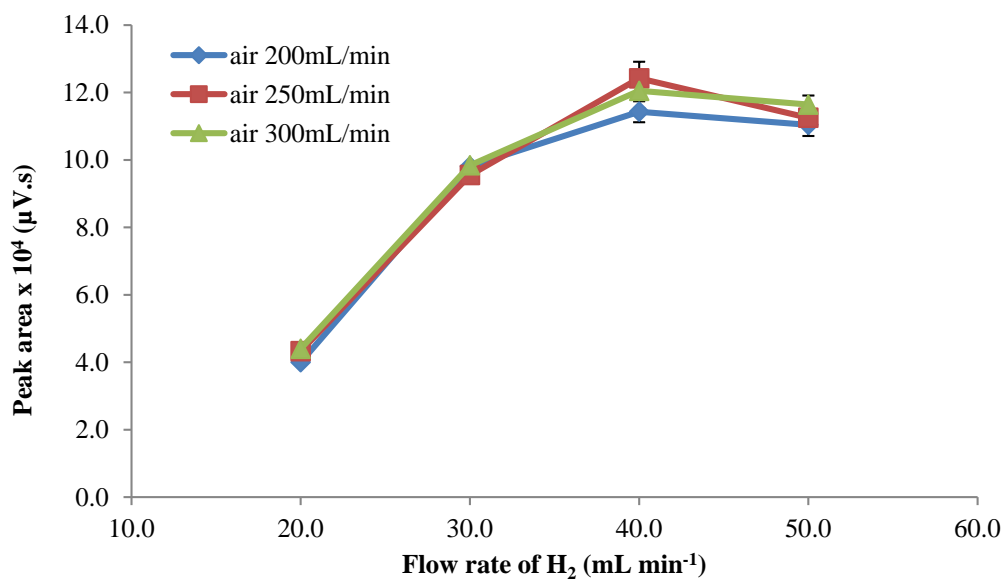


**Figure 4.9** Effect of the fuel and oxidant gas flow rate on the peak area of 5.0 ppm toluene (n = 5)

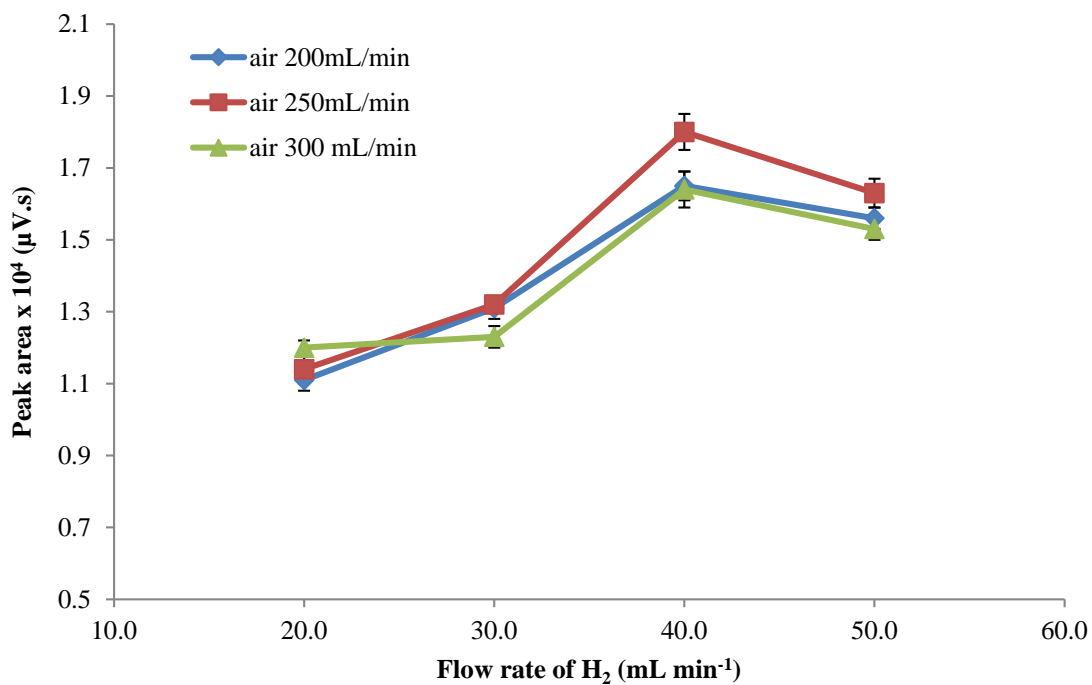


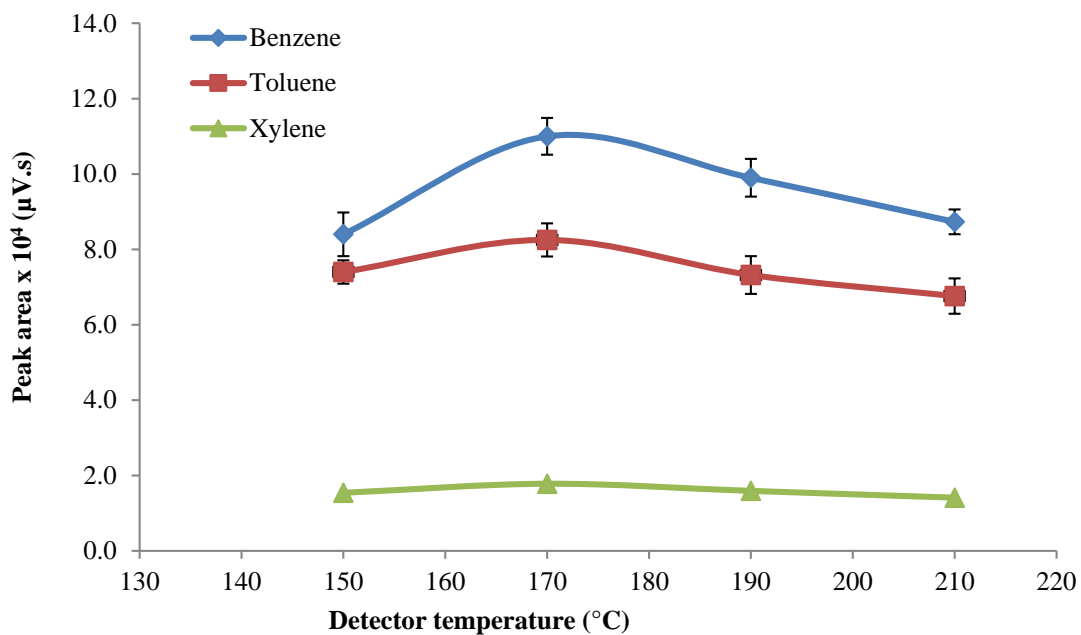
**Figure 4.10** Effect of the fuel and oxidant gas flow rate on the peak area of 5.0 ppm xylene (n = 5)

#### 4.3.1.4 Detector temperature

The detector temperature was optimized by varying the detector temperature from 150 to 210°C, and the optimum detector temperature was selected by considering the effect of the temperature on a peak area of BTX. The peak area of BTX increases with increase of detector temperature from 150 to 190°C. It was found that the highest peak areas of BTX was obtained at 170°C therefore, the detector temperature was fixed at 170°C for further studies. The data obtained for various detector temperature on peak area of BTX is summarized in Table 4.5 and Figure 4.11.

**Table 4.5** Peak area of 5.0 ppm BTX at various detector temperature (n = 5)

Detector temperature (°C)	Peak area ( $\times 10^4 \mu\text{V}\cdot\text{s}$ )					
	Benzene	%RSD	Toluene	%RSD	Xylene	%RSD
150	8.41 $\pm$ 0.58	6.9	7.43 $\pm$ 0.31	4.2	1.540 $\pm$ 0.091	5.9
170	11.00 $\pm$ 0.49	4.5	8.25 $\pm$ 0.44	5.3	1.780 $\pm$ 0.082	4.6
190	9.90 $\pm$ 0.51	5.1	7.32 $\pm$ 0.51	7.0	1.590 $\pm$ 0.062	3.9
210	8.73 $\pm$ 0.31	3.6	6.76 $\pm$ 0.47	7.0	1.42 $\pm$ 0.11	7.7

**Figure 4.11** Effect of the detector temperatures on the peak areas of 5.0 ppm BTX standard gas (n = 5)

### 4.3.1.5 Injector temperature

The injector temperature is one of the important part of the GC system. The injector temperature should be high enough to convert the injected analyte into the gas phase instantaneously in order to provide the rapid transfer of the analytes into the separation column. The injector temperature was varied from 150 to 210°C. The result showed that the peak area of the analyte BTX increased with increase of injector temperature from 150 to 190°C. Optimum peak area of BTX was obtained at injector temperature of 190°C which, was chosen as the optimum injector temperature. Table 4.6 and Figure 4.12 shows the summary of BTX various peak area obtained at different injector temperature.

**Table 4.6** Peak areas of 5.0 ppm BTX at various injector temperature (n = 5)

Injector temperature (°C)	Peak area ( $\times 10^4 \mu\text{V.s}$ )					
	Benzene	%RSD	Toluene	%RSD	Xylene	%RSD
150	8.29 $\pm$ 0.35	4.2	7.72 $\pm$ 0.37	4.8	1.240 $\pm$ 0.071	5.7
170	8.69 $\pm$ 0.18	2.1	8.02 $\pm$ 0.19	2.4	1.340 $\pm$ 0.032	2.4
190	9.27 $\pm$ 0.29	3.1	8.29 $\pm$ 0.21	2.5	1.430 $\pm$ 0.082	5.7
210	8.27 $\pm$ 0.32	3.9	7.32 $\pm$ 0.31	4.2	1.230 $\pm$ 0.031	2.5

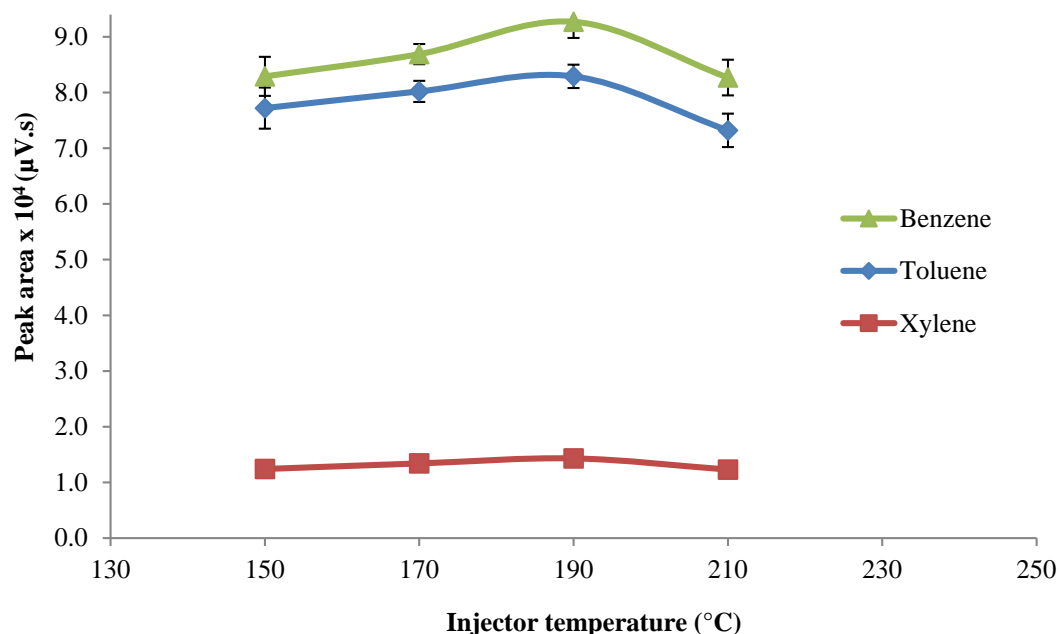


**Figure 4.12** Effect of the injector temperatures on the peak areas of 5.0 ppm BTX standard gas (n = 5)

#### 4.3.1.6 Column temperature programming

Column temperature programming is very much necessary in GC in order to minimize the eluting time of the target analytes and to obtain peak with narrow width and good resolutions. Column temperature programming is usually used for the unknown samples or samples of high complexity, with high-boiling components, which might not elute or be detected under isothermal conditions. Moreover it also helps “clean out” a column of remnant high-boiling species from the previous injections (Grob and Barry, 2004). For column temperature programming various column programs were studied as described in section 4.3.1.6, and the results are summarized as follows;

#### 4.3.1.6.1 Initial column temperature

The initial column temperature was varied from 35 to 50°C, and as the temperature was increased from 35 to 40°C, the peak area of BTX increases and after 40°C the peak area decreased with increased of temperature (Table 4.7 and Figure 4.13). The initial temperature at 40°C provided the highest peak area of BTX and it was selected as the optimum initial column temperature.

**Table 4.7** Peak areas of 5.0 ppm BTX at various initial column temperature (n = 5)

Initial column temperature (°C)	Peak area ( $\times 10^4 \mu\text{V.s}$ )					
	Benzene	%RSD	Toluene	%RSD	Xylene	%RSD
35	9.270 $\pm$ 0.081	0.87	6.93 $\pm$ 0.13	1.9	2.160 $\pm$ 0.041	1.9
40	9.74 $\pm$ 0.31	3.2	7.45 $\pm$ 0.44	5.9	2.300 $\pm$ 0.091	4.0
45	8.03 $\pm$ 0.21	2.6	5.89 $\pm$ 0.36	6.1	1.870 $\pm$ 0.072	3.9
50	7.63 $\pm$ 0.25	3.3	5.66 $\pm$ 0.21	3.7	1.720 $\pm$ 0.041	2.4

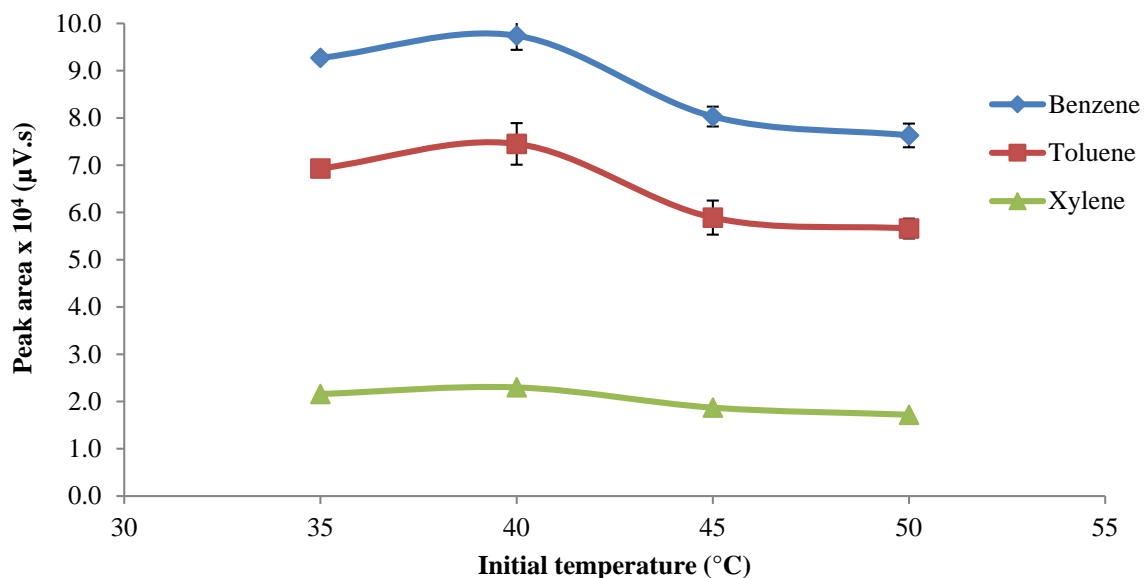


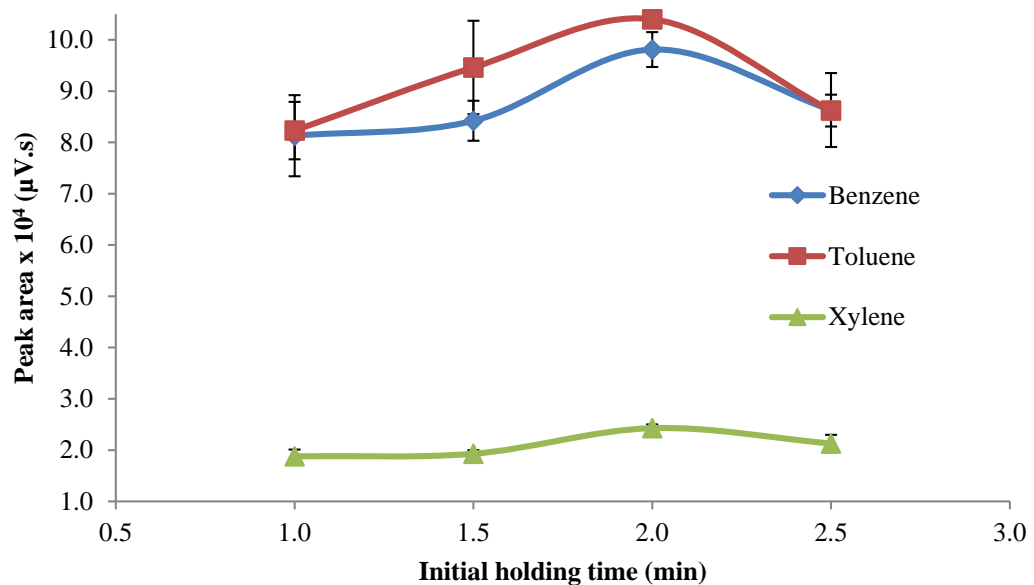
**Figure 4.13** Effect of the initial column temperatures on the peak areas of 5.0 ppm of BTX standard gas (n = 5)

#### 4.3.1.6.2 Initial column holding time

The initial column holding time was studied from 1.0 to 2.5 min. The results from the optimization on initial column holding time are summarized in Table 4.8 and Figure 4.14. Peak area of BTX increases with increase in initial holding time of 1.0 to 2.0 min, after that further increase of the initial holding time, the peak area decreased. This is because at the longer initial holding time the migration of analytes will be slower to the separation column leading to the peak broadening, and poor peak resolution and finally decrease in the peak area. Therefore, 2.0 min was chosen as the optimum initial column holding time.

**Table 4.8** Peak areas of 5.0 ppm BTX at various initial column holding time (n = 5)

Initial column holding time (min)	Peak area ( $\times 10^4 \mu\text{V.s}$ )					
	Benzene	%RSD	Toluene	%RSD	Xylene	%RSD
1.0	8.13 $\pm$ 0.79	9.7	8.230 $\pm$ 0.056	0.68	1.88 $\pm$ 0.13	6.9
1.5	8.42 $\pm$ 0.39	4.6	9.46 $\pm$ 0.91	9.6	1.930 $\pm$ 0.071	3.7
2.0	9.81 $\pm$ 0.34	3.5	10.44 $\pm$ 0.15	1.4	2.430 $\pm$ 0.072	3.0
2.5	8.63 $\pm$ 0.72	8.3	8.62 $\pm$ 0.31	3.6	2.13 $\pm$ 0.17	8.0

**Figure 4.14** Effect of the initial column holding time on the peak areas of 5.0 ppm of BTX standard gas (n = 5)

#### 4.3.1.6.3 Temperature ramp rate

The temperature ramp rate was studied from 15 to 30°C min<sup>-1</sup>. As the ramp rate increases from 15 to 25°C min<sup>-1</sup>, the peak area of BTX also increases and the retention time of the BTX decreases (data not shown). Further increase of the ramp rate the retention time still decreases but at the same time peak area also decreased. Therefore, the column temperature ramp rate was selected 25°C min<sup>-1</sup>. So, the column temperature was ramped from 40°C to the optimum final temperature with the temperature ramp rate of 25°C min<sup>-1</sup>. The result of temperature ramp rate is summarized in Table 4.9 and Figure 4.15.

**Table 4.9** Peak areas of 5.0 ppm BTX at various temperature ramp rates (n = 5)

Temperature ramp rate (°C min <sup>-1</sup> )	Peak area (×10 <sup>4</sup> μV.s)					
	Benzene	%RSD	Toluene	%RSD	Xylene	%RSD
15	9.83±0.60	6.1	8.61±0.47	5.5	2.53±0.13	5.1
20	10.37±0.43	4.1	9.00±0.41	4.6	2.61±0.19	7.1
25	11.08±0.52	4.7	9.47±0.43	4.5	2.74±0.25	9.1
30	10.21±0.36	5.1	8.78±0.36	4.1	2.37±0.23	9.7

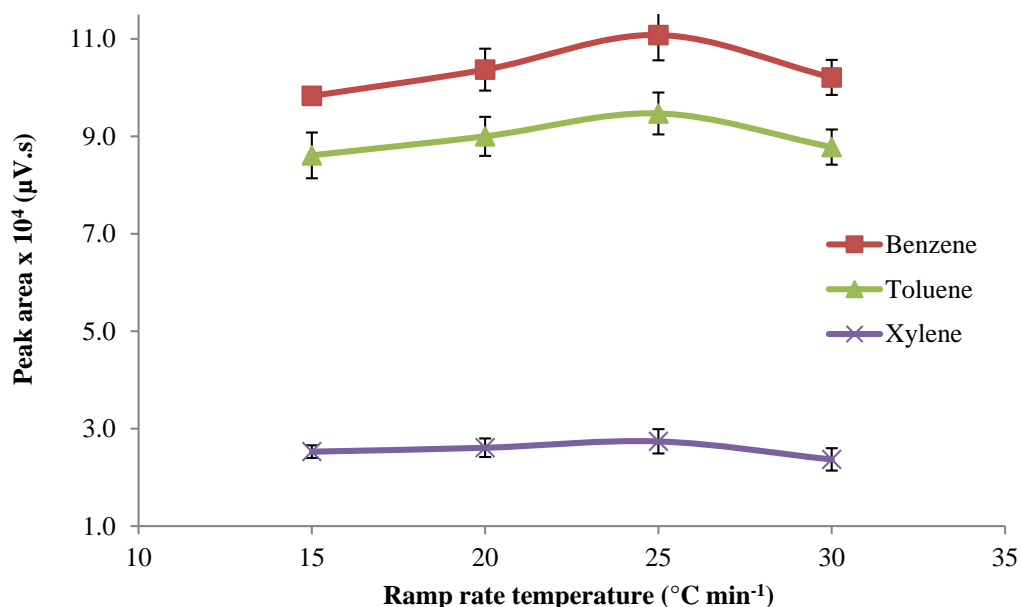


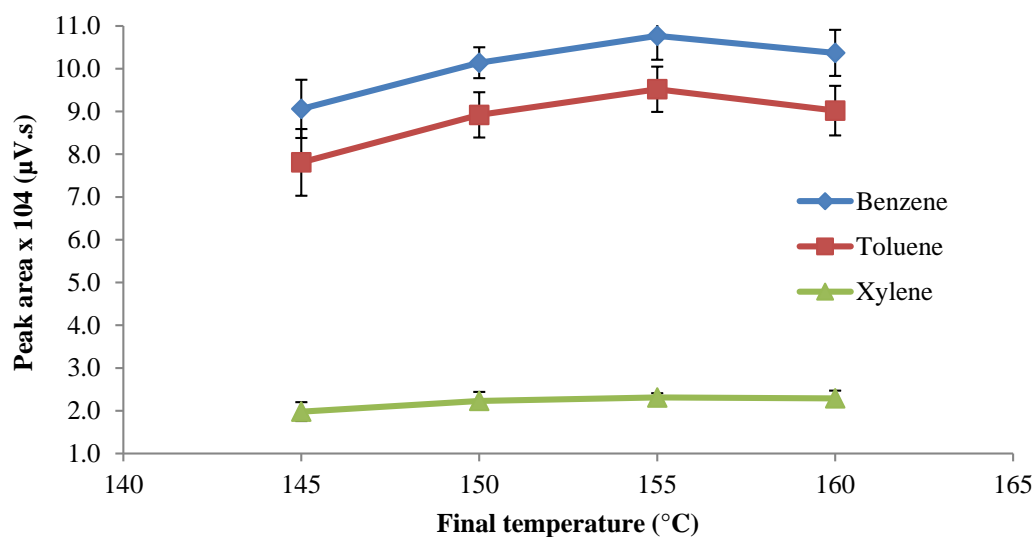
**Figure 4.15** Effect of the temperature ramp rate on the peak areas of 5.0 ppm of BTX standard gas (n = 5)

#### 4.3.1.6.4 Final column temperature

The final column temperature chosen should be sufficient to elute the more strongly retained component in the sample but it should not reach the upper temperature limit of the stationary phase. The results of the final temperatures optimization are shown in Table 4.10 and Figure 4.16. The final column temperature was varied from 145 to 160°C. The result shows that peak area of BTX increase with increase in final column temperature from 145 to 155°C. Above 155°C, the peak area of BTX slightly decreased. Therefore, 155°C was chosen as the optimum final column temperature.

**Table 4.10** Peak areas of 5.0 ppm BTX at various final column temperature (n = 5)

Final column temperature (°C)	Peak area ( $\times 10^4 \mu\text{V}\cdot\text{s}$ )					
	Benzene	%RSD	Toluene	%RSD	Xylene	%RSD
15	9.06 $\pm$ 0.68	7.5	7.81 $\pm$ 0.78	10.0	1.98 $\pm$ 0.22	11.1
20	10.14 $\pm$ 0.36	3.6	8.92 $\pm$ 0.53	5.9	2.23 $\pm$ 0.21	9.4
25	10.77 $\pm$ 0.56	5.2	9.52 $\pm$ 0.53	5.6	2.31 $\pm$ 0.11	4.8
30	10.37 $\pm$ 0.54	5.2	9.02 $\pm$ 0.58	6.4	2.29 $\pm$ 0.18	7.9

**Figure 4.16** Effect of the final column temperature on the peak areas of 5.0 ppm of BTX standard gas (n = 5)

#### 4.3.1.6.5 Final column holding time

The results of final column holding time summarized in Table 4.11 and Figure 4.17. The result shows that the final holding time did not affect much on the peak area of BTX. But there is slight increase in peak area of BTX as the final column holding time increases from 1.5 to 2.5 min. Therefore, 2.5 was chosen as the optimum final holding time.

**Table 4.11** Peak areas of 5.0 ppm BTX at various final column holding time (n = 5)

Final column holding time (min)	Peak area ( $\times 10^4 \mu\text{V.s}$ )					
	Benzene	%RSD	Toluene	%RSD	Xylene	%RSD
1.5	9.64 $\pm$ 0.12	1.2	8.230 $\pm$ 0.051	0.6	1.840 $\pm$ 0.051	2.8
2.0	10.09 $\pm$ 0.29	2.9	8.78 $\pm$ 0.25	2.8	2.030 $\pm$ 0.031	1.5
2.5	10.98 $\pm$ 0.41	3.7	9.79 $\pm$ 0.09	0.9	2.530 $\pm$ 0.052	2.1
3.0	10.64 $\pm$ 0.14	1.3	9.35 $\pm$ 0.13	1.4	2.460 $\pm$ 0.041	1.7

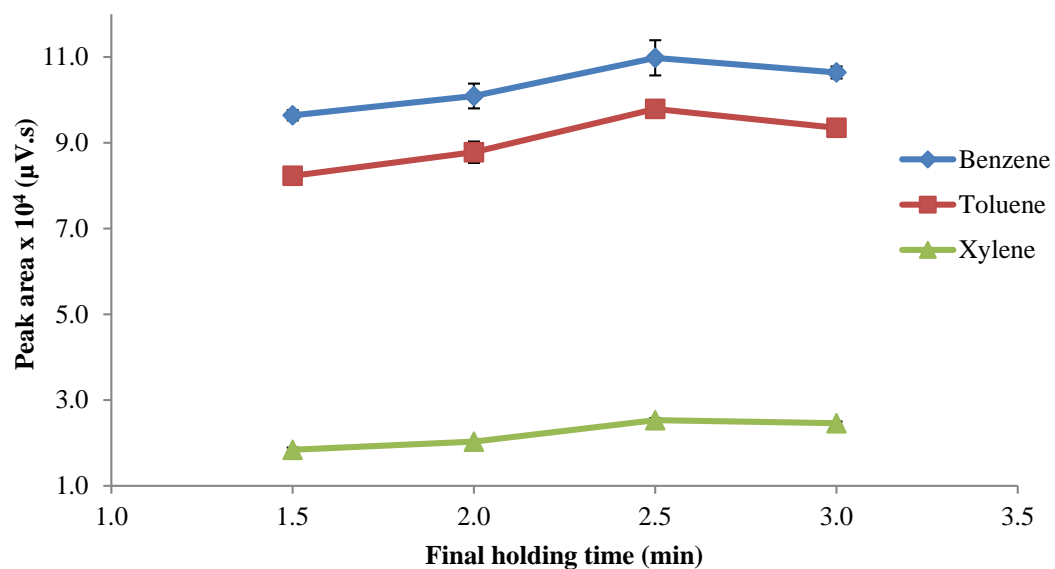


**Figure 4.17** Effect of the final column holding time on the peak areas of 5.0 ppm of BTX standard gas (n = 5)

Figure 4.18 shows the summary of the optimum conditions of the column temperature programming applied for the analysis of BTX by GC-FID.

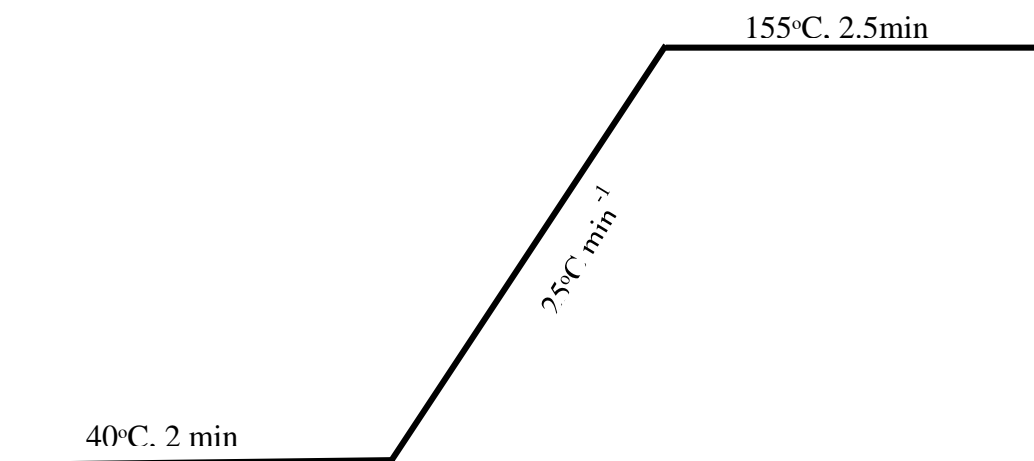


**Figure 4.18** Optimum column temperature programming for the analysis of BTX

#### 4.3.1.7 Summary of GC-FID optimum conditions

Various optimized parameters of GC-FID with their optimum value is summarized in Table 4.12. The chromatogram of BTX at the optimum condition is shown in Figure 4.19 with the retention time of BTX at 4.9, 6.1 and 7.3 respectively.

**Table 4.12** Summary of optimum GC-FID conditions for the determination of 5.0 ppm BTX standard gas

Parameters	Optimized values	Optimum values
Carrier gas (N <sub>2</sub> ) (mL min <sup>-1</sup> )	1.0-3.0	1.5
Make up gas (N <sub>2</sub> ) (mL min <sup>-1</sup> )	20-50	40
Fuel gas (H <sub>2</sub> ) (mL min <sup>-1</sup> )	20-50	40
Oxidant gas (Air) (mL min <sup>-1</sup> )	200-300	250
Injector temperature (°C)	150-210	190
Detector temperature (°C)	150-210	170
Column temperature program		
Initial column temperature (°C)	35-50	40
Initial column holding time (min)	1.0-2.5	2.0
Ramp rate (°C min <sup>-1</sup> )	15-30	25
Final temperature (°C)	145-160	155
Final holding time (min)	1.5-3.0	2.5

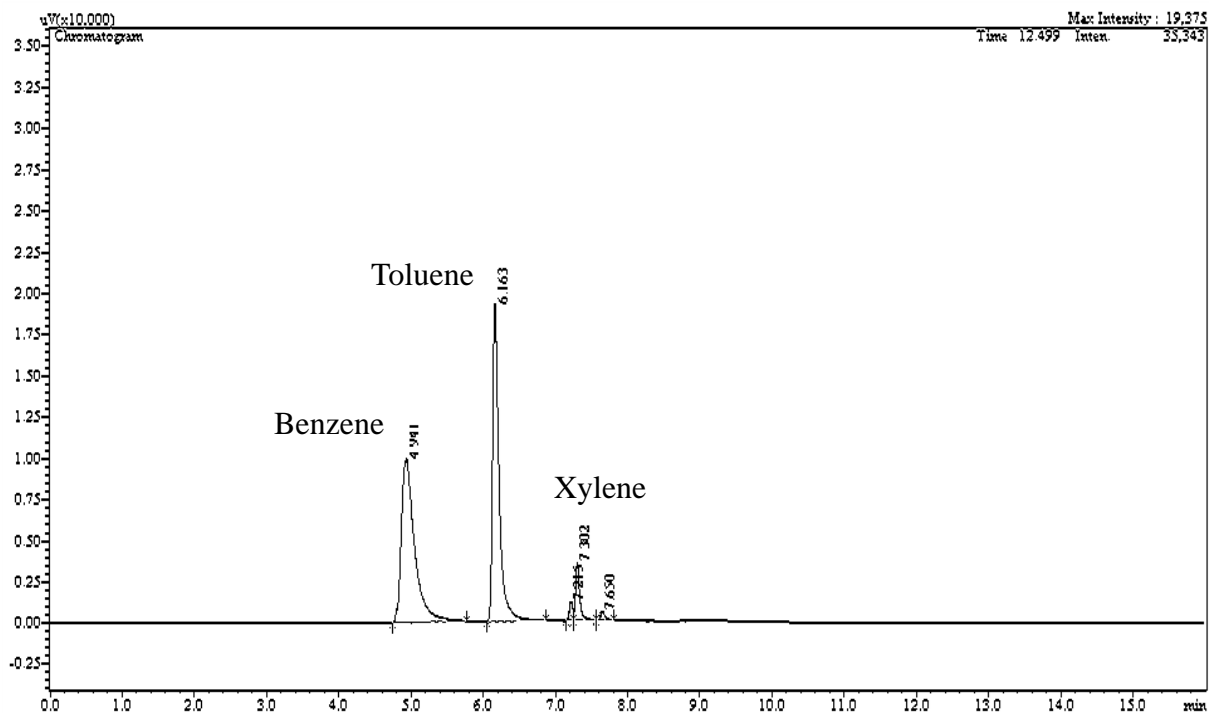


**Figure 4.19** Chromatogram of BTX 5.0 ppm at optimum GC-FID conditions

### 4.3.2 Analytical performance of the GC-FID

#### 4.3.2.1 Linear dynamic range of the GC-FID

Under the optimum GC-FID conditions, linear dynamic range was evaluated. For the evaluation of linear dynamic range a series (0.01 to 80 ppm) of standard BTX gas was injected into the GC-FID system. Then based on the obtained peak area, a calibration curve was plotted between the obtained peak area ( $\mu\text{V}\cdot\text{s}$ ) and the concentration of analyte BTX (ppm). The linear dynamic range is achieved when the  $R^2$  is equal or greater than 0.99 (Authority, 2004), because when the value of  $R^2$  get closer to 1 the slope of the regression line will provide the sensitivity of the regression and method to be validated (Miller and Miller, 2005). The GC-FID provided the linear dynamic range from 0.1 to 80 ppm for all

analyte benzene (Figure 4.20), toluene (Figure 4.21) and xylene (Figure 4.22) with  $R^2$  greater than 0.99 and relative standard deviations (RSD) lower than 4%.

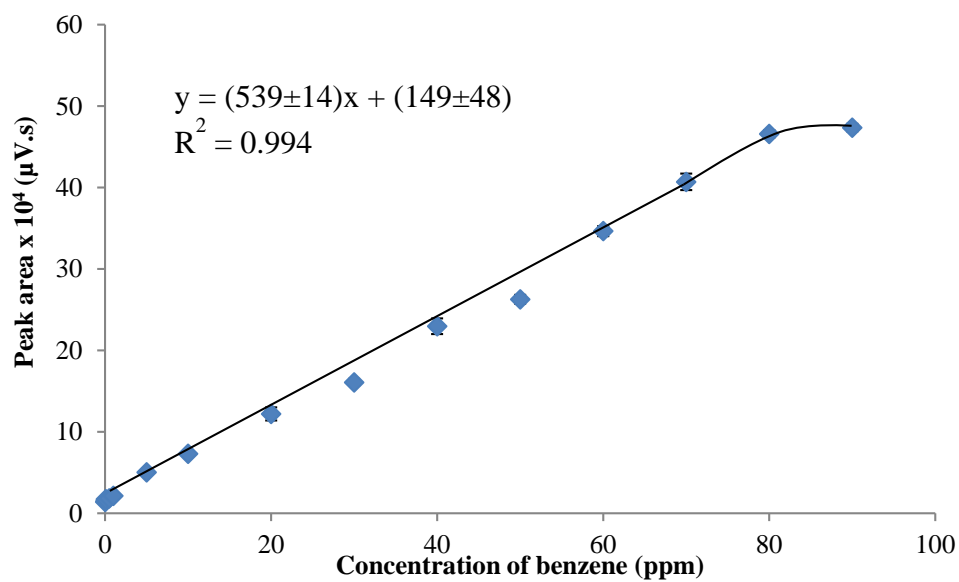


**Figure 4.20** Linear dynamic range of GC-FID for the determination of benzene

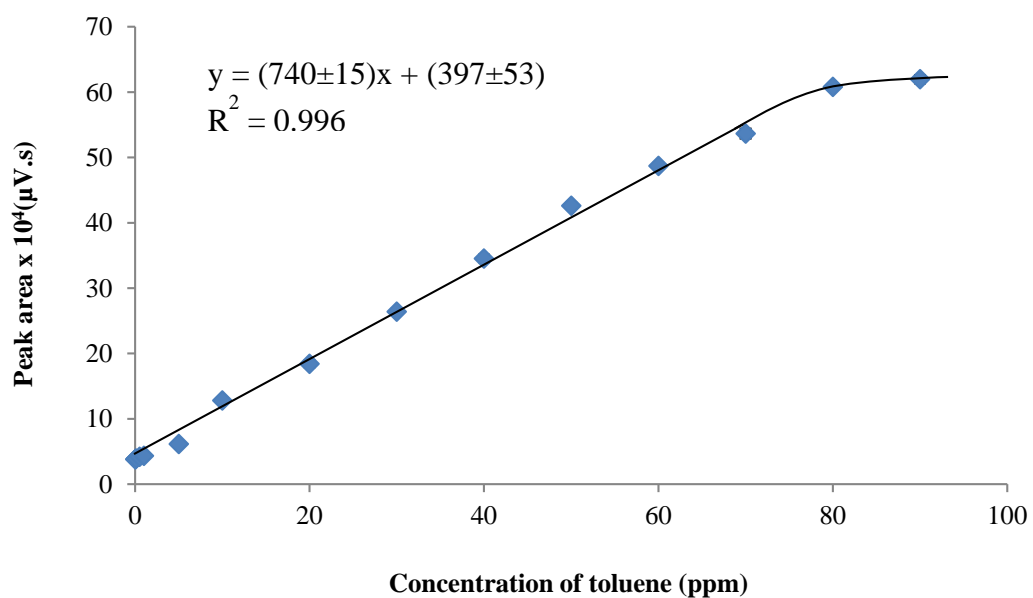


**Figure 4.21** Linear dynamic range of GC-FID for the determination of toluene

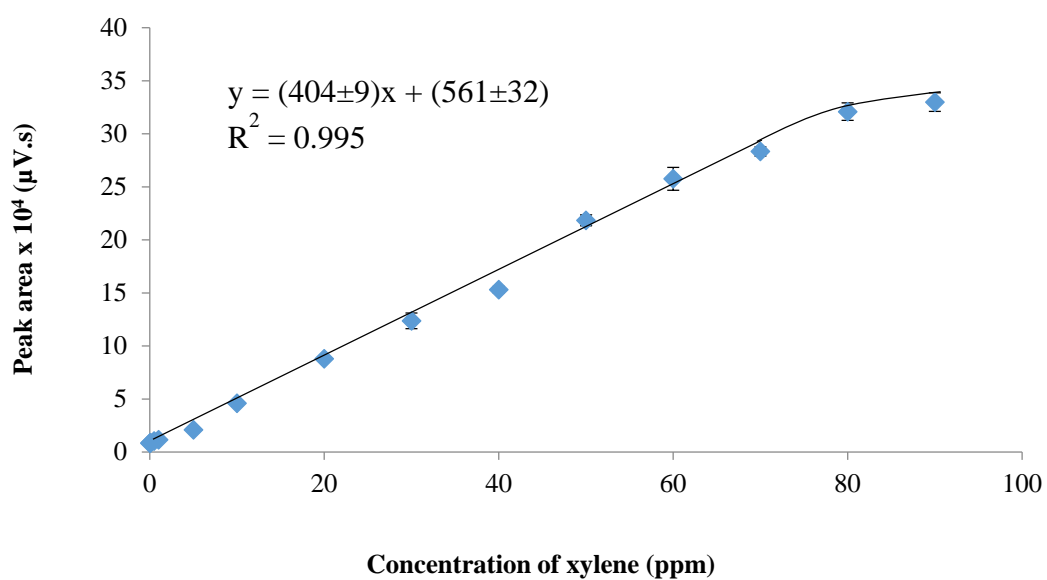


**Figure 4.22** Linear dynamic range of GC-FID for the determination of xylene

#### **4.3.2.2 Limit of detection (LOD) and limit of quantification (LOQ)**

LOD and LOQ of the GC-FID for the determination of BTX were evaluated based on IUPAC method (Long and Winefordner, 1983). The peak area of 20 blank injections are shown in Table 4.13. The LOD and LOQ (Table 4.14) were calculated using the equation 4.5.

**Table 4.13** The peak area of 20 blank injections at optimum GC-FID conditions

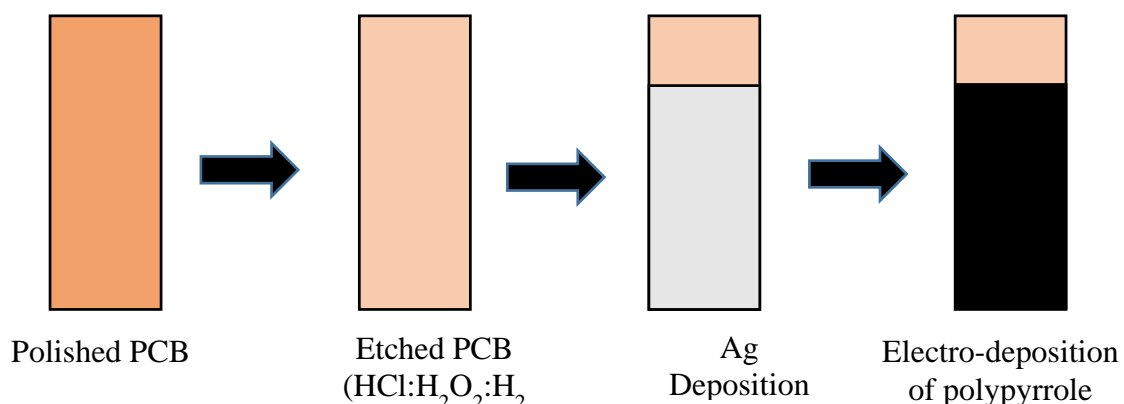
Number of injection	Peak area ( $\mu\text{V.s}$ )
1	47.13
2	52.42
3	46.33
4	48.51
5	51.23
6	57.18
7	65.67
8	52.33
9	55.12
10	56.24
11	58.40
12	54.55
13	55.24
14	58.92
15	49.38
16	56.71
17	63.11
18	62.16
19	56.31
20	59.82
Mean	57.18
SD	5.084
Linear equations	$y_{\text{benzene}} = (539 \pm 14)x + (149 \pm 48)$ $y_{\text{toluene}} = (740 \pm 15)x + (397 \pm 53)$ $y_{\text{xylene}} = (404 \pm 9)x + (561 \pm 32)$ $y = \text{Peak area } (\times 10^4 \mu\text{V.s})$ $x = \text{ppm}$

**Table 4.14** LOD and LOQ of the GC-FID for BTX detection

Compounds	LOD (ppb)	LOQ (ppb)
Benzene	28.3±2.1	94.3±6.4
Toluene	20.61±0.39	68.7±1.3
Xylene	37.8±6.1	125.8±2.0

### 4.3.3 Re-development of the printed circuit board (PCB) passive sampler

The PCB passive sampler was successfully re-developed by following the procedure (Saelim et al., 2013). The re-developed passive sampler was tested with standard BTX gas and it was found that the sampler can adsorb the BTX gas effectively. The re-developed PCB passive sampler was tested in the laboratory by injecting BTX standard gas in to the passive sampler before applying it for real ambient out door monitoring of BTX. Figure 4.23 shows the schematic diagram for the re-development of PCB passive samplers.

**Figure 4.23** Schematic diagram showing the development of PCB passive sampler

#### **4.3.4 Optimization of the thermal desorption and on-line micro-preconcentrator system**

For obtaining the highest desorption efficiency of the laboratory-built thermal desorption and on-line micro-preconcentrator system, various parameters were optimized. This was also to see after the analytes were adsorbed on the sorptive layer of the PCB passive sampler, they are desorbed effectively. The parameters like desorption temperature and desorption time of the thermal desorption device, and adsorption time, heating time and heating potential of the on-line micro-preconcentrator were optimized.

##### **4.3.4.1 The desorption temperature of the laboratory-built thermal desorption system**

The first parameter studied was desorption temperature of the laboratory-built thermal desorption system, it was studied from 190 to 220°C. The result shows that as desorption temperature increases there is increase in peak area of the analyte BTX till 210 °C (Table 4.15 and Figure 4.24). Then on further heating peak area slightly decreased and many contaminant peak appeared which might have come from the overheating of the passive sampler. So, 210 °C was selected as the optimum desorption temperature of the laboratory-built thermal desorption system.

**Table 4.15** Peak area of 1.0 ppm BTX at various desorption temperature of the laboratory-built thermal desorption system (n = 5)

Desorption temperature (°C)	Peak area $\times 10^3$ ( $\mu\text{V}\cdot\text{s}$ )					
	Benzene	%RSD	Toluene	%RSD	Xylene	%RSD
190	11.48 $\pm$ 0.96	8.4	8.00 $\pm$ 0.66	8.3	4.01 $\pm$ 0.22	5.5
200	14.80 $\pm$ 0.82	5.5	10.15 $\pm$ 0.96	9.5	4.22 $\pm$ 0.31	7.3
210	23.39 $\pm$ 0.95	4.1	15.9 $\pm$ 1.1	6.9	5.32 $\pm$ 0.37	7.0
220	21.08 $\pm$ 0.66	3.1	14.59 $\pm$ 0.86	5.9	5.31 $\pm$ 0.11	2.1

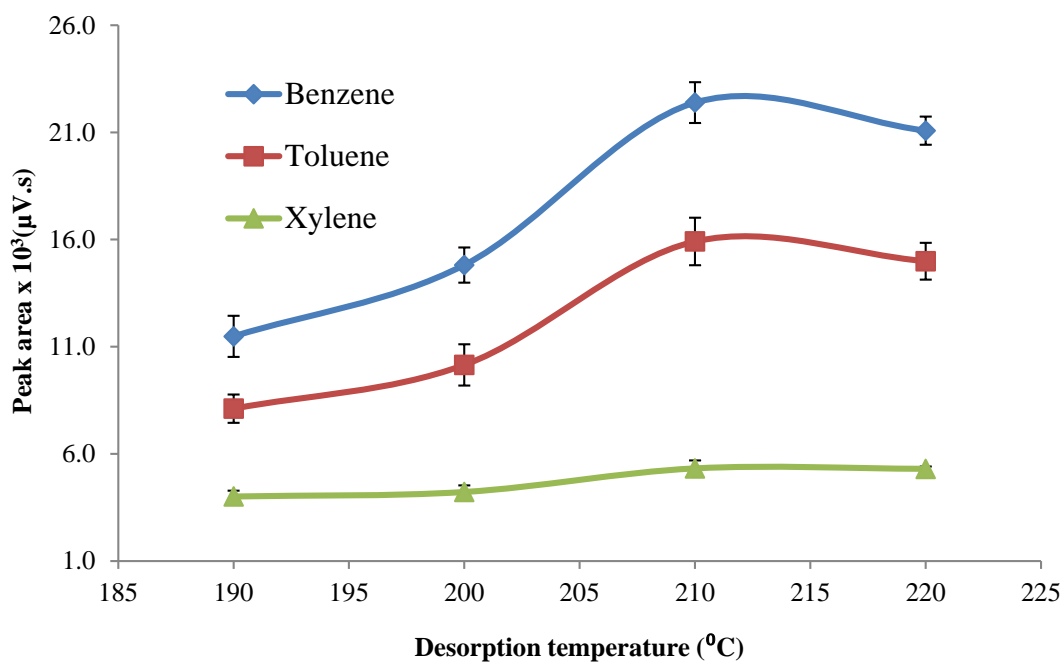


**Figure 4.24** Effect of the desorption temperature of the laboratory-built thermal desorption system on the peak area of 1.0 ppm BTX gas (n = 5)

#### 4.3.4.2 The desorption time of the laboratory-built thermal desorption system

The next parameter studied was desorption time of the laboratory-built thermal desorption system, desorption time was varied from 5 to 14 min. It was found that the peak area of the BTX increases with increase in desorption time from 5 – 12 min (Table 4.16 and Figure 4.25). And when desorption time was increased to 14 min it was found that peak area of BTX decreased and also there was peeling off of layer sorptive layer from PCB. Therefore, 12 min was selected as the optimum desorption time of the laboratory-built thermal desorption system.

**Table 4.16** Peak area of 1.0 ppm BTX at various desorption time of the laboratory-built thermal desorption system (n = 5)

Desorption time (min)	Peak area $\times 10^3$ ( $\mu\text{V.s}$ )					
	Benzene	%RSD	Toluene	%RSD	Xylene	%RSD
5	18.11 $\pm$ 0.64	3.5	7.62 $\pm$ 0.61	8.0	2.48 $\pm$ 0.28	11.3
8	27.2 $\pm$ 1.7	6.2	11.89 $\pm$ 0.58	4.9	3.76 $\pm$ 0.31	8.2
10	31.27 $\pm$ 0.91	2.9	15.47 $\pm$ 0.86	5.6	4.29 $\pm$ 0.11	2.0
12	35.0 $\pm$ 1.8	5.1	17.66 $\pm$ 0.84	4.8	5.56 $\pm$ 0.18	3.2
14	33.6 $\pm$ 1.1	3.3	16.5 $\pm$ 1.2	7.3	5.53 $\pm$ 0.21	3.8

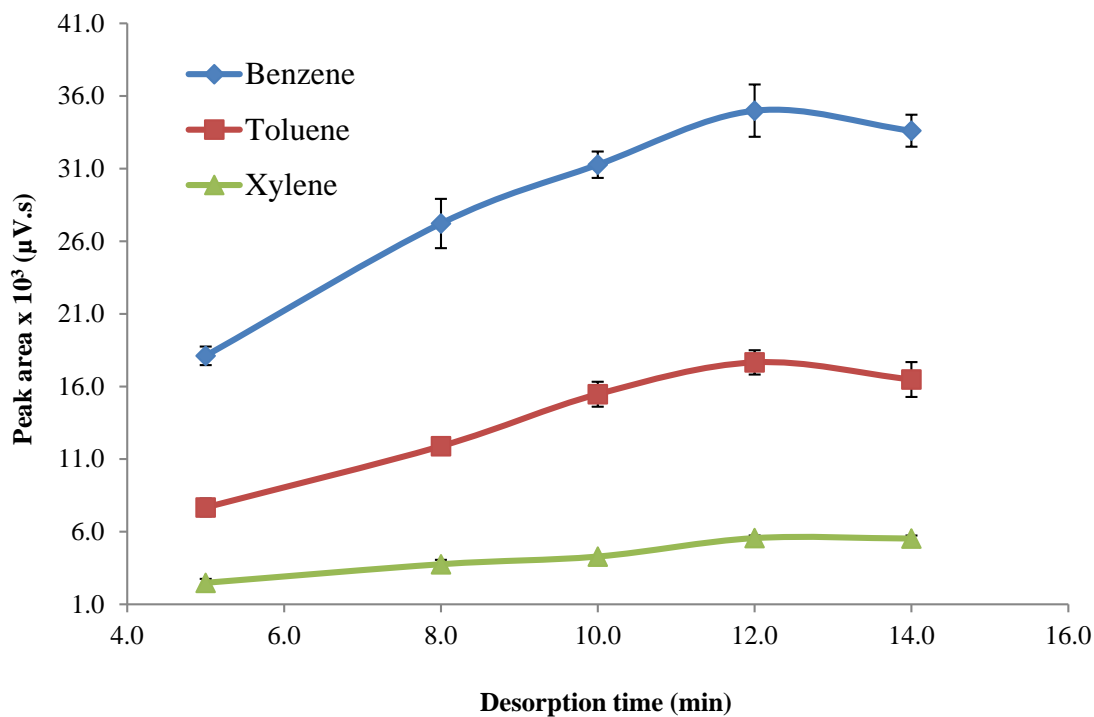


**Figure 4.25** Effect of the desorption time of the laboratory-built thermal desorption system on the peak area of 1.0 ppm BTX gas (n = 5)

#### 4.3.4.3 Adsorption time of the on-line micro-preconcentrator

To avoid the loss of analytes during the desorption step, the adsorption time of the analytes in the on-line micro-preconcentrator was studied. The adsorption time was studied from 5 to 14 min. And it was found that the peak area of BTX increases with increase of adsorption time from 5 – 12 min (Table 4.17 and Figure 4.26). After 12 min further increase in adsorption time the peak area almost remain constant, this might be because the 12 min adsorption time was enough for the analytes to get completely trapped by on-line micro-preconcentrator. Therefore, 12 min was selected as the optimum adsorption time for the on-line micro-preconcentrator.

**Table 4.17** Peak area of 1.0 ppm BTX at various adsorption time of the on-line micro-preconcentrator (n = 5)

Adsorption time (min)	Peak area $\times 10^4$ ( $\mu\text{V}\cdot\text{s}$ )					
	Benzene	%RSD	Toluene	%RSD	Xylene	%RSD
5.0	3.36 $\pm$ 0.12	3.6	2.42 $\pm$ 0.21	8.8	2.21 $\pm$ 0.16	7.2
8.0	3.80 $\pm$ 0.17	4.5	3.57 $\pm$ 0.13	3.6	2.73 $\pm$ 0.10	3.7
10	4.18 $\pm$ 0.11	2.6	3.91 $\pm$ 0.12	3.1	2.86 $\pm$ 0.14	4.9
12	4.75 $\pm$ 0.14	2.9	4.41 $\pm$ 0.12	2.7	3.52 $\pm$ 0.11	3.1
14	4.71 $\pm$ 0.12	2.5	4.30 $\pm$ 0.18	4.2	3.51 $\pm$ 0.15	4.3

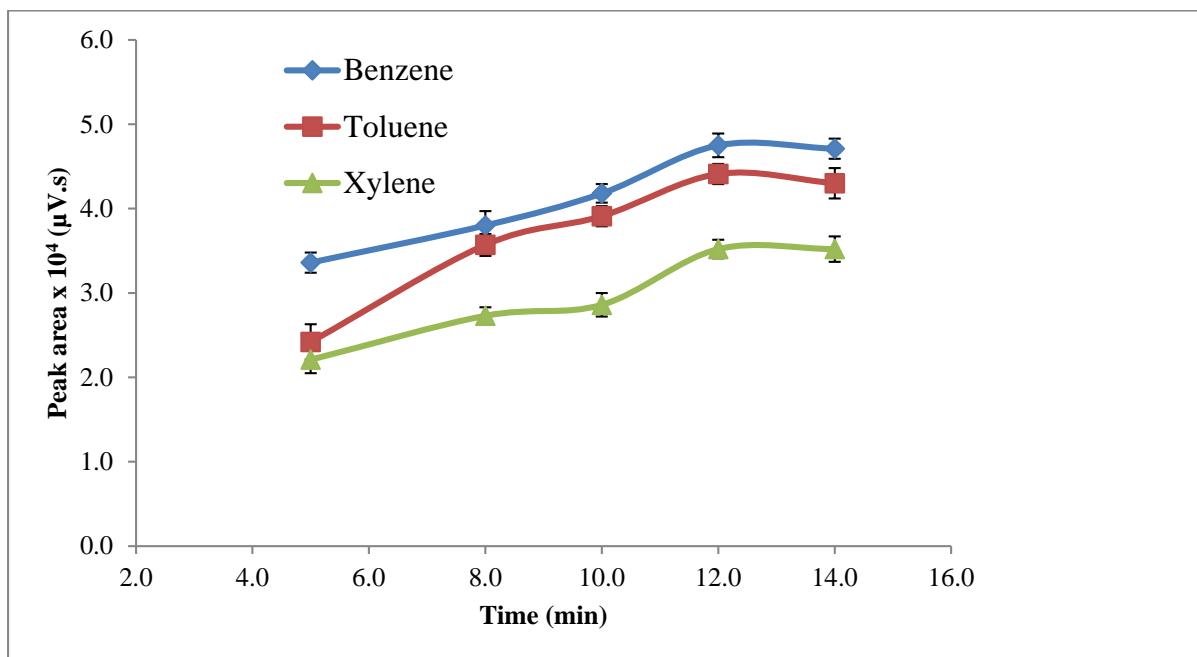


**Figure 4.26** Effect of the adsorption time of the on-line micro-preconcentrator on the peak area of 1.0 ppm BTX gas (n = 5)

#### 4.3.4.4 Heating potential of on-line micro-preconcentrator

To avoid the memory effects from the incomplete desorption of the analytes from the on-line micro-preconcentrator, the heating potential was optimized from 3.0 to 5.0 V. The result shows that at 3.0 V there was small peaks which cannot be integrated, but as the heating potential was increased from 3.5 to 4.5 V, there was increase in peak area, and the highest peak area was obtained at 4.0 V (Table 4.18 and Figure 4.27). With increase of heating potential to 4.5 V there was some contaminant peak appeared might be due to overheating of the adsorbent packed inside the on-line system and when 5.0 V heating potential was applied it heated the micro-preconcentrator too much resulting into damaging the on-line micro-preconcentrator. Therefore, 4.0 V of heating potential was chosen as the optimum heating potential.

**Table 4.18** Peak area of 1.0 ppm BTX at various heating potential of the on-line micro-preconcentrator (n = 5)

Heating potential (Volts)	Peak area $\times 10^4$ ( $\mu\text{V}\cdot\text{s}$ )					
	Benzene	%RSD	Toluene	%RSD	Xylene	%RSD
3.0	-	-	-	-	-	-
3.5	4.26 $\pm$ 0.19	4.5	4.07 $\pm$ 0.15	3.7	2.83 $\pm$ 0.13	4.6
4.0	4.63 $\pm$ 0.12	2.6	4.29 $\pm$ 0.17	4.0	3.26 $\pm$ 0.18	5.5
4.5	4.41 $\pm$ 0.16	3.6	3.91 $\pm$ 0.15	3.8	2.86 $\pm$ 0.11	3.8
5.0	-	-	-	-	-	-

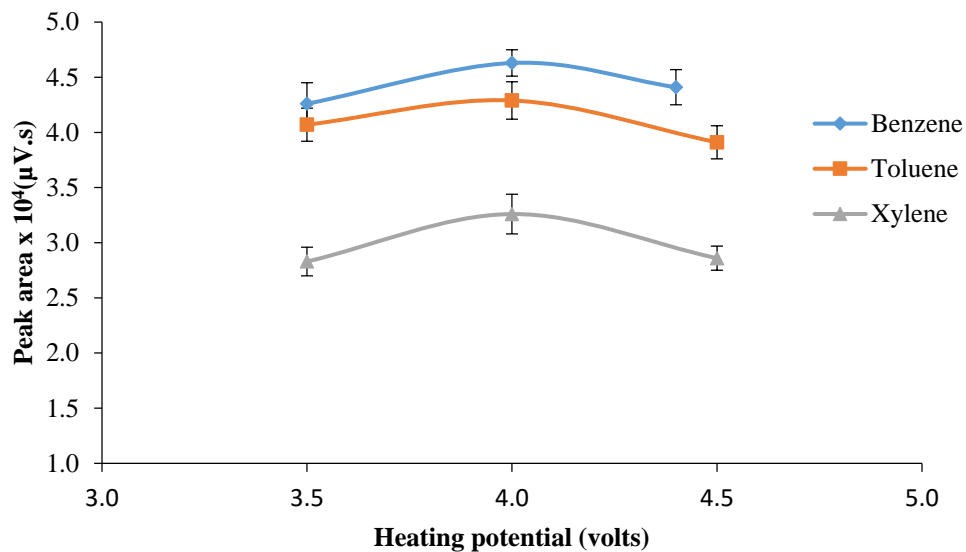


**Figure 4.27** Effect of heating potential of the on-line micro-preconcentrator on the peak area of 1.0 ppm BTX gas (n = 5)

#### 4.3.4.5 Heating time of the on-line micro-preconcentrator

The heating time of the on-line micro-preconcentrator was optimized by fixing the heating potential at 4.0 V and the effect of heating time was investigated at 0.5 to 2.0 s. The result shows that when heating time was increase from 0.5 s to 1 s, the peak area of BTX increases and after 1 s the peak area decreases and lots of contaminant peak appear, this might be because long heating of on-line micro-preconcentrator damages the adsorbent packed inside resulting into partial damage of the adsorbent (Table 4.19 and Figure 4.28). Thus, 1.0 s was selected as the optimum heating time of the on-line micro-preconcentrator.

**Table 4.19** Peak area of 1.0 ppm BTX at various heating time of the on-line micro-preconcentrator (n = 5)

Heating time (s)	Peak area $\times 10^4$ ( $\mu\text{V}\cdot\text{s}$ )					
	Benzene	%RSD	Toluene	%RSD	Xylene	%RSD
0.5	2.26 $\pm$ 0.22	9.7	2.26 $\pm$ 0.26	11.5	1.39 $\pm$ 0.11	7.9
1.0	3.63 $\pm$ 0.17	4.7	3.54 $\pm$ 0.31	8.8	2.42 $\pm$ 0.24	9.9
1.5	3.52 $\pm$ 0.12	3.4	3.36 $\pm$ 0.27	8.0	1.80 $\pm$ 0.14	7.8
2.0	3.24 $\pm$ 0.26	8.0	3.18 $\pm$ 0.11	3.5	1.73 $\pm$ 0.12	6.9

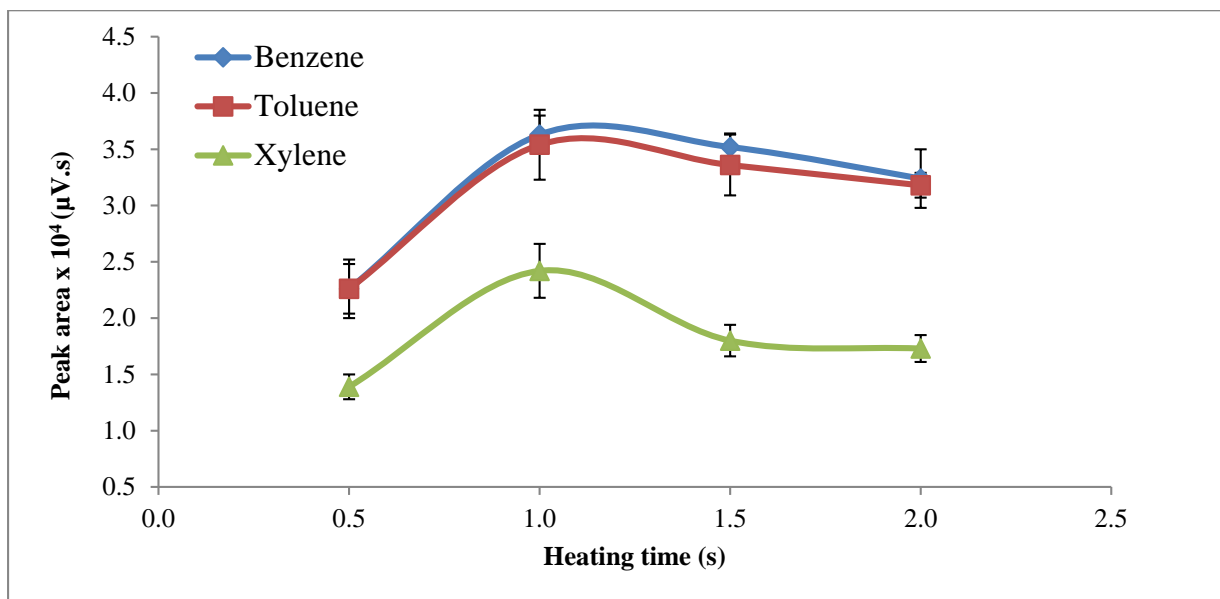


**Figure 4.28** Effect of heating time of the on-line micro-preconcentrator on the peak area of 1.0 ppm BTX gas (n = 5)

The various optimized parameters with their optimum values of the laboratory-built thermal desorption and on-line micro-preconcentrator system is summarized in table 4.20.

**Table 4.20** Optimum conditions of the laboratory-built thermal desorption and on-line micro-preconcentrator system.

<b>Parameters</b>	<b>Optimized values</b>	<b>Optimum value</b>
<i>Laboratory-built thermal desorption system</i>		
Desorption temperature (°C)	190, 200, 210, 220	210
Desorption time (min)	5.0, 8.0, 10, 12, 14	12
<i>On-line micro-preconcentrator</i>		
Adsorption time (min)	5.0, 8.0, 10, 12, 14	12
Heating potential (V)	3.0, 3.5, 4.0, 4.5, 5.0	4.0
Heating time (s)	0.5, 1.0, 1.5, 2.0	1.0

#### 4.3.4.6 Analytical performance of the system

The analytical performance of the system, i.e. the re-developed PCB passive sampler with the laboratory-built thermal desorption system coupled with on-line micro-preconcentrator and GC-FID were investigated using the various optimum conditions. For evaluation of LDR various concentration of standard BTX gas (0.1 to 100 ppm) was injected. The result shows a wide LDR and good linearity was obtained. The LDR of benzene was 0.06 – 5.6 µg with a linear equation of  $y = (1444 \pm 23)x + (647 \pm 48)$  and  $R^2 = 0.998$  (Figure 4.29), for toluene was 0.07 – 2.2 µg with a linear equation of  $y = (1419 \pm 48)x$

+ (344±44) and  $R^2 = 0.992$  (Figure 4.30) and for xylene was  $0.23 - 2.5 \mu\text{g}$  with a linear equation of  $y = (496\pm 13)x + (108\pm 15)$  and  $R^2 = 0.996$  (Figure 4.31). The LOD and LOQ were evaluated based on IUPAC method (Long and Winefordner, 1983) and was calculated using the equation 4.5 (Table 4.21)

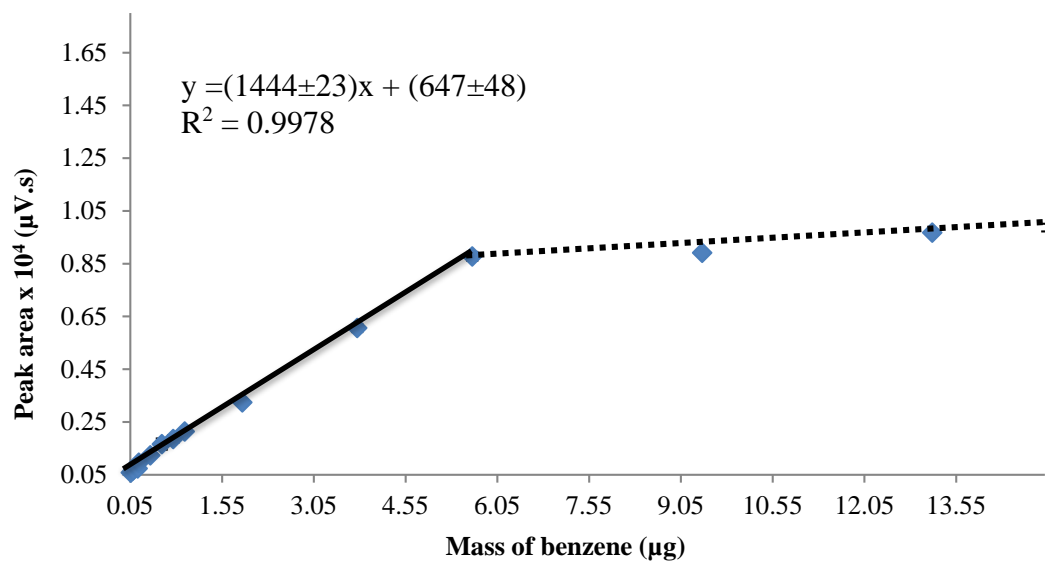


**Figure 4.29** Linear dynamic range of benzene at various mass uptake on the PCB passive sampler after desorption using the thermal desorption system coupled with the on-line micro-preconcentrator and GC-FID system

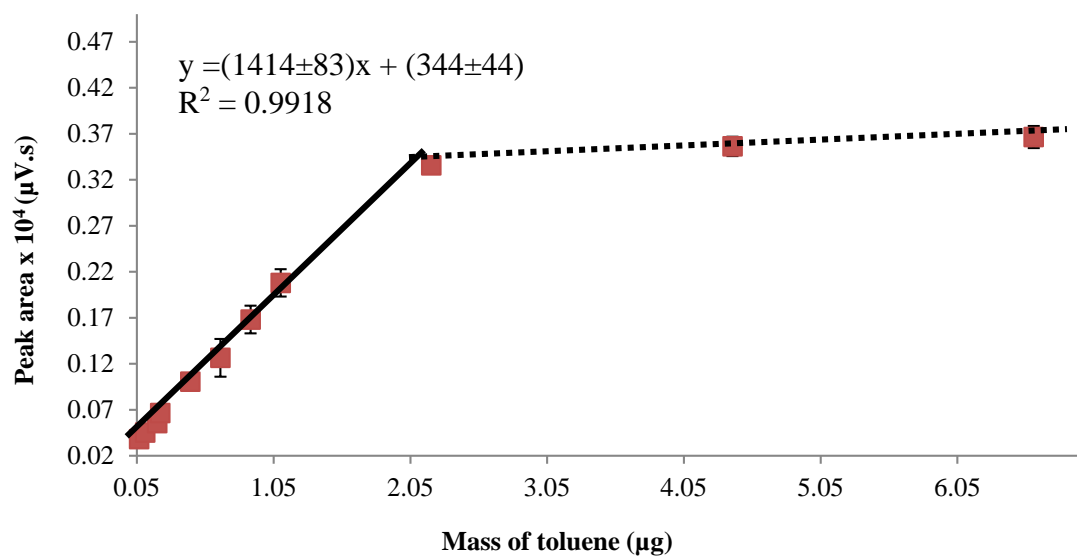


**Figure 4.30** Linear dynamic range of toluene at various mass uptake on the PCB passive sampler after desorption using the thermal desorption system coupled with the on-line micro-preconcentrator and GC-FID system

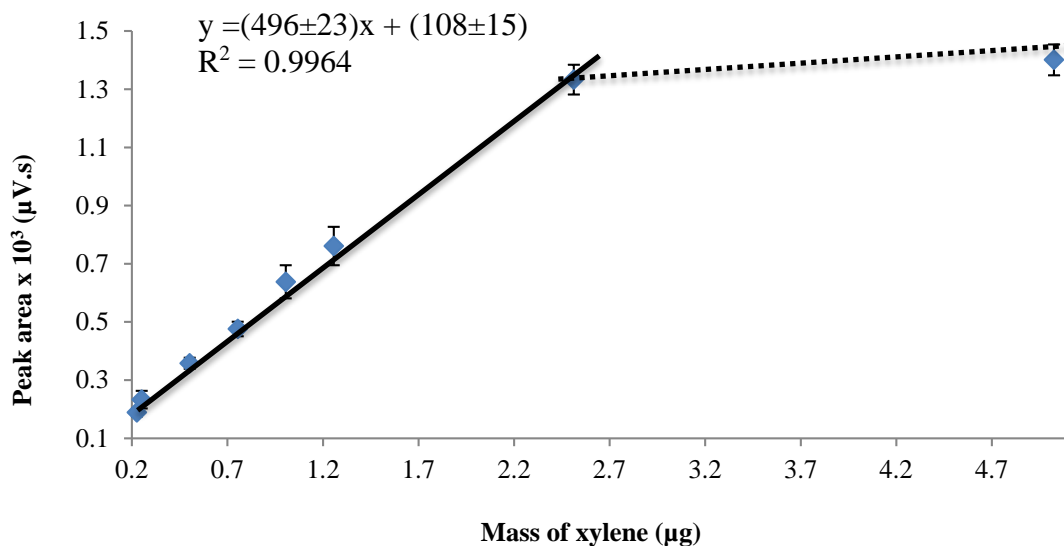


**Figure 4.31** Linear dynamic range of xylene at various mass uptake on the PCB passive sampler after desorption using the thermal desorption system coupled with the on-line micro-preconcentrator and GC-FID system

**Table 4.21** LOD and LOQ of BTX under optimum conditions of thermal desorption system and on-line micro-preconcentrator coupled with GC-FID.

Analyte	LOD (ng)	LOQ (ng)
Benzene	6.65±0.12	22.16±0.35
Toluene	6.81±0.23	23.63±0.78
Xylene	19.35±0.49	64.5±1.7

#### 4.3.4.7 Sampling time

Fig. 4.32 shows the amount of benzene, toluene and xylene from the passive samplers with different exposure time. Benzene was not detected when sampling for 1 and 2 days and xylene was not detected with a sampling time of 1 day. It can be clearly seen that the uptake of BTX by the PCB sampler increases with the exposure time. At 7 days, the PCB provided the maximum amount of BTX, indicated that the sampler has already reached its breakthrough point. In other words the adsorbent was saturated with the analytes and it could not adsorb any more target analytes. At 14 days, the uptake of BTX decreased, it was likely that part of the adsorbed analyte re-volatilized. Therefore, the effective sampling time for PCB passive sampler was fixed at 5 days to avoid the breakthrough point.

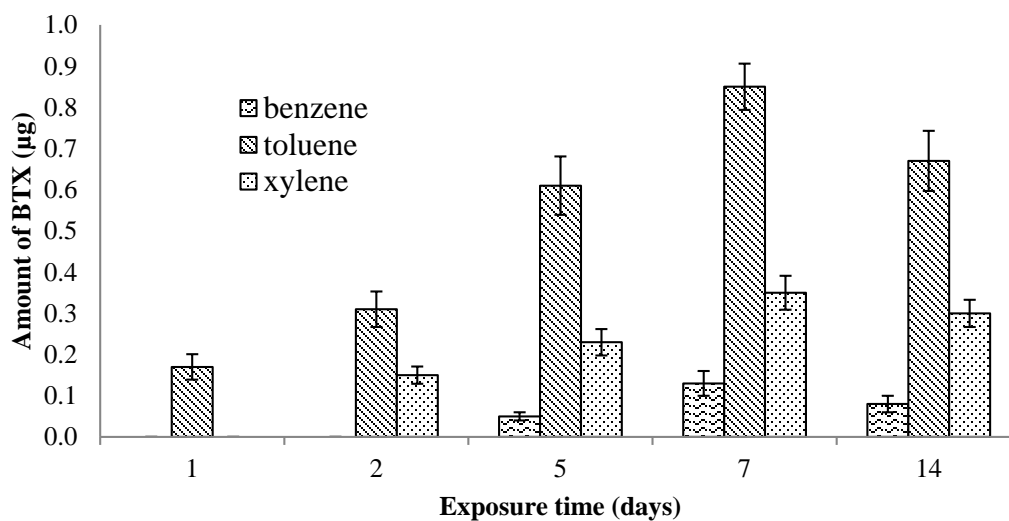


**Figure 4.32** The amount of BTX ( $\mu\text{g}$ ) adsorbed on to the PCB passive sampler for various exposure time

#### 4.3.4.8 Application of the PCB passive samplers

The PCB passive sampler was used for the mapping of BTX concentration in Hat Yai city. Sixteen sampling sites (Fig. 4.4) were selected based on their high or low traffic volume and to cover strategic area of the city as well as the sites where the monitoring of BTX in Hat Yai was done previously (Thammakhet *et al.*, 2004) to provide comparative results. Other criteria considered were vehicle and population density, most of the sites are either highly populated or is the corridor to the city. For the sampling, the PCB passive samplers were hung at a height of approximately 150-170 cm, the normal breathing height of a person. The passive samplers were exposed for 5 days after which they were collected and immediately analysed in the laboratory to avoid any loss of the adsorbed analytes.

#### 4.3.4.9 Concentration of BTX in Hat Yai city

The ambient level of BTX in Hat Yai city was found in the range of N.D-11.3±1.6, 4.50±0.76 – 49.6±3.7 and 1.10±0.23 – 39.6±3.1  $\mu\text{g m}^{-3}$ , respectively (Fig. 4.33). It was calculated using an equation based on the principle of passive sampler (equation 4.11) (Batterman et al., 2002; Górecki and Namieśnik, 2002)

$$Q = \frac{AD(C_1 - C_0)t}{L} \quad (4.11)$$

Where Q is the uptake amount of the analyte by the passive sampler ( $\mu\text{g}$ ), calculated from the linear equation by substituting the peak area obtained from the GC-FID of each analytes; A the surface area of the passive sampler ( $2.0 \text{ cm}^2$ ); D the diffusion rate of the analyte at  $25^\circ\text{C}$  (BTX 0.0928, 0.0829 and  $0.0756 \text{ cm}^2\text{s}^{-1}$  respectively) (US EPA on-line tool),  $C_1$  the concentration of the analyte adsorbed by the sampler ( unknown  $\text{g L}^{-1}$ ),  $C_0$  the concentration of the analyte at the surface of the sampler (  $0 \text{ g L}^{-1}$ ); t the exposure time (432000 s); and L the diffusion length from the stainless steel mesh (membrane) to the adsorbent film of the passive sampler (0.36 cm).

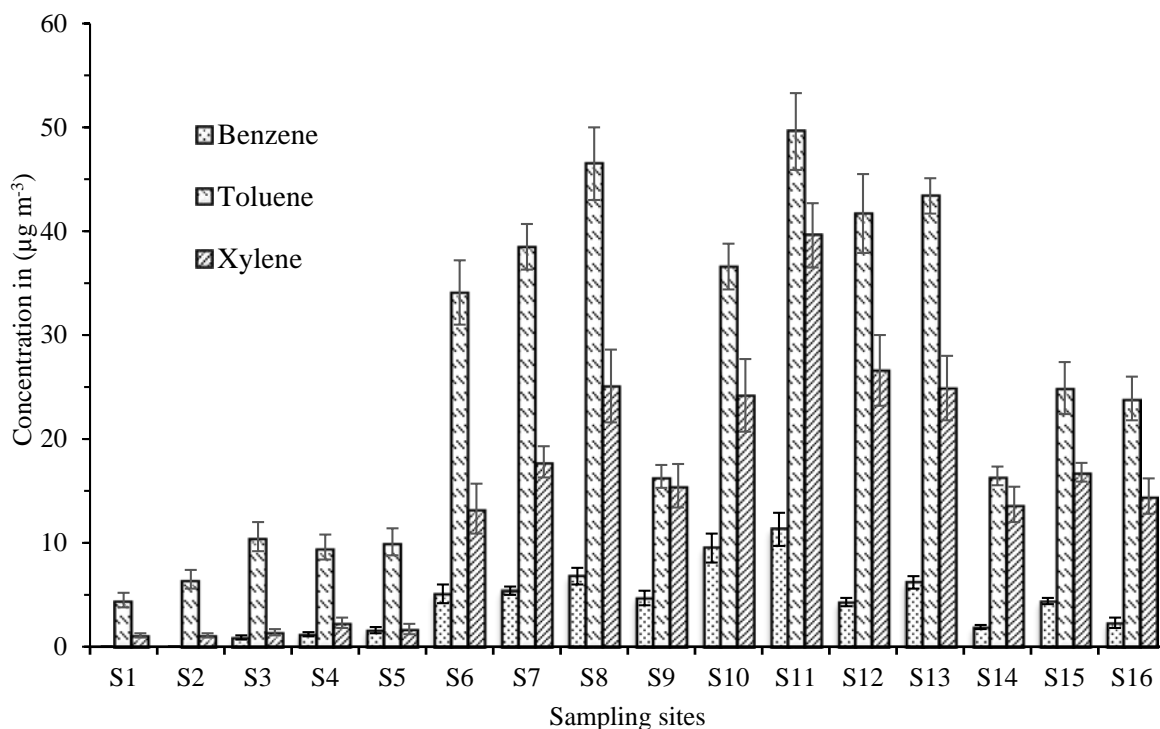


**Figure 4.33** Concentrations of BTX at different sampling sites

Sampling sites S1 and S2 showed very low concentration of toluene and xylene while benzene was not at all detected. This is as expected since these sites were chosen to be the background level of BTX due to very low traffic movement. The other possible reason could be the presence of lots of trees around these sites.

Sampling sites S3, S4 and S5 in Karnchanawanich Road were a little out of the city, connecting Hat Yai city to the Malaysian border. Though the road is quite busy in the morning and evening, the ambient concentration of BTX were found to be comparatively lower than other sites. This might be because there are no tall buildings to block the wind so the analytes might have been diluted and blown away. The wind speed recorded in these sites during sampling time was relatively high, in the range of 3.5 – 14.0 km h<sup>-1</sup>.

Sampling sites S6, S7 and S8 are at the center periphery of the city, around one of the biggest intersection between two main roads Rajyindee and Tamnoonwithi which connect to various part of the city. There is a huge inflow of traffic from all around the city to this intersection. A large number of small cars and motorcycles big buses and trucks also take these roads. As a result, the ambient concentration of BTX at these sites were higher than many of the sampling sites.

Sites S9, S10 and S11 are along a narrow street down town, among the main tourist attractions. There are hotels, restaurants, big plazas, shopping malls and tall buildings. A large number of cars go in and out of this area, dropping off and picking up tourists. Moreover, both sides of the street are packed with clothing stalls and fried food stands. Since, there are number of tall buildings, the wind speed in this area was recorded to be only in the range of  $0.5 - 7.5 \text{ km h}^{-1}$ . All these factors contribute to the higher concentration of BTX. In fact, the highest ambient concentration of BTX were found in this area (S11), *i.e.*,  $11.3 \pm 1.6 \mu\text{g m}^{-3}$ ,  $49.6 \pm 3.7 \mu\text{g m}^{-3}$  and  $39.6 \pm 3.1 \mu\text{g m}^{-3}$ , respectively. Among the three sampling sites, the concentration of BTX at S9 was the lowest, it might be because it was located at the junction of a cross-roads so, the wind can flow from any of the four directions. The wind speed at this site was relatively higher than the other two sides, thus the parts of analytes might have been diluted and blown away. At S10 and S11, the street becomes more narrow. So the BTX concentration trend increases from S9-S11.

Sampling sites S12 and S13 are within a gas station located along Phetkasem Road. The ambient concentrations of BTX in this gasoline station are from the exhaust emission and evaporative emissions (from car tank or from the station fuel tank). As expected, the concentration of BTX were high.

Sampling sites S14, S15 and S16 were along Niphat Songkhro 1 Road, which can connects to a few other provinces and a number of cars go in and out of the city via this road. Moreover, there are night hawkers on both sides along the street. Although the street is narrow there are no tall buildings and hotels around and the target analytes can be diluted and blown away by the wind. As a result the ambient concentration of BTX is lower than expected.

From all the sampling sites, the highest concentration of BTX was found on S11, which is located in the heart of the Hat Yai city. This is likely because of the large number of cars, vans, buses, motorcycles and tuk-tuk (open sided public transport minivan) operating in this area to pick-up and drop off the tourists visiting the city. Moreover, there are many hotels and tall building shopping malls which obstruct the free flow of the air, as a result the target analytes are more concentrated. From the pattern of the obtained results, it indicates that road traffic is the main source of BTX to the ambient environment. The more the number of vehicles the higher the ambient concentration of BTX. The presence of skyscraper buildings and narrow streets would also indirectly increase the ambient concentration of BTX by obstructing the free air flow in these areas.

#### **4.3.4.10 Conclusion**

The re-validated PCB passive sampler for BTX was successfully applied for the sampling of ambient outdoor air in and around Hat Yai city. The results indicate that there is a gradual increase of benzene concentration when compared to the studies in 2004. Since, US EPA and WHO do not recommend any safe level for benzene exposure, because of its highly toxic nature to humans, it is important to bring its concentration to be as low as possible. For toluene and xylene, a daily average that can be sustained for life time exposure is  $400 \mu\text{g m}^{-3}$  and  $100 \mu\text{g m}^{-3}$  (US EPA 2004b), respectively. So, as of now the ambient concentration of these two pollutants is still much lower than the recommended level.

But in time to come with the rapid increase of vehicle numbers, the ambient concentrations of BTX will certainly increase. Therefore, as a precaution some measures should be considered, for example by increasing the efficiency of a public transport system to reduce the traffic volume and going for environmentally friendly electric cars, motorcycles, and even buses. Another possibility is by introducing zero benzene content gasoline.

Since, BTX exposure is harmful to humans there is a need to monitor them from time to time. Commercial passive samplers are quite expensive, therefore, as shown in this work environmentally friendly, cheap passive samplers can be developed in laboratories for the monitoring of BTX, hence bringing down the overall cost of monitoring. This study also showed that the developed PCB passive sampler, in addition to the monitoring of styrene (Saelim *et al.*, 2013), can be used effectively for the monitoring of BTX and possibly for other VOCs.

## CHAPTER 5

### Distributions of SO<sub>2</sub> and NO<sub>2</sub> in the lower atmosphere of an industrial area in Bhutan

#### 5.1 Introduction

Air pollutants such as sulfur dioxide (SO<sub>2</sub>) and nitrogen dioxide (NO<sub>2</sub>) are mainly produced from the burning of oils and fossil fuels and are important industrial pollutants (Garg et al., 2006). SO<sub>2</sub> and NO<sub>2</sub> contribute to acidic deposition in terrestrial ecosystems (Cooper and Alley, 2002; Wang et al., 2001). In aerosol form, they can also impact visibility (Huang et al., 2014). NO<sub>2</sub> is of particular concern, as it is a precursor to the formation of photochemical oxidants which directly impact human health (Cox, 2003). SO<sub>2</sub> and NO<sub>2</sub> once released into the atmosphere, they undergo several processes of transformation due to atmospheric reactions. All these transformation processes play an important role in an environment. SO<sub>2</sub> may react immediately with hydroxyl radical in the atmosphere to produce SO<sub>3</sub>, which in turn reacts quickly with water vapor to produce sulfuric acid or depending on the meteorological conditions and local availability of oxidizing substances and it may be transported hundreds of kilometers before it reacts (Erduran and Tuncel, 2001). Studies have shown that high level of SO<sub>2</sub> exposure will lead to low birth weights (Rogers et al., 2000) and reduction in birth rates (Dejmek et al., 2000). NO<sub>2</sub> plays an important role in the atmospheric chemistry for the formation of secondary particulate nitrate (Millstein and Harley, 2010; Stock et al., 2013). Secondary particulates have huge negative impacts to an environment such as visibility, water body acidification and global climate change (Liu et al., 2012; Rodhe et al., 2002). Moreover previous studies have shown that NO<sub>2</sub> is one of the major components responsible for producing brown haze inhibiting the visibility (Lei and Wuebbles, 2013).

Since, SO<sub>2</sub> and NO<sub>2</sub> has hazardous properties, they are being measured and monitored by almost all countries. For example, in China central government has established national goal to reduce SO<sub>2</sub> emissions by about 10% in the stipulated time of

2001- 2005 and by another 10% in the year 2006-2010 (Schrefils et al., 2012). And most of the countries have regulated NO<sub>2</sub> as an indicator to assess the status of ambient air quality in urban environment (Baldasano et al., 2003; Ravindra et al., 2008).

Bhutan being a developing country, as of now the air quality in Bhutan has been considered as pristine, but with new developmental activities and setting up of new industries, it is placing pressure on pristine air quality of Bhutan (NEC, 2010). At the foothill of Bhutan bordering India one can see a clustered of industries. Industries being one of the main point source of air pollution, it is very important to monitor the air quality where industries are located. Monitoring of air pollutants at the local levels is important in order to know the levels and behaviors that atmospheric species show and then to apply plans and control strategies. Developed nations like America and Europe have many local studies (Gurjar et al., 2008; Parrish et al., 2011). Similarly, in Mediterranean countries air pollution problems are investigated due to high level of emissions in large cities and industrial areas (Baldasano *et al.*, 2003). Although the National Environment Commission (NEC) of Bhutan is doing its best to control air pollution in the industrial area of Bhutan, still to this date no researched data are available with regard to air pollution.

There are various technique available to monitor SO<sub>2</sub> and NO<sub>2</sub> pollutants such as ion chromatography (Krupińska et al., 2012), chemiluminescence (Sun et al., 2011) and spectrophotometry (Campos et al., 2010; Mahadevaiah et al., 2008). Out of which spectrophotometric technique is one of the simple and accurate methods commonly used for measuring SO<sub>2</sub> and NO<sub>2</sub>. So, in this work standard colorimetric methods, West-Gaeke for SO<sub>2</sub> determination and Saltzman method for NO<sub>2</sub> determination were used. Since, these methods are very simple and provide accurate results and has been used by the National Environmental Chemistry and Acoustics Laboratory (NECAL), Department of Health, Auckland, New Zealand (Graham, 1997), United State Department of Health, Education and Welfare, USA (US EPA, 1964) and Bureau of Indian Standards, India (Kamyotra and Saha, 2011). Two important air pollutants SO<sub>2</sub> and NO<sub>2</sub> were monitored using modified portable active sampler in an industrial area of Bhutan. The sampling was done for the spring season (March-May, 2015) in Bhutan.

## 5.2 Experimental

### 5.2.1 Apparatus and reagents

All chemicals used in this study were of analytical grade. *N*-1-naphthylethylenediamine dihydrochloride with 97% purity was from BDH Chemical Ltd., (Poole, UK), pararosaniline dye with 85% purity was from Sigma-Aldrich, (Steinheim, Germany), triethanolamine with 99% w/v purity was from Loba Chemie Pvt. Ltd., (Mumbai, India), glacial acetic acid with 99.9% w/v purity was from J.T. Baker, (Phillipsburg, USA), sodium sulfite with 99.9% purity was from Fisher Scientific, (Loughborough, UK), sodium nitrite with 97% purity was from Ajax Finechem, (Auckland, New Zealand), formaldehyde 37% was from Merck, (Darmstadt, Germany), hydrochloric acid 37% was from Merck KGaA, (Darmstadt, Germany), sulfamic acid 99.5% purity was from Fluka, (St. Gallen, Switzerland) and sulfanilic acid with 98% purity was from Fluka, (St. Gallen, Switzerland).

Absorbance was measured using a Mini 20 portable spectrophotometer (Milton Roy, Rochester New York, USA). Two midjet bubblers (Supelco, Bellefonte PA, USA) were used to trap SO<sub>2</sub> and NO<sub>2</sub> in their respective trapping reagent while the ambient air was pumped into the midjet bubblers using a mini 12V DC vacuum air pump (Xiamen AJK Technology Co., Ltd., Hong Kong). Flow rate was measured using soap film flow meter (Agilent, Florida, USA) and air flow rate was controlled by a flow controller (Cole-Parmer, Chicago, USA).

### 5.2.2 Methodology

For the study of SO<sub>2</sub> and NO<sub>2</sub> using standard colorimetric method *i.e.* West-Gaeke method for SO<sub>2</sub> and Saltzman method for NO<sub>2</sub>, simple active air sampler was assembled in the laboratory, then it was validated using the standard liquid gas as well as standard gas.

And after the validation of the proposed method, it was applied for sampling of SO<sub>2</sub> and NO<sub>2</sub> in the ambient out door air.

#### **5.2.2.1 Standard colorimetric method for SO<sub>2</sub> (West-Gaeke method)**

One of the biggest challenges for monitoring of air pollutants is the determination of SO<sub>2</sub> in air. It is one of the complicated process because of the presence of oxygen and the coexistence of the other pollutants, such as the ozone, oxides of nitrogen, hydrogen sulfide, disulfide etc. All these pollutants either react with the SO<sub>2</sub> during sampling or storage or interfere with subsequent analytical processes. Beside this, acidic or basic substances in air further contributes to the complexity of the determination. There are various techniques employed for the determination of SO<sub>2</sub>, they are conductometry, polarography, iodimetry, acidimetry, gas chromatography, flame photometry, coulometry, and ion chromatography. All these methods are expensive and requires lots of skills for operation. Therefore, the spectrophotometric method introduced by West and Gaeke in 1956 remains the top choice for critical studies because of its less interferences from the other pollutants and good sensitivity and its accuracy. This method has been used for determination of SO<sub>2</sub> as the reference method world-wide. It has been used for critical studies of air quality and is suitable for determining base-line values for “unpolluted” atmospheres. It is a preferred method for continuous air monitoring, provided the instrumentation employed is of good design and modification. Moreover, this method can be used for spot checks, monitoring, and field surveys.

The spectrophotometric method has been applied to many studies in the laboratories and responsible agencies throughout the world. Studies have proven that this method is very much reliable. And a number of minor modifications of the original procedure have been proposed mainly in the form of concentration changes of reagents and in some cases change of reagents. The procedure recommended is therefore, the original one modified only in minor details.

### 5.2.2.1.1 Principle of the West and Gaeke method

The basic principle of West-Gaeke method is based on the absorption and stabilization of SO<sub>2</sub> from air by a solution of sodium or potassium tetrachloromercurate II, to form the dichlorosulfitomecurate II complex. The sulfite complex resists oxidation by atmospheric oxygen and is even stable in the presence of small amounts of strong oxidants such as ozone and the oxides of nitrogen. Quantitative determinations of the collected SO<sub>2</sub> is accomplished by adding acid-bleached pararosaniline hydrochloride and formaldehyde to the sulfite complex and measuring the intensely deep purple colored pararosaniline methylsulfonic acid to produced (Figure 5.1)

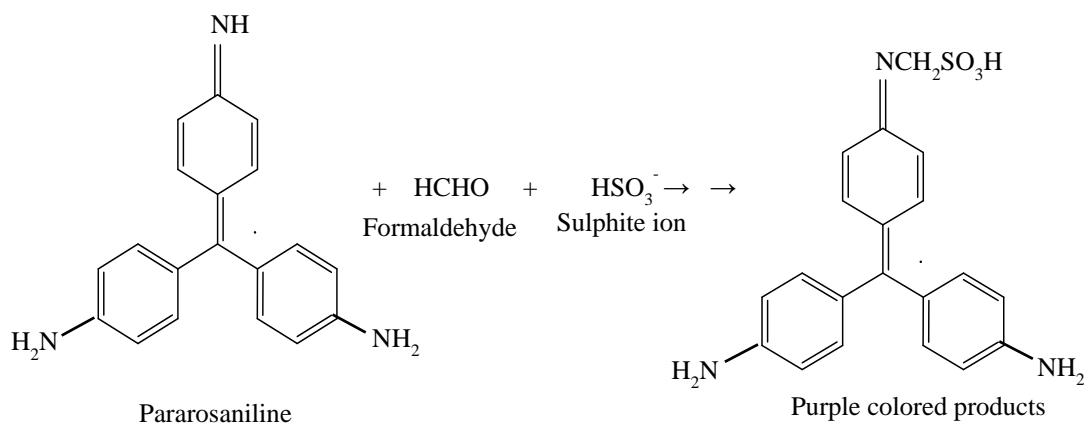


**Figure 5.1** Reaction mechanism of West and Gaeke method for determination of SO<sub>2</sub> (Munoz et al., 1989)

### 5.2.2.2 Colorimetric method for determination of NO<sub>2</sub> (Saltzman method)

Saltzman method is one of the first applications for colorimetric determination of NO<sub>2</sub> in air and was reported by B.E.Saltzman, and has since been known as the Saltzman method. In this method the absorber used is a mixture of sulfanilic acid and N-(1-naphthyl)-ethylenediamine, in acetic acid solutions.



### **5.2.3 Preparation of various absorbing solutions and standard solutions**

#### **5.2.3.1 Trapping solution for SO<sub>2</sub>**

Triethanoamine was used as the absorbing solution in place of tetrachloromercurate II used in West-Gaeke method for trapping SO<sub>2</sub>. For preparation of absorbing solution for SO<sub>2</sub>, 1.5 mL of triethanolamine was measured using pipette and was diluted to 100 mL with ultrapure water to get 1.5% solution of triethanolamine, 10 mL of this solution was used as absorbing solution for SO<sub>2</sub> (Geetha and Balasubramanian, 2000)

#### **5.2.3.2 Trapping solution for NO<sub>2</sub>**

Trapping solution of NO<sub>2</sub> was prepared by using 0.1% *N*-1-naphthylethylenediamine dihydrochloride stock solution which was prepared by accurately weighing 0.1 grams of *N*-1-naphthylethylenediamine dihydrochloride in a 100 mL volumetric flask, and was dissolved using ultrapure water and make it to the mark to obtain 0.1% of *N*-1-naphthylethylenediamine dihydrochloride stock solution.

Final absorbing solution of NO<sub>2</sub> was made by accurately weighing 0.5 gram of sulfanalic acid into a 100 mL volumetric flask, then it was dissolved using 14 mL of glacial acetic acid and ultrapure water to it 2 mL of 0.1% *N*-1-naphthylethylenediamine dihydrochloride was added and the solution was make up to mark by adding ultrapure water (Mousazadeh, 2009).

#### **5.2.3.3 Preparation of standard sulfite solution**

Standard sulfite solution was prepared by dissolving 0.40 g of sodium sulfite in 500 mL of deionized water. The SO<sub>2</sub> content in the solution was determined by the iodimetric

method (Jeffery et al., 1989) and found to be  $320 \mu\text{g mL}^{-1}$  (Mahadevaiah et al., 2008, ASTM, D 2914-01, 2007).

#### **5.2.3.4 Preparation of standard nitrite solution**

Standard nitrite solution was prepared by dissolving 0.0150 g of sodium nitrite in 500 mL of deionized water. This standard nitrite solution contain  $22 \mu\text{g mL}^{-1}$  as  $\text{NO}_2$  (Mousazadeh, 2009).

#### **5.2.4 Sampling train for active sampling**

*Active sampling system:* Figure 5.3 shows the schematic diagram of a convenient portable active sampler that was assembled in the laboratory. A sampling train consisting of mini air pump (12 V), nylon filter, flow controller and two fritted midget bubblers with respective absorbing reagents. Butt-to-butt connections was made with Tygon tubing. Before sampling, all the connections between the various components were made leak tight using greaseless ball joint fittings.

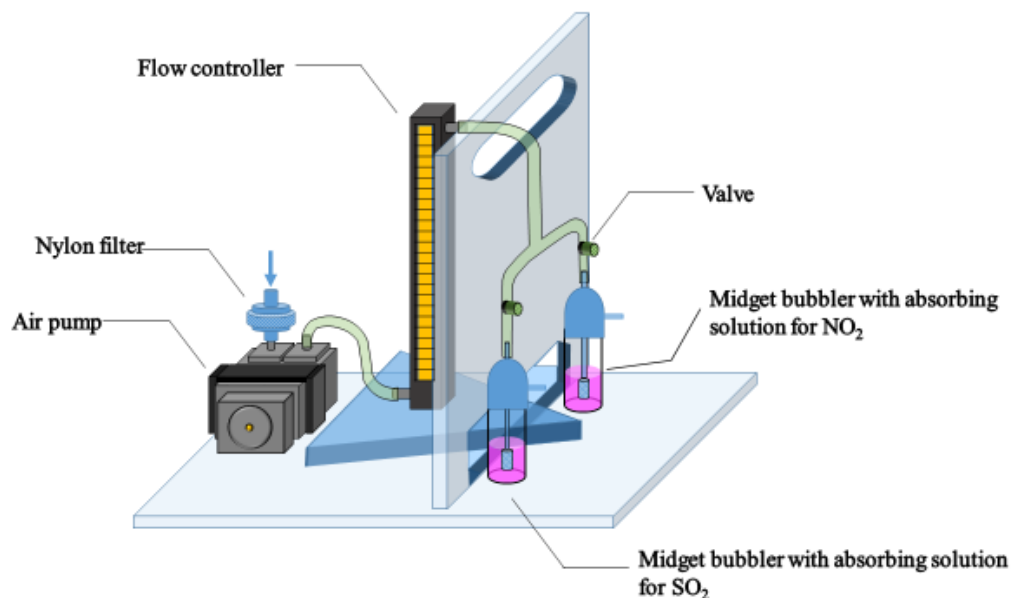


**Figure 5.3** Schematic diagram of active sampler assembled in the laboratory

*Colorimetric reagents:* For SO<sub>2</sub>, 10 mL of 1.5% TEA solution was used as the absorbing reagent. After trapping the air, it was transferred into a 25 mL volumetric flask and the color was developed by adding 1.0 mL of 0.50% sulfamic acid, 2.0 mL of 0.02% formaldehyde solution and 5.0 mL of pararosaniline dye solution and made to the mark (25 mL) by adding deionized water.

For NO<sub>2</sub>, first 0.10% *N*-1-naphthylethylenediamine dihydrochloride stock solution was prepared with deionized water. To prepare the absorbing reagent, 0.50 g of sulfanilic acid was dissolved with 14 mL of glacial acetic acid in a 100 mL volumetric flask together with 2.0 mL of 0.10% *N*-1-naphthylethylenediamine dihydrochloride stock solution and made to volume (100 mL) by adding deionized water. This solution (0.030 M sulfanilic acid, 2.4 M acetic acid and 4.0 mM *N*-1-naphthylethylenediamine dihydrochloride) was used as the absorbing reagent for NO<sub>2</sub>. This absorbing reagent develops a red-violet color directly in the presence of NO<sub>2</sub> and no additional reagents are required.

*Air sampling procedure:* To collect air samples, 10 mL of each absorbing reagents, were pipetted into each midget bubbler. Air sample was aspirated into the absorbing reagents at a certain flow rate. The flow rate at which the air need to be sampled and the sampling time was adjusted with fixed volume of absorbing reagent to obtain the best result (ASTM International D2914-01, 2007). During sampling, the volume of the absorbing reagent was fixed and air sampling rate and sampling time was varied. The air was sampled at different rates to find out the minimum time required for the color development by absorbing reagents. During sampling, the midget bubblers were covered with aluminum foil, to prevent the degradation of the absorbing reagents which are light sensitive. The absorber temperature was controlled to 10-15°C using ice bath, to prevent decomposition of the collected complex and loss of absorbing reagent by evaporations. The difference in temperature in the ice bath by 5.0 °C do not have any adverse effect on color developments (ASTM International D2914-01, 2007). The sampling rate and time were recorded along with the atmospheric pressure and temperature.

*Measurement:* For SO<sub>2</sub>, the atmospheric SO<sub>2</sub> absorbed in the reagent remains in the form of sulfite ions. After sampling, the absorbing reagent was transferred to a 25 mL volumetric flask and a specific volume of the color development reagents were added and kept in an ice bath (5°C) to avoid volatilization of formaldehyde and other reagents. The absorbed sulfite ion reacts with pararosaniline dye in the presence of formaldehyde to form a deep purple color product (from pale purple color) (Figure 5.1). The intensity of the developed purple color is proportional to the concentration of sulfite ions which was measured at 560 nm.

To minimize the release of toxic formaldehyde from the reaction mixture to the environment, the time for keeping the reaction mixture in the ice bath was varied. The presence of formaldehyde in the reaction mixture kept for various time was tested using a formaldehyde sol-gel sensor developed by Bunkoed and co-worker (Bunkoed *et al.*, 2010). For this, the reaction mixture kept for different time was transferred into the head space vial (30 mL) and was heated on a water bath (80 °C) for 20 min to volatilize the formaldehyde into gas form. Then, 10 µL of head space gas was drawn with the air tight syringe and was injected into another 15 mL head space vial, which contain 1.0 mL of

formaldehyde of sol-gel sensor. After which the sensor was left overnight for proper color development by diffusion of formaldehyde into the sol-gel sensor if present any. It was found that, there was decrease in yellow color intensity of the formaldehyde sol-gel sensor with increase of reaction time. When the reaction mixture was kept for 40 min, and tested for presence of formaldehyde, the sol-gel sensor did not show any color change, which shows that all formaldehyde added into the reaction mixture has been reacted completely, thereby its release into the environment was minimized to the least.

For NO<sub>2</sub>, the colorless sulfanilic acid in the absorbing reagent absorbs NO<sub>2</sub> to form diazosulfanilic acid which reacts with N-1-naphthylethylenediamine dihydrochloride present in the solution to form a red-violet color products (Figure 5.2) (Tanaka et al., 1998). The absorbance was measured at 550 nm as soon as possible to minimize any loss (Saltzman, 1949). The absorbance of the reagent blank which was not exposed to air was used as reference for both cases.

#### **5.2.4.1 Analytical performance and method validation**

The standard colorimetric methods for SO<sub>2</sub> (West-Gake 1956) and NO<sub>2</sub> (Saltzman 1949) were modified by changing some reagents and the assembling of various parts of an active sampler. To ensure that the results obtained are reliable the methods were validated using liquid and gas standards as follows.

##### **5.2.4.1.1 Linearity, limit of detection (LOD) and limit of quantitation (LOQ)**

Linearity, LOD and LOQ were determined using a series concentrations of SO<sub>2</sub> and NO<sub>2</sub> liquid standards. The SO<sub>2</sub> liquid standard was prepared by dissolving 0.40 g of sodium sulfite in 500 mL of deionized water. The SO<sub>2</sub> content in the solution was determined by the iodimetric method (Jeffery et al., 1989) and found to be 320 µg mL<sup>-1</sup> (Mahadevaiah et

al., 2008, ASTM, D 2914-01, 2007). For NO<sub>2</sub>, 0.015 g sodium nitrite was dissolved in 500 mL of deionized water, this solution contains 22 µg mL<sup>-1</sup> of NO<sub>2</sub> (Mousazadeh, 2009).

For the evaluation of the linearity of SO<sub>2</sub>, 10 mL of absorbing reagent was pipetted into a series of 25 mL volumetric flasks, five flasks were used for each concentration. Different concentration of liquid standard in the range of 0.050-1.0 µg mL<sup>-1</sup> were added followed by a specific volume of color development reagents (1.0 mL of 0.5% sulfamic acid, 2.0 mL of 0.02% formaldehyde solution and 5.0 mL of pararosaniline dye solution) and adjusted to 25 mL with deionized water. All flasks were kept in an ice bath for 40 min for color development and to make sure that the added formaldehyde reacted completely. The absorbance of the developed purple color was measured against the reagent blank (prepared in similar way without adding standard sulfite solution).

For NO<sub>2</sub>, various concentrations of NO<sub>2</sub> liquid standard (0.010-1.0 µg mL<sup>-1</sup>) were pipetted into series of 25 mL volumetric flasks and the volume was made up to mark by adding the absorbing solution of NO<sub>2</sub>. They were allowed to stand for 10 minutes at room temperature during this time color changed from colorless to red-violet color. The absorbance of the solution was measured using a reagent blank as reference.

Linearity was determined from the plots between the absorbance *versus* concentrations of SO<sub>2</sub> or NO<sub>2</sub>. LOD and LOQ was determined from 3.3σ/S and 10σ/S, respectively, where σ is the standard deviation of the intercept and S is the slope of the calibration curve (Swartz and Krull 1997).

#### **5.2.4.1.2 Precision**

Intraday and interday precisions of the method were studied by preparing five replicates of three different concentrations (0.3, 0.5, and 1.0 µg mL<sup>-1</sup>) of SO<sub>2</sub> and NO<sub>2</sub> liquid standards (ICH guidelines, 2005). For evaluation of SO<sub>2</sub> and NO<sub>2</sub> intraday and interday precisions, similar procedure was followed as described in section 2.2 and the absorbance was measured. This was to see if different time of sampling on same day and on different day have any effect on the overall results during final sampling. For validating the intraday

precisions the absorbance of the developed color was measured at different time of the day and for interday the absorbance was measured consecutively for three different days (Halima *et al.*, 2012). Intraday and interday precisions were evaluated using freshly prepared standards for every new set of measurements.

#### **5.2.4.1.3 Calibration of liquid standard and gas standard**

Since most of the validation was done using the liquid standards to ensure its applicability, the responses of the liquid standards were compared with those of the gas standards, prepared in air tight headspace vials based on the stoichiometric calculations (Averill and Eldredge 2006). Three different concentrations (0.3, 0.7 and 1.0  $\mu\text{g mL}^{-1}$ ) of liquid and gas standards of  $\text{SO}_2$  and  $\text{NO}_2$  were tested. The gas standards were injected, using a gas tight syringe, into the respective absorbing reagents in the air tight head space vials. The slopes of the two curves were compared and analyzed by Two-Way ANOVA to see any significant difference in their slopes. The absorbance obtained from the two standards were also compared with paired t-test.

#### **5.2.4.1.4 Flow rate and sampling time**

Since this work focusses on a short-term sample collection, the flow rate was measured at the sampling site (ASTM D 2914, 2007). Soap flow meter was used to measure the flow rate and to calibrate the flow controller by connecting it to the outlet of the flow controller. The flow rate was controlled using the adjustable knob of the flow controller. During sampling the flow meter was removed and the outlet of the flow controller was connected as shown in Figure 5.3. The suitable flow rate was selected based on the minimum time required for the color development by the absorbing reagent placed on the midjet bubbler. The flow rate was monitored through the calibrated flow controller ensure a constant flow of the sampled air. After each sampling the flow rate was confirmed again with the flow meter.

### 5.2.5 Sampling sites

Bhutan being a developing country and with a number of developmental activities taking place, there is increasing trend of industries in Bhutan. So, it would be good to know the ambient air quality in the industrial areas which will provide the concerned authority with some guidelines to control the environment. The selected sampling site was Pasakha industrial estate, which is located at the foot hill of Bhutan, bordering India (26°50' N, 89°26' E, 342 m above sea level) and with no prior study on air pollution in this area. Some of the industries located in this industrial area are ferro alloy, metal, silicon, ceramic, and carbide. Since SO<sub>2</sub> and NO<sub>2</sub> are mainly emitted to ambient air from combustion of oil, coal and combustion chamber with very high temperatures (Meng *et al.*, 2008) and almost all these industries make use of coal as the main fuel (NEC, 2009). So, there is a possibility of SO<sub>2</sub> and NO<sub>2</sub> emission from these industrial areas.

Sampling was carried out during the spring of 2015 (April-June). Twenty five sampling stations were selected (S1-S25). Sampling stations included all the catchment areas like staff quarters, schools, shops and villages, to make sure that the people living around the industrial areas should be made aware of their ambient environment. Samples were collected using active sampler, at the height of 150-160 m above the ground on a daily basis. From each sampling site, samples were collected, three times a day, morning (7.00-9.00 AM), afternoon (1.00-3.00 PM) and evening (5.00-7.00 PM) to find the average daily concentration of the two pollutants and to see the two pollutants concentration levels at different time of the day. Wind speed, temperature, and pressure were also recorded. After sampling, the absorbance of the color developed were measured on the site. And the final concentration of the pollutants were calculated based on the absorbance reading and the slope obtained from the calibration curve.

Figure 5.4 shows the two industrial areas and the 25 different sampling stations (S1-S25). S1 and S2, were located inside the industrial area I and II, the sources of emission. When compared in-terms of number of factories and overall area, area I is bigger. For area II the settlements around it are much fewer. S1 and S2, were selected to see the

concentration of  $\text{SO}_2$  and  $\text{NO}_2$  level within the industrial area I and II. S3, S4 and S8, were the nearby staff quarters with S3 and S4 were 50 m and 300 m away from area I, and S8 400 m from area I and II. S5 and S6 were located around 300m away on the slope facing area I, selected to see the two pollutants level at nearby areas from the emission source. Moreover, S6 is the small Buddhist monastic school with about 40 monks. S7 and S11 are the nearby communities with a few shops. S9, S10, S12-S22 are the settlement areas along with some agricultural fields. Among these, four sites were the main settlement areas located on the slopes facing the industrial areas, S13 and S14 facing area I while, S12 and S17 facing area II. The rest were located further away either on the slope facing area I or on the opposite side of the hill to area I. S23-S25 were the farthest about 2.5-3.0 km from area I and II. A staff quarter for the Bhutan power corporation working on the power station (S23) was located at 2.5 km away from the area I and II. S24, is the only school with about 700 students located on a hill top around 3.0 km away from the area I and II. S25 is the farthest settlement area located on the top of the hill, similar to that of S24.



**Figure 5.4** Map showing the industrial area of Bhutan and sampling stations

### 5.2.6 Calculation of ambient concentration of SO<sub>2</sub> and NO<sub>2</sub>

After sampling the final concentration of SO<sub>2</sub> and NO<sub>2</sub> was calculated by the relationship (Equation 5.1) this equation was first used for converting the volume of air sampled to the volume in liter at the reference conditions of 25°C and 760 mmHg.

$$V_R = V \times \frac{P}{760} \times \frac{298}{(t + 273)} \quad (5.1)$$

Where;

V<sub>R</sub> = volume of air at 25°C and 760 mmHg in liter

V = volume of air sampled in liter

P = barometric pressure in mmHg

t = temperature in °C

Final ambient concentration of SO<sub>2</sub> or NO<sub>2</sub> in µg m<sup>-3</sup> can be calculated using equation (5.2)

$$C(\mu\text{g m}^{-3}) = \frac{(A - A_0) \times B \times 10^3}{V_R} \times D \quad (5.2)$$

Where;

A = absorbance of a sample

A<sub>0</sub> = absorbance of blank reagent

V<sub>R</sub> = volume of air sampled at 25°C and 760 mmHg

B = calibration factor (µg or absorbance unit)

D = dilution factor for 30 min and 1 hour sampling; D = 1 and for 24 hour sampling D = 10

## 5.2.7 Results and Discussion

### 5.2.7.1 Analytical performance of the system

#### 5.2.7.1.1 Linear dynamic range (LDR), limit of detection (LOD) and limit of quantification (LOQ)

Using liquid standards, a good linearity for both analytes were obtained, in the range of 0.050-1.0  $\mu\text{g mL}^{-1}$  for  $\text{SO}_2$  with a linear equation of  $y = (89.8 \pm 1.6)x + (1.03 \pm 0.83)$ , ( $R^2 = 0.998$ ) and 0.010-1.0  $\mu\text{g mL}^{-1}$  for  $\text{NO}_2$  with a linear equation of  $y = (73.2 \pm 2.9)x + (2.7 \pm 1.1)$ , ( $R^2 = 0.997$ ). The LOD for  $\text{SO}_2$  and  $\text{NO}_2$  were  $30.0 \pm 1.0$  and  $50.0 \pm 2.0$   $\text{ng mL}^{-1}$  and LOQ were  $90.0 \pm 2.0$  and  $150.0 \pm 6.0$   $\text{ng mL}^{-1}$ , respectively (Table 5.1).

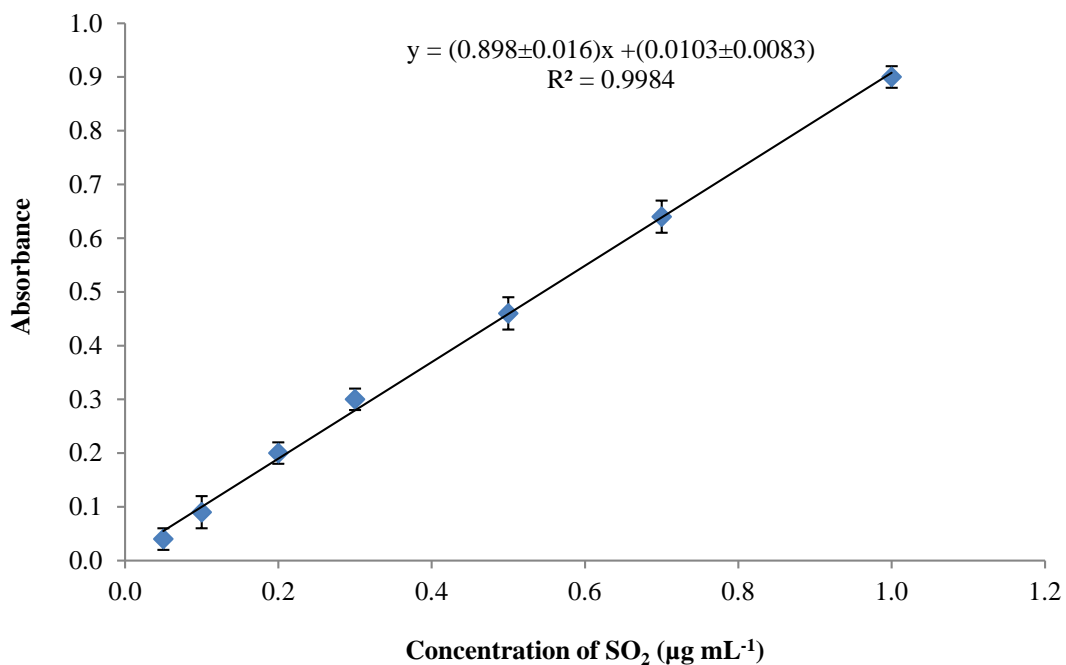


**Figure 5.5** Linear plot of  $\text{SO}_2$  in the concentration range of 0.05-1.0  $\mu\text{g mL}^{-1}$  ( $n = 5$ )

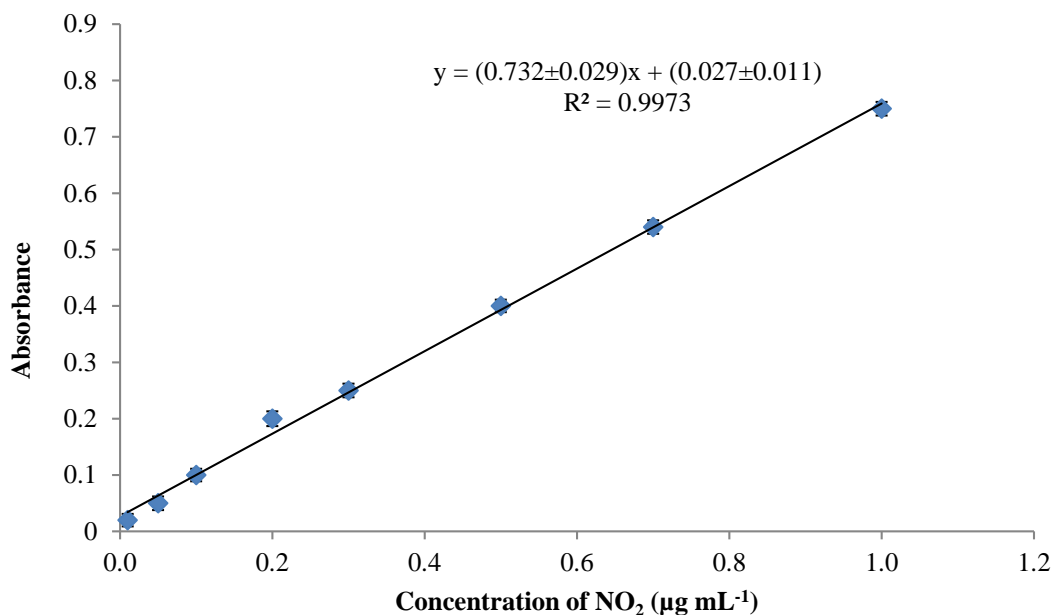


**Figure 5.6** Linear plot of NO<sub>2</sub> in the concentration range of 0.05-1.0 µg mL<sup>-1</sup> (n = 5)

**Table 5.1** LOD and LOQ of SO<sub>2</sub> and NO<sub>2</sub>

Analyte	LOD (ng mL <sup>-1</sup> )	LOQ (ng mL <sup>-1</sup> )
SO <sub>2</sub>	30.0±1.0	90.0±2.0
NO <sub>2</sub>	50.0±2.0	150.0±6.0

### 5.2.7.2 Precision

Tables 5.2 and 5.3 show the intraday and interday precisions of SO<sub>2</sub> and NO<sub>2</sub>, respectively. It can be concluded that the absorbance measured during different times of the day and on different days are similar. The results, reported as %RSD, were lower than 5.0% which is acceptable as per AOAC guidelines of 8% for 1 µg mL<sup>-1</sup> concentration (AOAC, 2002). The intraday and interday precisions confirmed that this method is stable and reliable *i.e.* the system can be used any time and any day.

**Table 5.2** Intraday and interday precision for SO<sub>2</sub> (n = 5)

<b>Intraday</b>				
<b>Concentration</b> ( $\mu\text{g mL}^{-1}$ )	<b>Absorbance</b> <b>(Morning)</b>	<b>Absorbance</b> <b>(Afternoon)</b>	<b>Absorbance</b> <b>(Evening)</b>	<b>Average</b> <b>%RSD</b>
0.3	0.25±0.01	0.26±0.01	0.24±0.01	4.0
0.5	0.41±0.01	0.39±0.01	0.40±0.01	2.5
1.0	0.74±0.01	0.73±0.01	0.74±0.01	1.4
<b>Interday</b>				
	<b>Day1</b>	<b>Day 2</b>	<b>Day 3</b>	
0.3	0.24±0.01	0.25±0.01	0.25±0.01	4.1
0.5	0.41±0.01	0.40±0.01	0.40±0.01	2.5
1.0	0.74±0.02	0.73±0.02	0.73±0.02	2.7

**Table 5.3** Intraday and interday precision for NO<sub>2</sub> ( $n = 5$ )

<b>Intraday</b>				
<b>Concentration</b> ( $\mu\text{g mL}^{-1}$ )	<b>Absorbance</b> <b>(Morning)</b>	<b>Absorbance</b> <b>(Afternoon)</b>	<b>Absorbance</b> <b>(Evening)</b>	<b>Average</b> <b>%RSD</b>
0.3	0.21±0.01	0.22±0.01	0.22±0.01	4.6
0.5	0.38±0.01	0.39±0.01	0.38±0.01	2.6
1.0	0.70±0.01	0.71±0.01	0.70±0.01	1.4
<b>Interday</b>				
	<b>Day1</b>	<b>Day 2</b>	<b>Day 3</b>	
0.3	0.20±0.01	0.21±0.01	0.21±0.01	4.9
0.5	0.40±0.01	0.39±0.01	0.39±0.01	2.6
1.0	0.71±0.01	0.71±0.01	0.70±0.02	1.9

### 5.2.7.3 Calibration of liquid and gas standards

After plotting the calibration curves of liquid and gas standard of SO<sub>2</sub> and NO<sub>2</sub>, the two slopes were tested by Two-Way ANOVA. The comparison showed that statistically there was no significant difference in the sensitivity of liquid and gas standards ( $P > 0.05$ ). Although their sensitivities (slopes) were the same, it should be noted that the absorbance of the gas standards were slightly lower than that of liquid standards. It was likely because there was some loss of gas while transferring from one head space vial to another head space vial for dilution. However, when the absorbance obtained from the liquid and gas standards were analysed using paired t-test, it also showed that statistically there was no

significant difference in the absorbance reading obtained from liquid and gas standards ( $P > 0.05$ ).

**Table 5.4** Table showing the accuracy of absorbance of SO<sub>2</sub> and NO<sub>2</sub> liquid standard and gas standard ( $n=5$ )

Concentration ( $\mu\text{g mL}^{-1}$ )	SO <sub>2</sub>		NO <sub>2</sub>	
	Absorbance (liquid standard)	Absorbance (gas standard)	Absorbance (liquid standard)	Absorbance (gas standard)
0.3	0.25 $\pm$ 0.01	0.23 $\pm$ 0.01	0.22 $\pm$ 0.01	0.20 $\pm$ 0.01
0.7	0.55 $\pm$ 0.01	0.53 $\pm$ 0.02	0.53 $\pm$ 0.01	0.51 $\pm$ 0.01
1.0	0.75 $\pm$ 0.01	0.74 $\pm$ 0.01	0.71 $\pm$ 0.01	0.70 $\pm$ 0.01

#### 5.2.7.4 Flow rate and sampling time

The flow rate of the air flowing into the absorbing solution and the sampling time was selected based on the flow rate and the minimum time required for the color development by the absorbing reagent at the sampling site. It was found that when the flow rate was fixed at 0.20 L min<sup>-1</sup> (maximum flow rate provided by the mini air 12 V DC vacuum air pump) the minimum time required for color development by the absorbing reagent was 2 h, which provided the least absorbance reading on spectrophotometer compared to the blank. Less than 2 h of sampling provided same reading as that of blank. So, the flow rate for collection of air sample was fixed at 0.20 L min<sup>-1</sup> and the sampling time for 2 h.

#### 5.2.7.5 Sampling result

During the sampling period, the temperature was recorded in the range of 24-35°C, wind speed of 0-5 km h<sup>-1</sup> and atmospheric pressure of 690-760 mm Hg. The ambient concentration of SO<sub>2</sub> and NO<sub>2</sub> at morning, afternoon, evening and average are shown in the form of histogram in Figure 5.7.

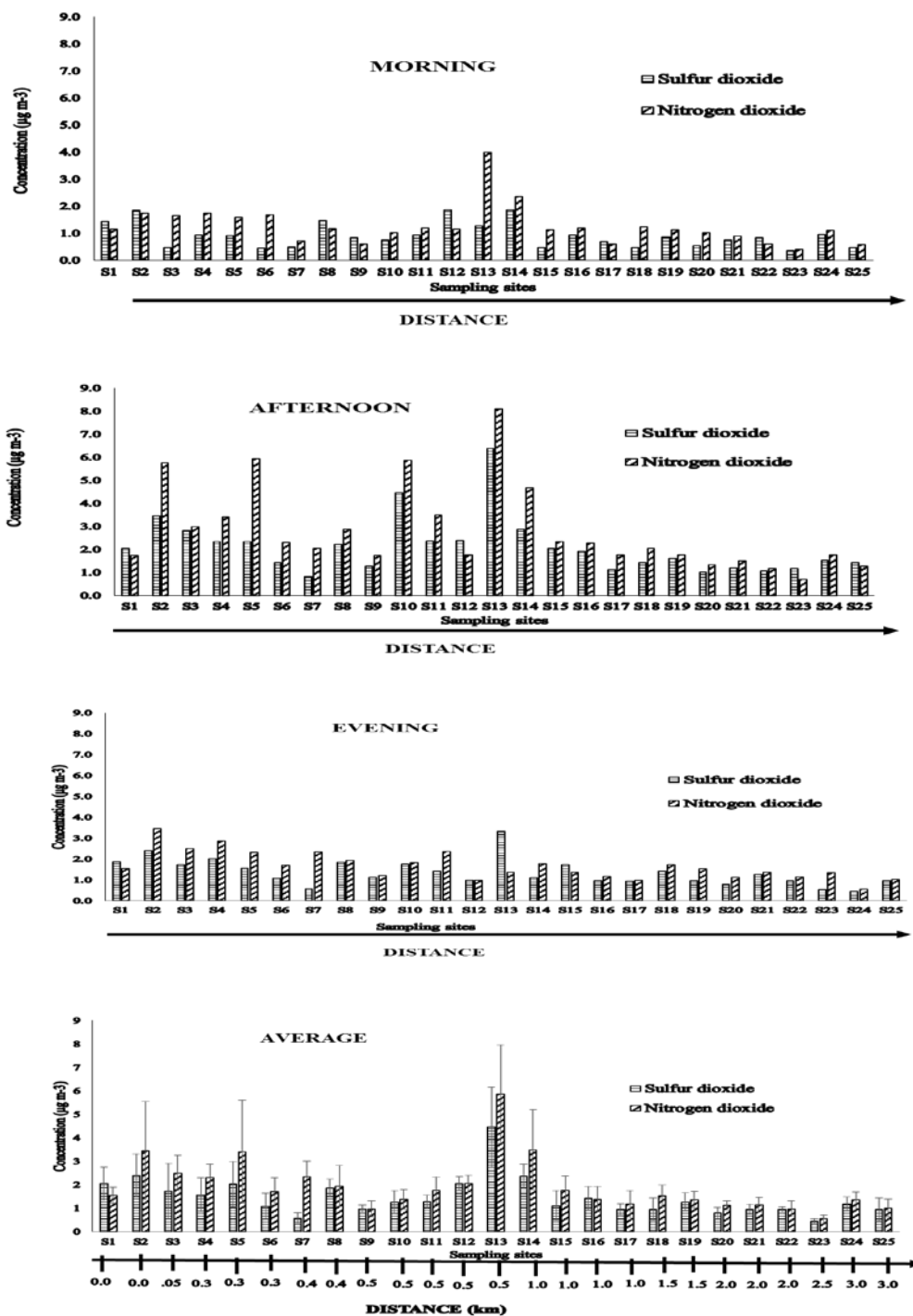


**Figure 5.7** Histogram showing the ambient concentration of SO<sub>2</sub> and NO<sub>2</sub> in morning afternoon, evening and average at different sampling stations with distance in km.

In general, the concentration of SO<sub>2</sub> and NO<sub>2</sub> varied throughout the day, were lowest in the morning, peak in the afternoon and come slightly down in the evening. This was likely because the normal working hour is from 8.00 AM-5.00 PM and the factories are in full operation in the day time. At night they are partially operated.

From the sampling result, it was found that the concentration of SO<sub>2</sub> and NO<sub>2</sub> differed mainly because of the distance from the emission source and the topography of the sampling sites. In sampling sites S1 and S2 within the emission source, the concentration of SO<sub>2</sub> and NO<sub>2</sub> were in the range of 2.04±0.71-2.39±0.92 and 1.55±0.34-3.45±2.1 µg m<sup>-3</sup>, respectively. These results, as expected, were on the higher side compared to many other sites. The concentration of the two pollutants more or less decreased with increase in distance from the emission source area I and II, except for sampling sites S13 and S14. Though, these two sampling sites were located about 0.50-1.0 km away from the emission source area I, the concentration of SO<sub>2</sub> and NO<sub>2</sub> were higher. In fact the highest concentration of both pollutants were found at S13 (Singye village) which was 4.46±1.7 and 5.86±2.1 µg m<sup>-3</sup>, respectively. It might be because of the topography of this village that is located over the slope facing the major industrial area I. The emitted pollutants are directly blown towards this village by the wind and can get concentrated over this village area. When compared to S13 the concentration of SO<sub>2</sub> and NO<sub>2</sub> were slightly lower at S14 (2.36±0.51 and 3.49±1.7 µg m<sup>-3</sup>) though geographically this site was similar to S13. This was likely because it was located (1.0 km) further away from the emission source area I. The lowest concentration of SO<sub>2</sub> and NO<sub>2</sub> (0.45±0.09 and 0.56±0.15 µg m<sup>-3</sup>) was found in Bhutan power colony (S23) which is located approximately 2.5 km from the area I and II. This was likely because this site is located quite far from the emission source (area I and II) and in a valley surrounded by hills and slopes, thus the pollutants emitted from the source are probably diluted by moisture present in the air before reaching this sampling station (Tan and Piri, 2013, Zhang and Tie, 2011).

The results also showed that the concentration of SO<sub>2</sub> and NO<sub>2</sub> were affected by the topography of the sampling site. When the sites were on a slope facing the emission source the concentrations of the two pollutants were generally quite high. For example,

comparing between S2 and S5 that was located over a slope facing area I, though S5 was about 300 m away from the emission source area I, the concentration of SO<sub>2</sub> and NO<sub>2</sub> (2.02±0.97 and 3.41±2.2 µg m<sup>-3</sup>) were similar to that of S2 (2.39±0.92 and 3.45±2.1) within the emission source. Similarly S12 which is located around 0.50 km away and facing the emission source area II, the concentration of SO<sub>2</sub> and NO<sub>2</sub> was found to be 2.05±0.29 and 1.36±0.35 µg m<sup>-3</sup>, which was comparatively higher than other sites. On the other hand S9 that was located in the shallow valley surrounded by small hills, the concentration of SO<sub>2</sub> and NO<sub>2</sub> (0.97±0.15 and 0.97±0.4 µg m<sup>-3</sup>) were much lower than many sampling sites (S10-S11) with the same distance from the emission source area I (500 m). In this case the wind blowing from the emission source cannot reach this site directly since it is blocked by the surrounding hills.

Among the sampling stations there are two schools (S6, S24) that are classified as one of the two sensitive sites (hospitals and schools) as per National Environment Commission (NEC) of Bhutan guideline 2010. The monastic school (S6) is located just 300 m above the source of emission over a plateau. The concentration of SO<sub>2</sub> and NO<sub>2</sub> at this site was found at 1.09±0.55 µg m<sup>-3</sup> and 1.71±0.58 µg m<sup>-3</sup>, respectively. These were lower than expected, compared to S5, since both sites were located at a similar distance from area I. The wind can easily carry the emitted pollutants towards it. Moreover, the slope above the school can block the wind flow thereby accumulating the pollutants. This low concentration might be because of the overnight rains before the sampling day which might have washed down all the accumulated pollutants. For the middle secondary school (S24), located about 3.0 km away from the source of emission (area I), the concentration of SO<sub>2</sub> and NO<sub>2</sub> was 1.17±0.30 µg m<sup>-3</sup> and 1.35±0.35 µg m<sup>-3</sup>, respectively. Though, the school is located quite far from the area I the concentration of SO<sub>2</sub> and NO<sub>2</sub> was still a little higher than some other sites of similar distance (S25). Again, possibly because the school is located on the slope facing the area I. For S25 the concentration was lower, this might be because the pollutants are diluted by the moisture present in the air as it is blown towards it.

### 5.2.8 Conclusion

From this study, it is clear that the ambient concentration of SO<sub>2</sub> and NO<sub>2</sub> in an industrial area of Bhutan, in the range of 0.45±0.09-4.46±1.7 µg m<sup>-3</sup> and 0.56±0.15-5.68±2.1 µg m<sup>-3</sup>, for spring season, respectively, were still much lower than the maximum permissible limits (MPL) set by National Environment Commission of Bhutan (80 µg m<sup>-3</sup>) (NEC, 2010) for a day average in a mixed area consisting of a settlement and commercial activities. Literature suggested that, the presence of high moisture content in air can dissolve the two pollutants forming an acid (Tan and Pirie, 2013, Zhang and Tie, 2011). Therefore, it is expected, the level of SO<sub>2</sub> and NO<sub>2</sub> would be much higher during dry season. Therefore, further sampling need to be done to include all seasons so as to obtain the annual average concentration of SO<sub>2</sub> and NO<sub>2</sub>. During the sampling time it was observed that the majority of the factories operating were not following the standard operating process. Many factories were releasing its smoke without any treatment. So, if this process is not controlled at the earliest there are chances that the concentration of air pollutants and perhaps particulate matters would increase dramatically within a short span of time. Therefore, a regulating body like NEC should set a strict guidelines for all factories with regards to pollution. One of the way to reduce pollution level can be achieved by fixing filters on the chimneys so that toxic pollutants are not released out directly into an environment.

## CHAPTER 6

### Conclusions

This thesis work is based on monitoring of various air pollutants in an ambient air using both active and passive sampling technique, using different analysis technique. The air pollutants like benzene, toluene, and xylene which are volatile organic compounds and causes serious damages to environment and human health were monitored in Hat Yai city of Thailand using the passive sampling technique. And sulfur dioxide and nitrogen dioxide was monitored in an industrial area of Bhutan using active sampling technique to set-up the baseline data for future references.

For monitoring of benzene, toluene and xylene in Hat Yai city, printed circuit board passive sampler was re-developed and it was re-validated in the laboratory before monitoring the ambient air in Hat Yai city. The re-developed and re-validated PCB passive sampler was used in mass for monitoring of BTX in Hat Yai city. The PCB passive sampler was thermally desorbed by using laboratory-built thermal desorption system and with on-line micro-preconcentrator coupled with GC-FID. The ambient concentration of benzene, toluene and xylene in Hat Yai city were found in the range of N.D –  $11.3 \pm 1.6$ ,  $4.5 \pm 0.76$  –  $49.6 \pm 3.7$  and  $1.0 \pm 0.21$  –  $39.6 \pm 3.1$   $\mu\text{g m}^{-3}$  respectively. The minimum concentration of BTX was found in Prince of Songkla University reservoir area, since the traffic volume in this area was comparatively low. And the maximum concentration of BTX was detected in major down town area which is the tourist hot spot of the city. Thus, this area has high number of traffic flow plus tall buildings with many shopping malls. This study proves that the main source of BTX in ambient air in Hat Yai city is from automobile exhaust. It also shows that the concentration of benzene is slowly increasing as compared to previous study and that of toluene and xylene are remaining almost constant as compared to previous study. The ambient concentration level of toluene and xylene is still under control but since, benzene is highly carcinogenic, therefore any amount of benzene in air is harmful to human

health. So, it is better to take precautionary measures to control the ambient concentration of benzene as far as possible.

Monitoring of SO<sub>2</sub> and NO<sub>2</sub> were carried out for the spring season in an industrial area of Bhutan using the active sampling technique and standard colorimetric method. Monitoring of SO<sub>2</sub> and NO<sub>2</sub> has not been carried out in this area before. Since, the number of factories are increasing year by year it would be good to develop the baseline data for these two major air pollutants which are mainly emitted from the factories and industries. For this study, the standard colorimetric method like West and Gaeke method for SO<sub>2</sub> and Saltzman method for NO<sub>2</sub> were used. Since, West and Gaeke method used highly toxic chemicals like mercury and formaldehyde, it was modified little by replacing the mercury containing compound with environmentally friendly compound triethanolamine, and the concentration of formaldehyde was reduced to the minimum so that all formaldehyde are used up for the colour development reaction. So, simple and portable active sampler was developed in the laboratory and was re-validated for monitoring of SO<sub>2</sub> and NO<sub>2</sub> in the ambient air. After validating the developed active sampler it was transported to the sampling site in Bhutan and SO<sub>2</sub> and NO<sub>2</sub> were sampled from 25 different locations keeping certain distance from the emission source. The ambient concentration of SO<sub>2</sub> and NO<sub>2</sub> was found in the range of 0.45 – 4.46 and 0.56 – 5.68 µg m<sup>-3</sup> respectively. From this study it can be concluded that the ambient concentration of SO<sub>2</sub> and NO<sub>2</sub> are far below the maximum permissible limit as set by national environment commission of Bhutan (80 µg m<sup>-3</sup> for 24 hour average). But, it still is an alarming sign for a small country like Bhutan. And this research data would serve as a base line data for future studies.

### References

- American Society for Testing and Materials, International, 2007. Standards test methods for sulfur dioxide content of the atmosphere (West-Gaeke Method). D 2914-01.
- AOAC, 2002. Guidelines for single laboratory validation of chemical methods for dietary supplements and botanicals.
- Arthur, C.L., Pawliszyn, J., 1990. Solid-phase microextraction with thermal desorption using silica optical fibers. 62, 2145–2148.
- Augusto, F., Luiz Pires Valente, A., 2002. Applications of solid-phase microextraction to chemical analysis of live biological samples. *TrAC Trends Anal. Chem.* 21, 428–438.
- Averill, B. A., and Eldredge, P. 2006. *General Chemistry: Principles, Patterns and Applications*. Flat World Knowledge, one bridge street suite 105, Irvington, New York.
- Bai, Z., Xie, C., Zhang, S., Xu, W., Xu, J., 2011. Microwave sintering of ZnO nanopowders and characterization for gas sensing. *Mater. Sci. Eng. B* 176, 181–186.
- Baldasano, J.M., Valera, E., Jiménez, P., 2003. Air quality data from large cities. *Sci. Total Environ.* 307, 141–165.
- Barrero, M.A., Orza, J.A.G., Cabello, M., Cantón, L., 2015. Categorisation of air quality monitoring stations by evaluation of PM10 variability. *Sci. Total Environ.* 524–525, 225–236.
- Barták, P., Čáp, L., 1997. Determination of phenols by solid-phase microextraction. *J. Chromatogr. A* 767, 171–175.
- Batterman, S., Metts, T., Kalliokoski, P., Barnett, E., 2002. Low-Flow Active and Passive Sampling of VOCs Using Thermal Desorption Tubes: Theory and Application at an Offset Printing Facility. *Journal of Environmental Monitoring* 4, 361–370.
- Beauchamp, J., Gutmann, R., Herbig, J., Hansel, A., 2008. On the use of Tedlar bags for breath-gas sampling and analysis. *J. Breath Res.* 046001, 1–19.
- Beckerman, B., Jerrett, M., Brook, J.R., Verma, D.K., Arain, M.A., Finkelstein, M.M., 2008. Correlation of nitrogen dioxide with other traffic pollutants near a major expressway. *Atmos. Environ.* 42, 275–290.
- Bell, M.L., Davis, D.L., Gouveia, N., Borja-Aburto, V.H., Cifuentes, L.A., 2006. The avoidable health effects of air pollution in three Latin American cities: Santiago, São Paulo, and Mexico City. *Environ. Res.* 100, 431–440.

- Beránek, J., Kubátová, A., 2008. Evaluation of solid-phase microextraction methods for determination of trace concentration aldehydes in aqueous solution. *J. Chromatogr. A* 1209, 44–54.
- Billionnet, C., Gay, E., Kirchner, S., Leynaert, B., Annesi-Maesano, I., 2011. Quantitative assessments of indoor air pollution and respiratory health in a population-based sample of French dwellings. *Environ. Res.* 111, 425–434.
- Bishop, E.J., Mitra, S., 2007. Measurement of nitrophenols in air samples by impinger sampling and supported liquid membrane micro-extraction. *Anal. Chim. Acta* 583, 10–14.
- Boyd-Boland, A.A., Pawliszyn, J.B., 1995. Solid-phase microextraction of nitrogen-containing herbicides. *J. Chromatogr. A* 704, 163–172.
- Briggs, D.J., de Hoogh, K., Morris, C., Gulliver, J., 2008. Effects of travel mode on exposures to particulate air pollution. *Environ. Int.* 34, 12–22.
- Buczynska, A.J., Krata, A., Stranger, M., Locateli Godoi, A.F., Kontozova-Deutsch, V., Bencs, L., Naveau, I., Roekens, E., Van Grieken, R., 2009. Atmospheric BTEX-concentrations in an area with intensive street traffic. *Atmos. Environ.* 43, 311–318.
- Campos, V.P., Cruz, L.P.S., Godoi, R.H.M., Godoi, A.F.L., Tavares, T.M., 2010. Development and validation of passive samplers for atmospheric monitoring of SO<sub>2</sub>, NO<sub>2</sub>, O<sub>3</sub> and H<sub>2</sub>S in tropical areas. *Microchem. J.*, Brazilian National Meeting of Analytical Chemistry, 2009 96, 132–138.
- Cariou, S., Guillot, J.-M., 2006. Double-layer Tedlar bags: a means to limit humidity evolution of air samples and to dry humid air samples. *Anal Bioanal Chem* 384, 468–474.
- Carotta, M.C., Martinelli, G., Crema, L., Malagù, C., Merli, M., Ghiotti, G., Traversa, E., 2001. Nanostructured thick-film gas sensors for atmospheric pollutant monitoring: quantitative analysis on field tests. *Sens. Actuators B Chem.*, Proceeding of the Eighth International Meeting on Chemical Sensors IMCS-8 - Part 1 76, 336–342.
- Carrieri, M., Bartolucci, G.B., Paci, E., Sacco, P., Pignini, D., Zaratin, L., Cottica, D., Scapellato, M.L., Tranfo, G., 2014. Validation of a radial diffusive sampler for measuring occupational exposure to 1,3-butadiene. *J. Chromatogr. A, Method Validation* 1353, 114–120.
- Cavalcante, R.M., Campelo, C.S., Barbosa, M.J., Silveira, E.R., Carvalho, T.V., Nascimento, R.F., 2006. Determination of carbonyl compounds in air and cancer risk assessment in an academic institute in Fortaleza, Brazil. *Atmos. Environ.* 40, 5701–5711.
- Cetin, D., Odabasi, M., Seyfioglu, R., 2003. Ambient volatile organic compound concentrations around a petrochemical complex and a petroleum refinery. *The Science of the Total Environment* 312, 103–112.

- Chang, C.-C., Lo, S.-J., Lo, J.-G., Wang, J.-L., 2003. Analysis of methyl tert-butyl ether in the atmosphere and implications as an exclusive indicator of automobile exhaust. *Atmos. Environ.* 37, 4747–4755.
- Chang, C.-C., Sree, U., Lin, Y.-S., Lo, J.-G., 2005. An examination of 7:00–9:00 PM ambient air volatile organics in different seasons of Kaohsiung city, southern Taiwan. *Atmos. Environ.* 39, 867–884.
- Ciarrocca, M., Caciari, T., Ponticiello, B.G., Gioffre, P.A., Tomei, G., Sancini, A., Schifano, M.P., Palermo, P., Nardone, N., Scimitto, L., Fiaschetti, M., Tomei, F., 2011. Folicle-stimulating hormone levels in female workers exposed to urban pollutants. *Int. J. Environ. Health Res.* 28, 1–11.
- Cooper, C.D., Alley, F.C., 2002. *Air Pollution Control-A Design Approach*, Third Edition. ed. Waveland Press, Inc. Long Grove, NJ.
- Cox, R.M., 2003. The use of passive sampling to monitor forest exposure to O<sub>3</sub>, NO<sub>2</sub> and SO<sub>2</sub>: a review and some case studies. *Environ. Pollut.* 126, 301–311.
- Dart, A., Thornburg, J., 2008. Collection efficiencies of bioaerosol impingers for virus-containing aerosols. *Atmos. Environ.* 42, 828–832.
- Dejmek, J., Jelinek, R., Solansky, I., Sram, R., 2000. Fecundability and parental exposure to ambient sulfur dioxide. *Environ. Health Perspect.* 108, 647–654.
- Demeestere, K., Dewulf, J., De Witte, B., Van Langenhove, H., 2007. Sample preparation for the analysis of volatile organic compounds in air and water matrices. *J. Chromatogr. A, Advances in Sample Preparation Part II* 1153, 130–144.
- Desauziers, V., 2004. Traceability of pollutant measurements for ambient air monitoring. *TrAC Trends Anal. Chem.* 23, 252–260.
- Dettmer, K., Engewald, W., 2002. Adsorbent materials commonly used in air analysis for adsorptive enrichment and thermal desorption of volatile organic compounds 373, 490–500.
- Dewulf, J., Van Langenhove, H., Huybrechts, T., 2006. Developments in the analysis of volatile halogenated compounds. *TrAC Trends Anal. Chem., Organohalogen Analysis* 25, 300–309.
- Domeño, C., Martínez-García, F., Campo, L., Nerín, C., 2004. Sampling and analysis of volatile organic pollutants emitted by an industrial stack. *Anal. Chim. Acta, Papers presented at the VIIIth International Symposium on Analytical Methodology in the Environmental Field and XIIIth Meeting of the Spanish Society of Analytical Chemistry, University of A Coruna, Spain - 21-24 October 2003* 524, 51–62.
- Dutta, K., Bhowmik, B., Hazra, A., Chattopadhyay, P.P., Bhattacharyya, P., 2015. An efficient BTX sensor based on p-type nanoporous titania thin films. *Microelectron. Reliab.* 55, 558–564.

- Elbir, T., Cetin, B., Cetin, E., Bayram, A., Odabasi, M., 2007. Characterization of Volatile Organic Compounds (VOCs) and Their Sources in the Air of Izmir, Turkey 149–160.
- Erduran, M.S., Tuncel, S.G., 2001. Gaseous and Particulate air pollutants in the Mediterranean coast. *Science of the Total Environment* 281, 205–215.
- Feng, Y., Wen, S., Wang, X., Sheng, G., He, Q., Tang, J., Fu, J., 2004. Indoor and outdoor carbonyl compounds in the hotel ballrooms in Guangzhou, China. *Atmos. Environ.* 38, 103–112.
- Franklin, P.J., 2007. Indoor air quality and respiratory health of children. *Paediatr. Respir. Rev.* 8, 281–286.
- Gallego, E., Roca, F.X., Guardino, X., Rosell, M.G., 2008. Indoor and outdoor BTX levels in Barcelona City metropolitan area and Catalan rural areas. *J. Environ. Sci.* 20, 1063–1069.
- Garg, A., Shukla, P.R., Kapshe, M., 2006. The sectoral trends of multigas emissions inventory of India. *Atmos. Environ.* 40, 4608–4620.
- Geetha, K., Balasubramanian, N., 2000. An indirect method for the determination of sulfur dioxide using Methyl Red. *Microchem. J.* 65, 45–49.
- Gibson, L.T., Cooksey, B.G., Littlejohn, D., Tennent, N.H., 1997. Determination of experimental diffusion coefficients of acetic acid and formic acid vapours in air using a passive sampler. *Anal. Chim. Acta.* 341: 1–10.
- Górecki, T., Namieśnik, J., 2002. Passive sampling. *TrAC Trends Anal. Chem.* 21, 276–291.
- Graham, B. W. L. 1980. A general review of some of the early air pollution monitoring in Auckland. *Chemistry in New Zealand*, p. 18-20.
- Gurjar, B.R., Butler, T.M., Lawrence, M.G., Lelieveld, J., 2008. Evaluation of emissions and air quality in megacities. *Atmos. Environ.* 42, 1593–1606.
- Halima, O. A., Aneesh, T. P., Reshma, G., and Thomas, N. R., 2012. Development and validation of UV spectrophotometric method for the estimation of asenapine maleate in bulk and pharmaceutical formulation. *Der Pharma Chemica*, 4: 644-649.
- Harper, M., 2000. Sorbent trapping of volatile organic compounds from air. *J. Chromatogr. A* 885, 129–151.
- Hazrati, S., Harrad, S., 2007. Calibration of polyurethane foam (PUF) disk passive air samplers for quantitative measurement of polychlorinated biphenyls (PCBs) and

- polybrominated diphenyl ethers (PBDEs): Factors influencing sampling rates. *Chemosphere* 67, 448–455.
- Helmig, D., 1996. Artifact-free preparation, storage and analysis of solid adsorbent sampling cartridges used in the analysis of volatile organic compounds in air. *J. Chromatogr. A* 732, 414–417.
- Helmig, D., Greenberg, J.P., 1994. Automated in situ gas chromatographic-mass spectrometric analysis of ppt level volatile organic trace gases using multistage solid-adsorbent trapping. *J. Chromatogr. A* 677, 123–132.
- Heo, G.S., Lee, J.-H., Kim, D.W., Lee, D.W., 2001. Comparison of analytical methods for ozone precursors using adsorption tube and canister. *Microchem. J.*, Papers Presented at the Sixth International Symposium on Advanced Analytical Techniques and Applications 70, 275–283.
- Hogan Jr, C.J., Kettleson, E.M., Lee, M.-H., Ramaswami, B., Angenent, L.T., Biswa, P., 2005. Sampling methodologies and dosage assessment techniques for submicrometre and ultrafine virus aerosol particles. *J. Appl. Microbiol.* 99, 1422–1434.
- Holopainen, S., Luukkonen, V., Nousiainen, M., Sillanpää, M., 2013. Determination of chlorophenols in water by headspace solid phase microextraction ion mobility spectrometry (HS-SPME-IMS). *Talanta* 114, 176–182. doi:10.1016/j.talanta.2013.04.023
- Hoque, R.R., Khillare, P.S., Aggarwal, T., Shridhar, V., Balachandran, S., 2008. Spatial and temporal variation of BTEX in the urban atmosphere of Delhi, India. *Science of The Total Environment* 392, 30–40.
- Hsieh, C.-C., Horng, S.-H., Liao, P.-N., 2003. Stability of Trace-Level Volatile Organic Compounds Stored in Canisters and Tedlar bags. *Aerosol Air Qual. Res.* 3, 17–28.
- Huang, R.J., Zhang, Y.L., Bozzetti, C., Ho, K.F., 2014. High secondary aerosol contribution to particulate pollution during haze events in China. *Nature* 514, 218–222.
- Huybrechts, T., Dewulf, J., Van Langenhove, H., 2003. State-of-the-art of gas chromatography-based methods for analysis of anthropogenic volatile organic compounds in estuarine waters, illustrated with the river Scheldt as an example. *J. Chromatogr. A, A Century of Chromatography 1903-2003* 1000, 283–297.
- ICH harmonized Tripartite Guidelines, 2005. Validation of analytical procedures: text and methodology, Q2 (R).
- Ji, J., Deng, C., Shen, W., Zhang, X., 2006. Field analysis of benzene, toluene, ethylbenzene and xylene in water by portable gas chromatography–microflame ionization detector combined with headspace solid-phase microextraction. *Talanta* 69, 894–899.

- Jeffery, G. H., Bassett, J., Mendhan, J., and Denny, R. C. 1989. Vogel's Textbook of Quantitative Chemical Analysis. ELBS, Longman, Essex, p. 398.
- Kamyotra, S. J. S., and Saha, D., 2011. Guidelines for the measurement of the ambient air pollutants volume I. Central pollution control board, New Delhi.
- Kanda, K., Maekawa, T., 2005. Development of a WO<sub>3</sub> thick-film-based sensor for the detection of VOC. *Sens. Actuators B Chem.*, Proceedings of the Tenth International Meeting on Chemical Sensors IMCS - 10 2004 108, 97–101.
- Kataoka, H., Lord, H.L., Pawliszyn, J., 2000. Applications of solid-phase microextraction in food analysis. *J. Chromatogr. A* 880, 35–62.
- Kennedy, E.R., 2010. Introduction to work place air sampling. *J. Chem. Health Saf.* 17, 4–9.
- Kirchner, M., Jakobi, G., Feicht, E., Bernhardt, M., Fischer, A., 2005. Elevated NH<sub>3</sub> and NO<sub>2</sub> air concentrations and nitrogen deposition rates in the vicinity of a highway in Southern Bavaria. *Atmos. Environ.* 39, 4531–4542.
- Kolb, B., Ettre, L.S., 2006. *Static Headspace-Gas Chromatography: Theory and Practice*, 2nd Edition. ed. Wiley-Interscience, USA.
- Kot-Wasik, A., Zabiegała, B., Urbanowicz, M., Dominiak, E., Wasik, A., Namieśnik, J., 2007. Advances in passive sampling in environmental studies. *Anal. Chim. Acta* 602, 141–163.
- Król, S., Zabiegała, B., Namieśnik, J., 2010. Monitoring VOCs in atmospheric air II. Sample collection and preparation. *TrAC Trends Anal. Chem.* 29, 1101–1112.
- Krupa, S.V., Legge, A.H., 2000. Passive sampling of ambient, gaseous air pollutants: an assessment from an ecological perspective. *Environ. Pollut.* 107, 31–45.
- Krupińska, B., Worobiec, A., Rotondo, G.G., Novaković, V., Kontozova, V., Ro, C., Grieken, R.V., Wael, K.D., 2012. Assessment of the air quality (NO<sub>2</sub>, SO<sub>2</sub>, O<sub>3</sub> and particulate matter) in the Plantin-Moretus Museum/Print room in Antwerp, Belgium, in different seasons of the year. *Microchemical Journal* 102, 49–53.
- Kumar, A., Víden, I., 2007. Volatile Organic Compounds: Sampling Methods and their Worldwide Profile in Ambient Air. *Environ. Monit. Assess.* 131, 301–321.
- Kume, K., Ohura, T., Amagai, T., Fusaya, M., 2008. Field monitoring of volatile organic compounds using passive air samplers in an industrial city in Japan. *Environ. Pollut.* 153, 649–657.
- Kuncharin, W., Mohamed, B., 2013. Cross-border shopping motivation, behaviours and Ethnocentrism of Malaysian in Hat Yai, Thailand. *International Scholarly and Scientific Research and Innovation* 7, 451–461.
- Kuntasal, Ö.O., Karman, D., Wang, D., Tuncel, S.G., Tuncel, G., 2005. Determination of volatile organic compounds in different microenvironments by multibed adsorption

- and short-path thermal desorption followed by gas chromatographic–mass spectrometric analysis. *J. Chromatogr. A* 1099, 43–54.
- Lan, T.T.N., Binh, N.T.T., 2012. Daily roadside BTEX concentrations in East Asia measured by the Lanwatsu, Radiello and Ultra I SKS passive samplers. *Sci. Total Environ.* 441, 248–257.
- Lan, T.T.N., Minh, P.A., 2013. BTEX pollution caused by motorcycles in the megacity of HoChiMinh. *J. Environ. Sci.* 25, 348–356.
- Laowagul, W., Garivait, H., Limpaseni, W., Yoshizumi, K., 2008. Ambient Air concentrations of Benzene, Toluene, Ethylbenzene and Xylene in Bangkok, Thailand during April-August in 2007. *Asian Journal of Atmospheric Environment* 2-1, 14–25.
- Laowagul, W., Yoshizumi, K., 2009. Behavior of benzene and 1,3-butadiene concentrations in the urban atmosphere of Tokyo, Japan. *Atmos. Environ.* 43, 2052–2059.
- Lau, A.K.H., Yuan, Z., Yu, J.Z., Louie, P.K.K., 2010. Source apportionment of ambient volatile organic compounds in Hong Kong. *Science of the Total Environment* 408, 4138–4149.
- Lee, S.C., Chiu, M.Y., Ho, K.F., Zou, S.C., Xinming, W., 2002. Volatile organic compounds (VOCs) in urban atmosphere of Hong Kong. *Chemosphere* 48, 375–382.
- Lei, H., Wuebbles, D.J., 2013. Chemical competition in nitrate and sulfate formation and its effects on air quality. *Atmos. Environ.* 80, 472–477.
- Liu, L., Zhang, Y., Wang, G., Li, S., Wang, L., Han, Y., Jiang, X., Wei, A., 2011. High toluene sensing properties of NiO–SnO<sub>2</sub> composite nanofiber sensors operating at 330 °C. *Sens. Actuators B Chem.* 160, 448–454.
- Liu, Q., Sun, G., Wang, S., Lin, Q., Zhang, J., Li, X., 2014. Analysis of the variation in scent components of Hosta flowers by HS-SPME and GC–MS. *Sci. Hortic.* 175, 57–67.
- Liu, X.G., Zhang, Y.H., Cheng, Y.F., Hu, M., Han, T.T., 2012. Aerosol hygroscopicity and its impact on atmospheric visibility and radiative forcing in Guangzhou during the 2006 PRIDE-PRD campaign. *Atmos. Environ.* 60, 59–67.
- Llop, S., Ballester, F., Estarlich, M., Esplugues, A., Rebagliato, M., Iñiguez, C., 2010. Preterm birth and exposure to air pollutants during pregnancy. *Environ. Res.* 110, 778–785.
- Long, G.L., Winefordner, J.D., 1983. Limit of detection. A closer look at the IUPAC definition. *Analytical Chemistry* 55, 712A–724A.

- Lü, H., Cai, Q.-Y., Wen, S., Chi, Y., Guo, S., Sheng, G., Fu, J., Katsoyiannis, A., 2010. Carbonyl compounds and BTEX in the special rooms of hospital in Guangzhou, China. *J. Hazard. Mater.* 178, 673–679.
- Lupo, P.J., Symanski, E., Waller, D.K., Chan, W., Langlois, P.H., Canfield, M.A., Mitchell, L.E., 2011. Maternal exposure to ambient levels of benzene and neural tube defects among offspring: Texas, 199-2004. *Health Perspect* 119, 397–402.
- Mahadevaiah, Abdul Galil, M.S., Kumar, M.S.Y., Sathish, M.A., Nagendrappa, G., 2008. Simple spectrophotometric method for the determination of Sulphur dioxide by its decolorizing effect on the peroxovanadate complex. *Journal of Analytical Chemistry* 63, 239–243.
- Ma, H., Xu, Y., Rong, Z., Cheng, X., Gao, S., Zhang, X., Zhao, H., Huo, L., 2012. Highly toluene sensing performance based on monodispersed Cr<sub>2</sub>O<sub>3</sub> porous microspheres. *Sens. Actuators B Chem.* 174, 325–331.
- Malik, A.K., Kaur, V., Verma, N., 2006. A review on solid phase microextraction—High performance liquid chromatography as a novel tool for the analysis of toxic metal ions. *Talanta* 68, 842–849.
- Mangani, G., Berloni, A., Maione, M., 2003. “Cold” solid-phase microextraction method for the determination of volatile halocarbons present in the atmosphere at ultra-trace levels. *J. Chromatogr. A* 988, 167–175.
- Marion, M., Tiffonnet, A.L., Santa-Cruz, A., Makhoulfi, R., 2011. Study of the resistances to transfer of gaseous pollutant between material and indoor air. *Build. Environ.* 46, 356–362.
- Marlet, C., Lognay, G., 2010. Development and validation by accuracy profile of a method for the analysis of monoterpenes in indoor air by active sampling and thermal desorption-gas chromatography-mass spectrometry. *Talanta* 82, 1230–1239.
- Marple, V.A., 2004. History of Impactors—The First 110 Years. *Aerosol Sci. Technol.* 38, 247–292.
- Matisová, E., Škrabáková, S., 1995. Carbon sorbents and their utilization for the preconcentration of organic pollutants in environmental samples. *J. Chromatogr. A*, 11th International Symposium on Preparative and Industrial Chromatography 707, 145–179.
- Mendell, M.J., 2007. Indoor residential chemical emissions as risk factors for respiratory and allergic effects in children: a review. *Indoor Air* 17, 259–277.
- Meng, Z.Y., Ding, G.A., Xu, X.B., Xu, X.D., Yu, H.Q., Wang, S.F., 2008. Vertical distributions of SO<sub>2</sub> and NO<sub>2</sub> in the lower atmosphere in Beijing urban areas, China. *Sci. Total Environ.* 390, 456–465.
- Miljevic, B., Modini, R.L., Bottle, S.E., Ristovski, Z.D., 2009. On the efficiency of impingers with fritted nozzle tip for collection of ultrafine particles. *Atmos. Environ.* 43, 1372–1376.

- Millstein, B.E., Harley, R.A., 2010. Effects of retrofitting emission control systems on in-use heavy diesel vehicles. *Environ. Sci. Technol.* 5042–5048.
- Mishra, N., Bartsch, J., Ayoko, G.A., Salthammer, T., Morawska, L., 2015. Volatile Organic Compounds: Characteristics, distribution and sources in urban schools. *Atmos. Environ.* 106, 485–491.
- Moodley, K.G., Singh, S., Govender, S., 2011. Passive monitoring of nitrogen dioxide in urban air: A case study of Durban metropolis, South Africa. *J. Environ. Manage.* 92, 2145–2150.
- Mousazadeh, S. 2009. Determination of nitrogen oxides concentration in the atmosphere of the faculty of pharmacology's laboratories. *Iranian Journal of Toxicology*, 2: 281-286
- Mori, M., Nishimura, H., Itagaki, Y., Sadaoka, Y., 2009. Potentiometric VOC detection in air using 8YSZ-based oxygen sensor modified with SmFeO<sub>3</sub> catalytic layer. *Sens. Actuators B Chem.* 142, 141–146.
- Munoz, M. P., Rueda, F. J. M. D. V. and Diez, L. M. P. 1989. Determination of Formaldehyde in air by flow injection using pararosaniline and spectrophotometric detection. *Analyst* 114: 1469-1471.
- Musteata, F.M., Pawliszyn, J., 2007. In vivo sampling with solid phase microextraction. *J. Biochem. Biophys. Methods, Sample Preparation* 70, 181–193.
- Myers, G., Myrmel, K., Guild, L.V., Harper, M., 2005. Research report on validation of benzene using SKC passive sampler 575-001. Publ. No 1312 Rev 9812 Benzene.
- NEC, 2009. Compliance monitoring report- industries. National Environment Commission Secretariat.
- NEC, 2010. Strategy for air quality assessment and management in Bhutan. National Environment Commission Secretariat.
- Ng, S.P., Dimitroulopoulou, C., Grossinho, A., Chen, L.C., Kendall, M., 2005. PM<sub>2.5</sub> exposure assessment of the population in Lower Manhattan area of New York City after the World Trade Center disaster. *Atmos. Environ.* 39, 1979–1992.
- Nicoletti, S., Dori, L., Cardinali, G.C., Parisini, A., 1999. Gas sensors for air quality monitoring: realisation and characterisation of undoped and noble metal-doped SnO<sub>2</sub> thin sensing films deposited by the pulsed laser ablation. *Sens. Actuators B Chem.* 60, 90–96.
- Parrish, D.D., Singh, H.B., Molina, L., Madronich, S., 2011. Air quality progress in North American megacities: A review. *Atmos. Environ.* 45, 7015–7025.

- Pawliszyn, J., 2012. 2 - Theory of Solid-Phase Microextraction, in: Pawliszyn, J. (Ed.), *Handbook of Solid Phase Microextraction*. Elsevier, Oxford, pp. 13–59.
- Pawliszyn, J., 1997. *Solid Phase Microextraction: Theory and Practice*.
- Pimpisut, D., Jinsart, W., Hooper, M.A., 2005. Modelling of the BTX species based on an emission inventory of sources at the Map Ta Phut industrial estate in Thailand. *Science Asia* 31, 103–112.
- Plaisance, H., Gerboles, M., Piechocki, A., Detimmerman, F., de Saeger, E., 2007. Radial diffusive sampler for the determination of 8-h ambient ozone concentrations. *Environ. Pollut.* 148, 1–9.
- Pongiachan, S., Pongnailert, S., Ho, K.F., Cao, J., 2014. Diurnal variation and vertical distribution of carbonaceous aerosols in the Southern part of Thailand. *WIT Transactions on Ecology and the Environment* 183.
- Purcaro, G., Picardo, M., Barp, L., Moret, S., Conte, L.S., 2013. Direct-immersion solid-phase microextraction coupled to fast gas chromatography mass spectrometry as a purification step for polycyclic aromatic hydrocarbons determination in olive oil. *J. Chromatogr. A* 1307, 166–171.
- Ramírez, N., Cuadras, A., Rovira, E., Borrull, F., Marcé, R.M., 2010. Comparative study of solvent extraction and thermal desorption methods for determining a wide range of volatile organic compounds in ambient air. *Talanta* 82, 719–727.
- Rao, P., Ansari, M.F., Gavane, A.G., Pandit, V.I., Nema, P., Devotta, S., 2007. Seasonal Variation of Toxic Benzene Emissions in Petroleum Refinery. *Env. Monit Assess* 128, 323–328.
- Ras-Mallorquí, M.R., Marcé-Recasens, R.M., Borrull-Ballarín, F., 2007. Determination of volatile organic compounds in urban and industrial air from Tarragona by thermal desorption and gas chromatography–mass spectrometry. *Talanta* 72, 941–950.
- Ras, M.R., Borrull, F., Marcé, R.M., 2009. Sampling and preconcentration techniques for determination of volatile organic compounds in air samples. *TrAC Trends Anal. Chem.* 28, 347–361.
- Ravindra, K., Sokhi, R., Van Grieken, R., 2008. Atmospheric polycyclic aromatic hydrocarbons: Source attribution, emission factors and regulation. *Atmos. Environ.* 42, 2895–2921.
- Rodhe, H., Deutener, F., Schulz, M., 2002. The global distribution of acidifying wet deposition. *Environ. Sci. Technol.* 36, 4382–4388.
- Rogers, J.F., Thompson, S.J., Addy, C.L., Mc Keown, R.E., Cowen, D.J., Docufle, P., 2000. Association of very low birth weight with exposures to environmental sulfur dioxide and total suspended particulates. *Am J Epidemiol* 151, 602–613.

- Roukos, J., Locoge, N., Sacco, P., Plaisance, H., 2011. Radial diffusive samplers for determination of 8-h concentration of BTEX, acetone, ethanol and ozone in ambient air during a sea breeze event. *Atmos. Environ.* 45, 755–763.
- Saelim, J., Kanatharana, P., Thavarungkul, P., Thammakhet, C., 2013. Novel fabricated silver particles/polypyrrole printed circuit board passive samplers for volatile organic compounds monitoring. *Microchem. J.* 108, 180–187.
- Saltzman, B. E. 1949. Colorimetric Micro-determination of Nitrogen Dioxide in the Atmosphere. Division of special Health service, U. S. Department of Health, Education, and Welfare, Cincinnati, Ohio.
- Schrefils, J.J., Fu, Y., Wilson, E.J., 2012. Sulfur dioxide control in China: policy evaluation during the 10th and 11th Five-year plan and lesson for the future. *Energy Policy* 48, 779–789.
- Seethapathy, S., Górecki, T., Li, X., 2008. Passive sampling in environmental analysis. *J. Chromatogr. A, 50 Years Journal of Chromatography* 1184, 234–253.
- Singer, B.C., Hodgson, A.T., Hotchi, T., Kim, J.J., 2004. Passive measurement of nitrogen oxides to assess traffic-related pollutant exposure for the East Bay Children's Respiratory Health Study. *Atmos. Environ.* 38, 393–403.
- Sivacoumar, R., Bhanarkar, A.D., Goyal, S.K., Gadkari, S.K., Aggarwal, A.L., 2001. Air pollution modeling for an industrial complex and model performance evaluation. *Environ. Pollut.* 111, 471–477.
- Škarek, M., Čupr, P., Bartoš, T., Kohoutek, J., Klánová, J., Holoubek, I., 2007. A combined approach to the evaluation of organic air pollution —A case study of urban air in Sarajevo and Tuzla (Bosnia and Herzegovina). *Sci. Total Environ.* 384, 182–193.
- Skov, H., Lindskog, A., Palmgren, F., Christensen, C.S., 2001. An overview of commonly used methods for measuring benzene in ambient air. *Atmos. Environ., Selected Papers Presented at the Venice Conference 35, Supplement 1*, S141–S148.
- Slama, R., Theibauges, O., Goua, V., Aussel, L., Sacco, P., Bohet, A., Forhan, A., Ducot, B., Annesi-Maesanao, I., Heinrich, J., Magnin, G., Schweitzer, M., Kaminski, M., Charles, M., 2009. EDEN Mother-Child Cohort Study Group. Maternal personal exposure to airborne benzene and intrauterine growth. *Environ. Health Perspect* 117, 1313–1321.
- Spietelun, A., Pilarczyk, M., Kloskowski, A., Namieśnik, J., 2011. Polyethylene glycol-coated solid-phase microextraction fibres for the extraction of polar analytes—A review. *Talanta* 87, 1–7.
- Srivastava, A., Devotta, S., 2007. Indoor Air Quality of Public Places in Mumbai, India in Terms of Volatile Organic Compounds 133, 127–138.
- Srivastava, A., Sengupta, B., Dutta, S., 2005. Source apportionment of ambient VOCs in Delhi City. *Science of the Total Environment* 343, 207–220.

- Stock, Z.S., Russo, M.R., Butler, T.M., Archibald, A.T., Lawrence, M.G., Telford, P.J., Abraham, N.L., Pyle, J.A., 2013. Modeling the impact of megacities on local, regional and global tropospheric ozone and the deposition of nitrogen species. *Atmos. Chem. Phys.* 13, 12215–12231.
- Strandberg, B., Sunesson, A.-L., Olsson, K., Levin, J.-O., Ljungqvist, G., Sundgren, M., Sällsten, G., Barregard, L., 2005. Evaluation of two types of diffusive samplers and adsorbents for measuring 1,3-butadiene and benzene in air. *Atmos. Environ.* 39, 4101–4110.
- Stranger, M., Krata, A., Kontozova-Deutsch, V., Bencs, L., Deutsch, F., Worobiec, A., Naveau, I., Roekens, E., Van Grieken, R., 2008. Monitoring of NO<sub>2</sub> in the ambient air with passive samplers before and after a road reconstruction event. *Microchem. J.* 90, 93–98.
- Sun, C., Su, X., Xiao, F., Niu, C., Wang, J., 2011. Synthesis of nearly monodisperse Co<sub>3</sub>O<sub>4</sub> nanocubes via a microwave-assisted solvothermal process and their gas sensing properties. *Sens. Actuators B Chem.* 157, 681–685.
- Swartz, M., and Krull, I. D. 1997. Analytical method development and validation (2<sup>nd</sup> edition). New York.
- Tanaka, T., Ohyama, T., Maruo, Y.Y., Hayashi, T., 1998. Coloration reactions between NO<sub>2</sub> and organic compounds in porous glass for cumulative gas sensor. *Sens. Actuators B Chem.* 47, 65–69.
- Tan, S. P., and Piri, M. 2013. Modeling the solubility of nitrogen dioxide in water using perturbed-chain statistical associating fluid theory. *Industrial and Engineering Chemistry Research*, 52: 16031-16043.
- Tankiewicz, M., Morrison, C., Biziuk, M., 2013. Multi-residue method for the determination of 16 recently used pesticides from various chemical groups in aqueous samples by using DI-SPME coupled with GC–MS. *Talanta* 107, 1–10.
- Tao, S., Liu, Y.N., Lang, C., Wang, W.T., Yuan, H.S., Zhang, D.Y., Qiu, W.X., Liu, J.M., Liu, Z.G., Liu, S.Z., Yi, R., Ji, M., Liu, X.X., 2008. A directional passive air sampler for monitoring polycyclic aromatic hydrocarbons (PAHs) in air mass. *Environ. Pollut.* 156, 435–441.
- Tolnai, B., Hlavay, J., Möller, D., Prümke, H.-J., Becker, H., Dostler, M., 2000. Combination of canister and solid adsorbent sampling techniques for determination of volatile organic hydrocarbons. *Microchem. J.*, ANALYTICAL TECHNIQUES IN 67, 163–169.
- US EPA, 1964. Method of measuring and monitoring atmospheric sulfur dioxide. US Department of Health, Education and welfare.

- Wang, D., Austin, C., 2006. Determination of complex mixtures of volatile organic compounds in ambient air: an overview. *Anal Bioanal Chem* 386, 1099–1120.
- Wang, T., Cheung, V.T.F., Lam, K.S., Kok, G.L., Harris, J.M., 2001. The characteristics of ozone and related compounds in the boundary layer of the South China coast: temporal and vertical variations during autumn season. *Atmos. Environ.* 35, 2735–2746.
- Webb, P.A., 2003. *Introduction to Chemical Adsorption Analytical Techniques and their Applications to Catalysis*.
- West, Gaeke, 1956. Determination of Sulfur Dioxide by the West-Gaeke Method. *Anal. Chem.*, 28.
- Woolfeden, E., 2010. Sorbent-based sampling methods for volatile and semi-volatile organic compounds in air Part 1: Sorbent-based air monitoring options 1217, 2674–2684.
- Wu, C.-H., Feng, C.-T., Lo, Y.-S., Lin, T.-Y., Lo, J.-G., 2004. Determination of volatile organic compounds in workplace air by multisorbent adsorption/thermal desorption-GC/MS. *Chemosphere* 56, 71–80.
- Xie, Z., Selzer, J., Ebinghaus, R., Caba, A., Ruck, W., 2006. Development and validation of a method for the determination of trace alkylphenols and phthalates in the atmosphere. *Anal. Chim. Acta* 565, 198–207.
- Yurdakul, S., Civan, M., Tuncel, G., 2013. Volatile organic compounds in suburban Ankara atmosphere, Turkey: Sources and variability. *Atmospheric Res.* 120–121, 298–311.
- Zabiegała, B., Górecki, T., Przyk, E., Namieśnik, J., 2002. Permeation passive sampling as a tool for the evaluation of indoor air quality. *Atmos. Environ.* 36, 2907–2916.
- Zhang, Q. and Tie, X. 2011. High solubility of SO<sub>2</sub>: evidence in an intensive fog event measure in the NCP region, China. *Atmos. Chem. Phys. Discuss.*, 11: 2931–2947.
- Zhu, B.L., Xie, C.S., Wang, W.Y., Huang, K.J., Hu, J.H., 2004. Improvement in gas sensitivity of ZnO thick film to volatile organic compounds (VOCs) by adding TiO<sub>2</sub>. *Mater. Lett.* 58, 624–629.
- Zielinska, B., Fujita, E., 1994. *Environmental Sampling for Trace Analysis*. VCH Verlagsgesellschaft mbH.
- Zou, S.C., Lee, S.C., Chan, C.Y., Ho, K.F., Wang, X.M., Chan, L.Y., Zhang, Z.X., 2003. Characterization of ambient volatile organic compounds at a landfill site in Guangzhou, South China. *Chemosphere* 51, 1015–1022.

**VITAE**

**Name** Mr. Jas Raj Subba

**Student ID** 5510230032

**Education attainment**

<b>Degree</b>	<b>Name of Institution</b>	<b>Year of Graduation</b>
Master of Science (Inorganic Chemistry)	Madras University (India)	2007
Bachelor of Science (Biology and Chemistry)	Sherubtse College (Bhutan)	2000

**Scholarship Awards during Enrolment**

Prince of Songkla University, Ph.D. Scholarship

**List of Publication**

1. Subba, J. R., Thammakhet, C., Thavarungkul, P and Kanatharant, P. Sampling of BTX in Hat Yai city using cost effective laboratory-built PCB passive sampler Journal of Environmental Health and Science Part A. Accepted manuscript, February 25, 2016.
2. Subba, J. R., Thammakhet, C., Thavarungkul, P and Kanatharant, P. Distributions of SO<sub>2</sub> and NO<sub>2</sub> in the lower atmosphere of an industrial area in Bhutan. Journal of Environmental Health and Science Part A. Submitted manuscript, March 12, 2016

**Presentation****Oral presentation**

Subba, J. R., Kanatharana, P., Thammakhet, C., and Thavarungkul, P. Sampling of BTX in Hat Yai city using cost effective laboratory-built PCB passive sampler. 113<sup>th</sup> TRF Seminar Series in Basic Research “From Basic Research to Applications”. Faculty of Science, Prince of Songkla University, Thailand. September 25<sup>th</sup>, 2015.

**Presentation Awards**

Outstanding Oral Presentation Award: Sampling of BTX in Hat Yai city using cost effective laboratory-built PCB passive sampler. 113<sup>th</sup> TRF Seminar Series in Basic Research “From Basic Research to Applications”. Faculty of Science, Prince of Songkla University, Thailand. September 25<sup>th</sup>, 2015.